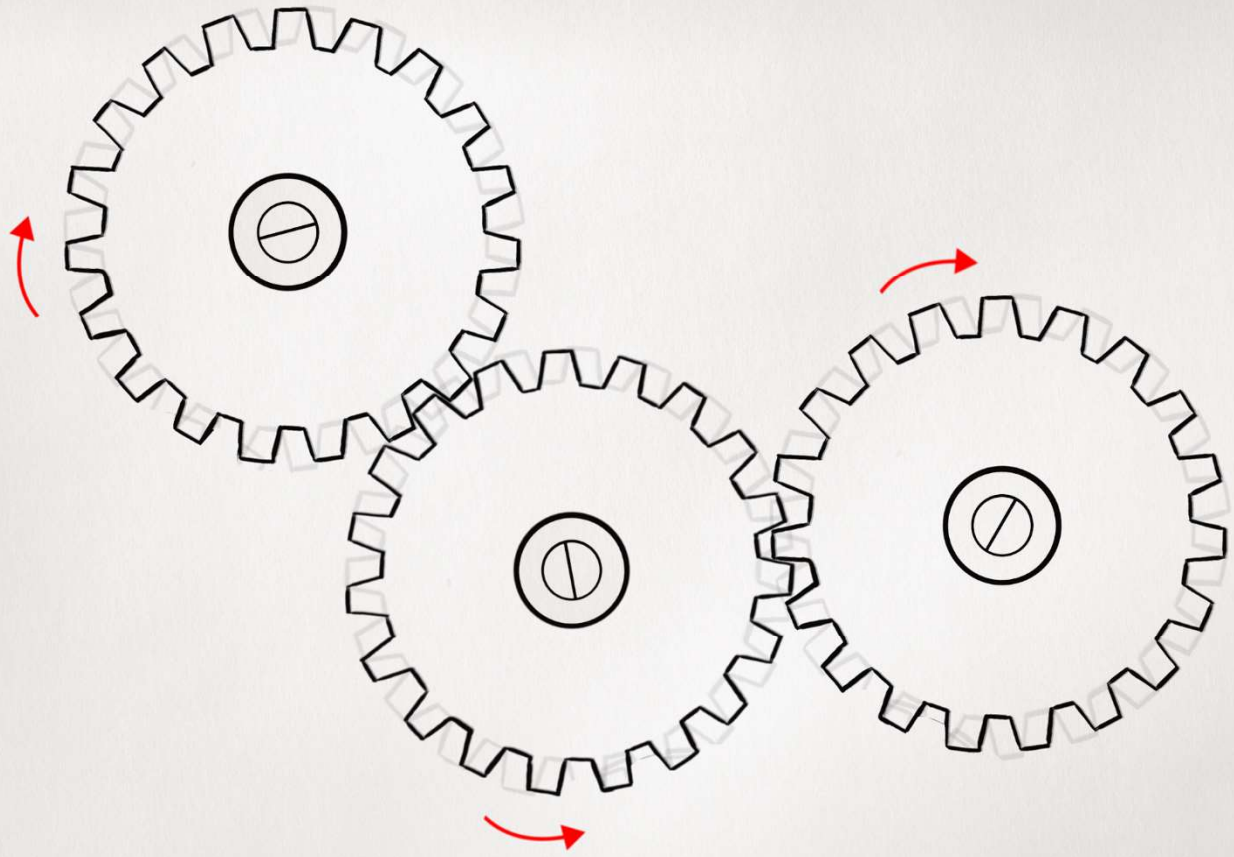
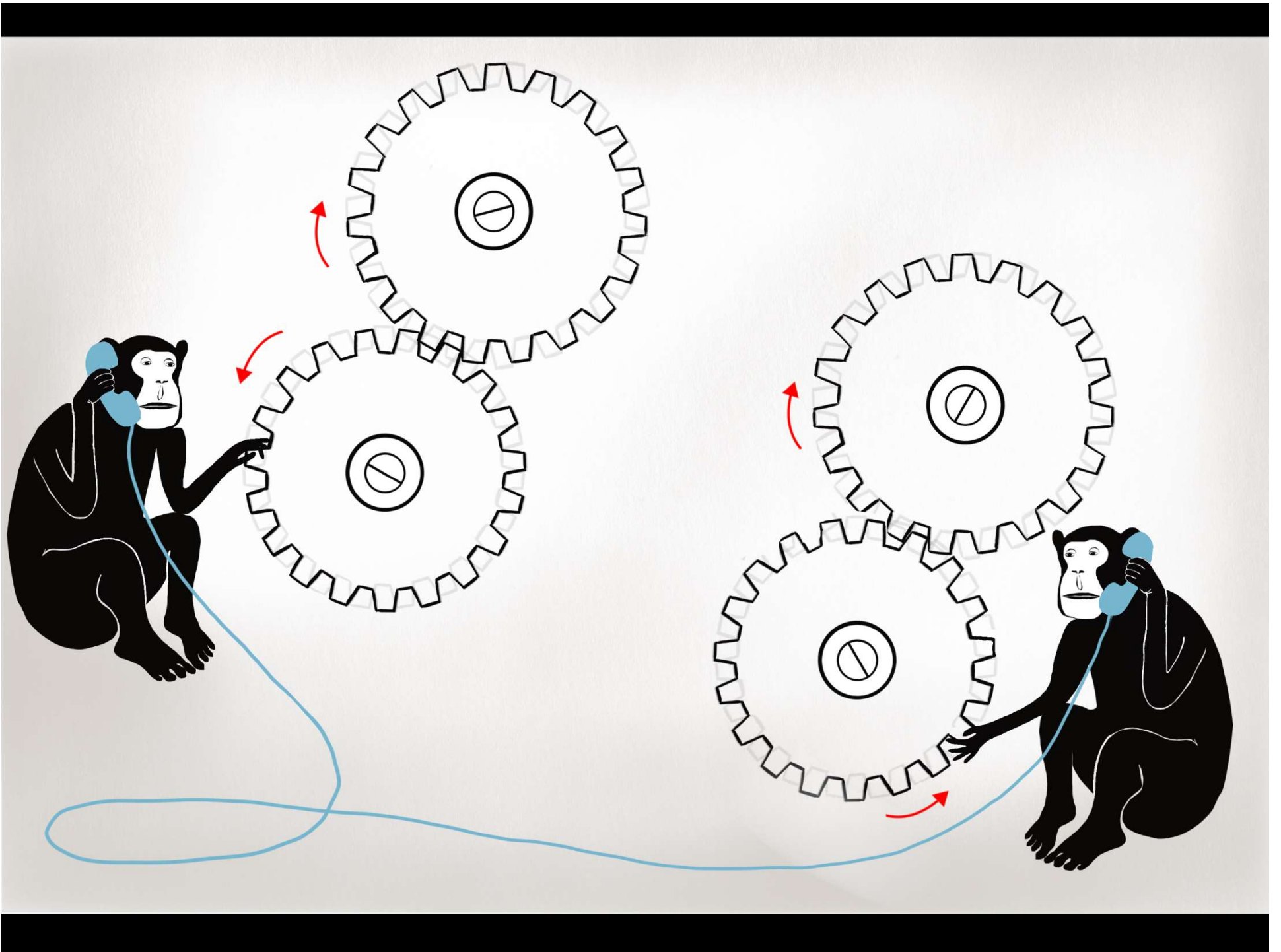
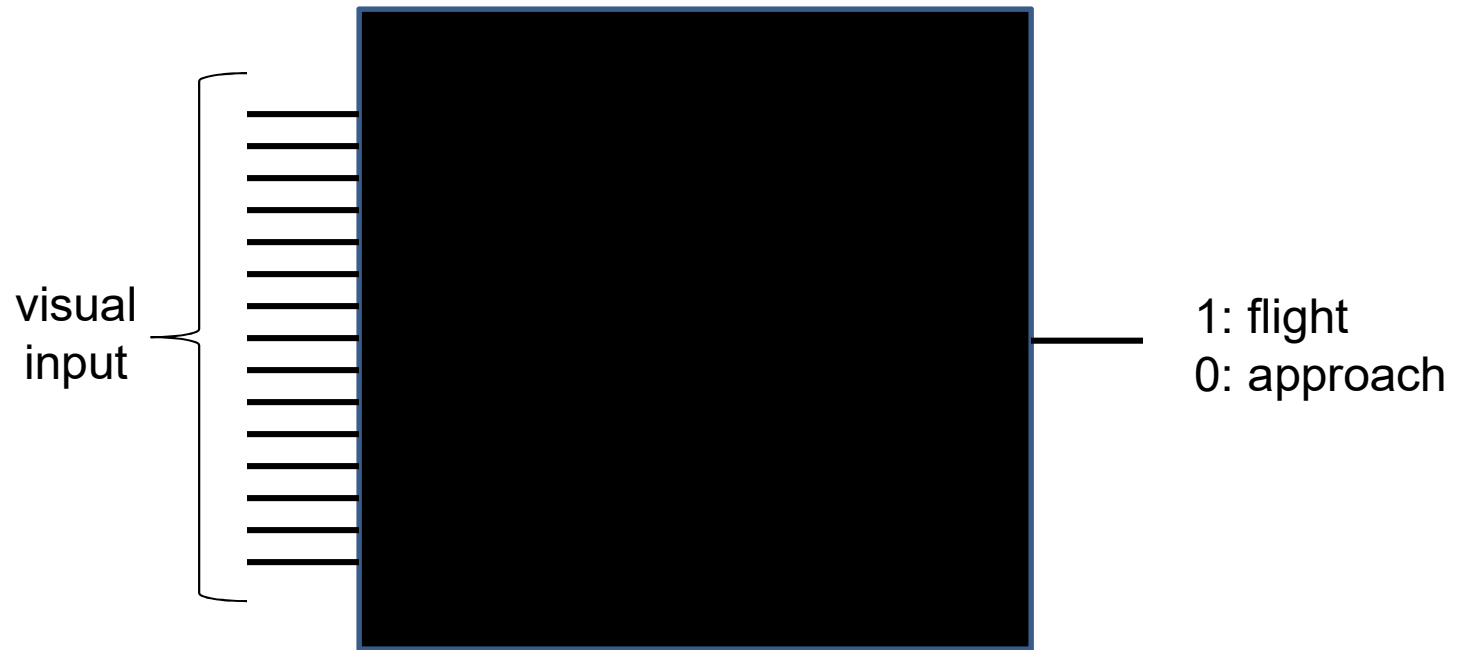


Animation: Julia Kuhl

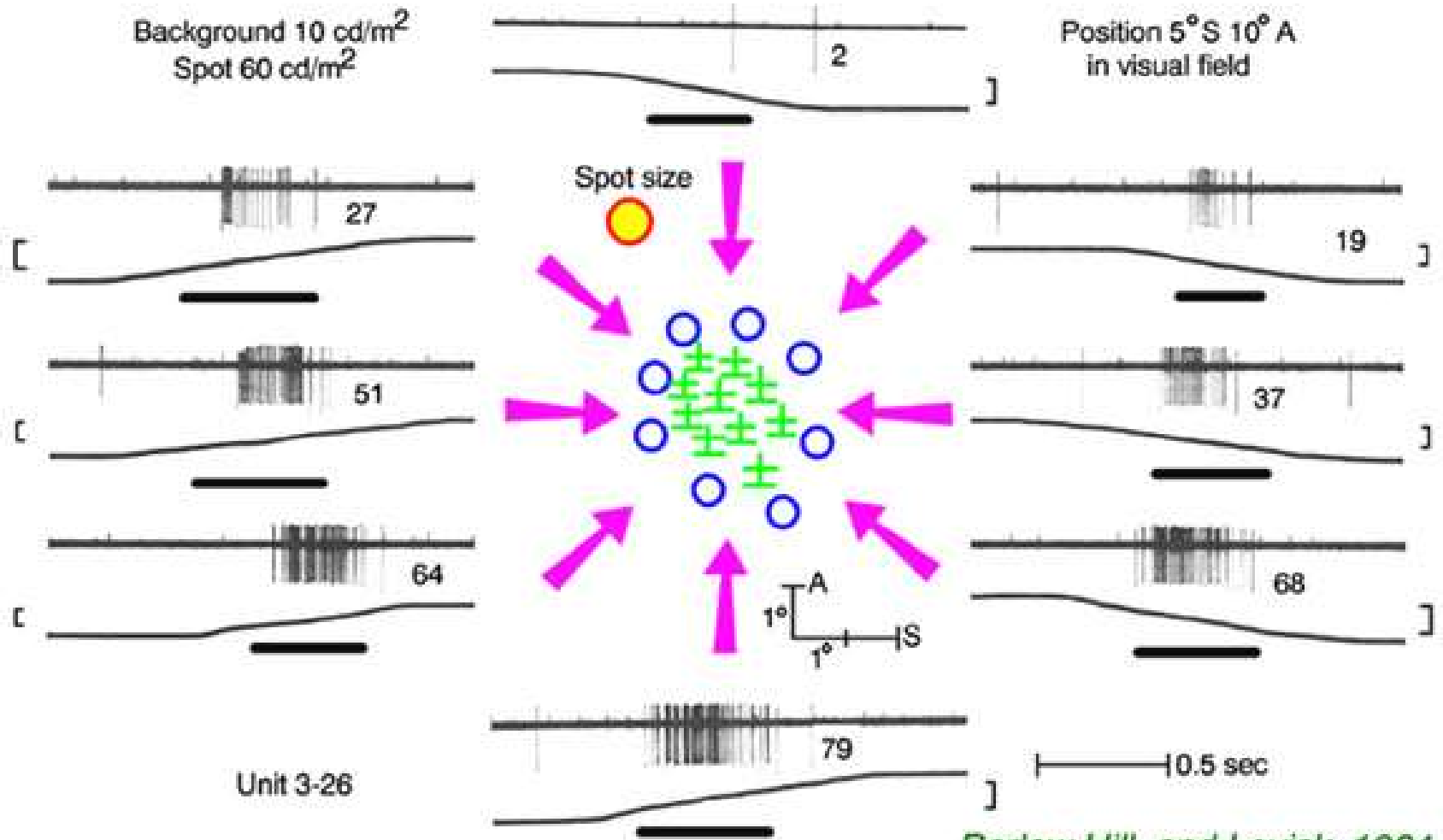




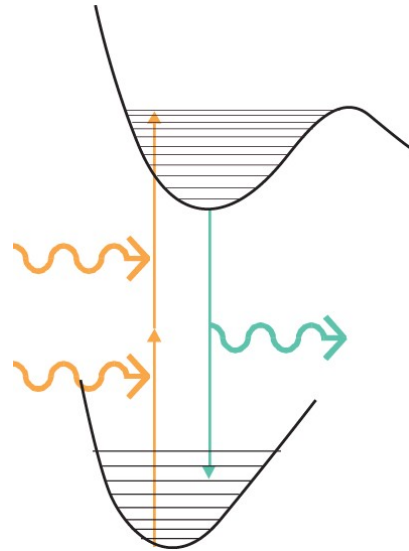
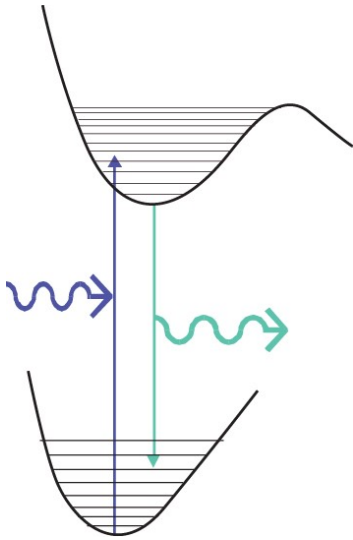
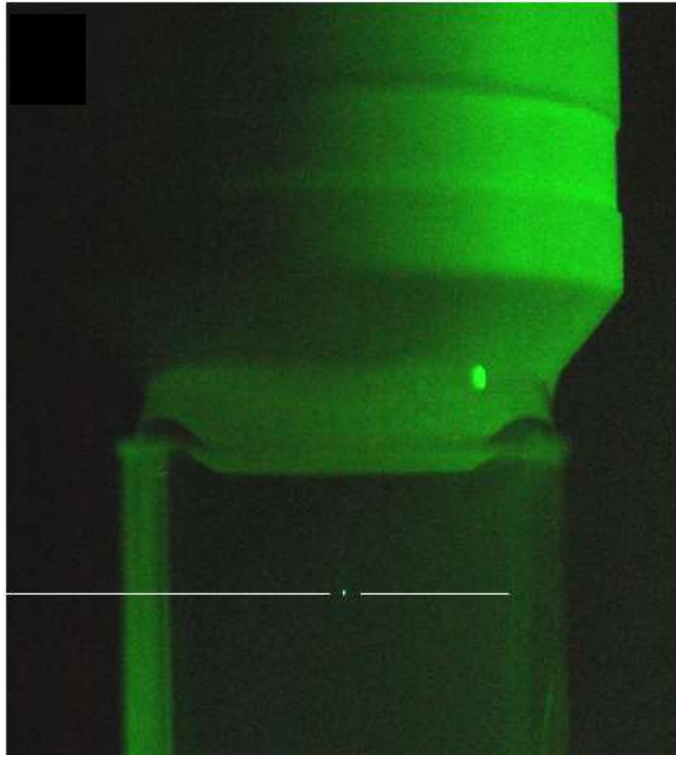
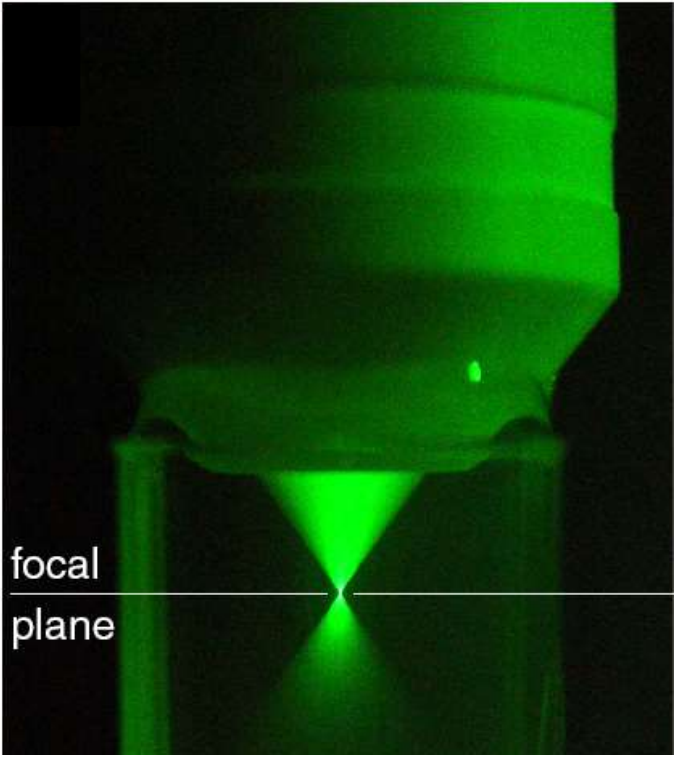


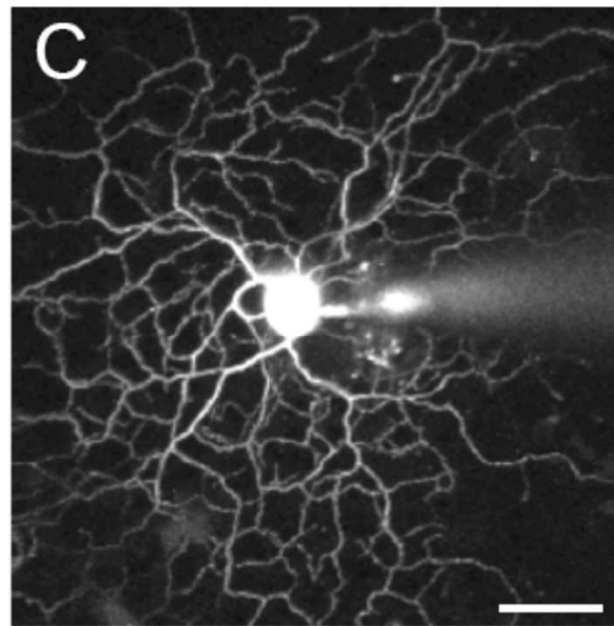
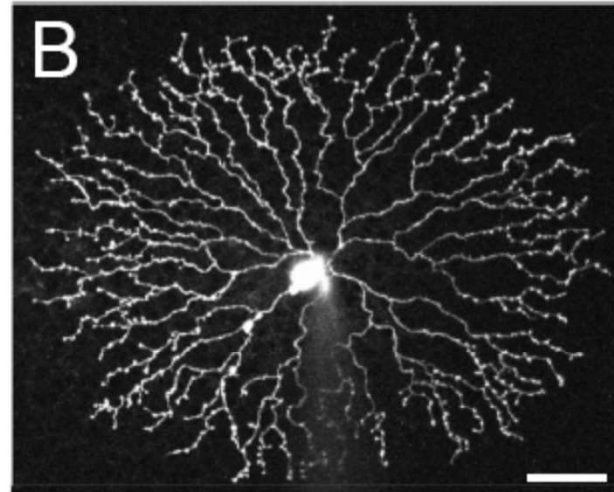
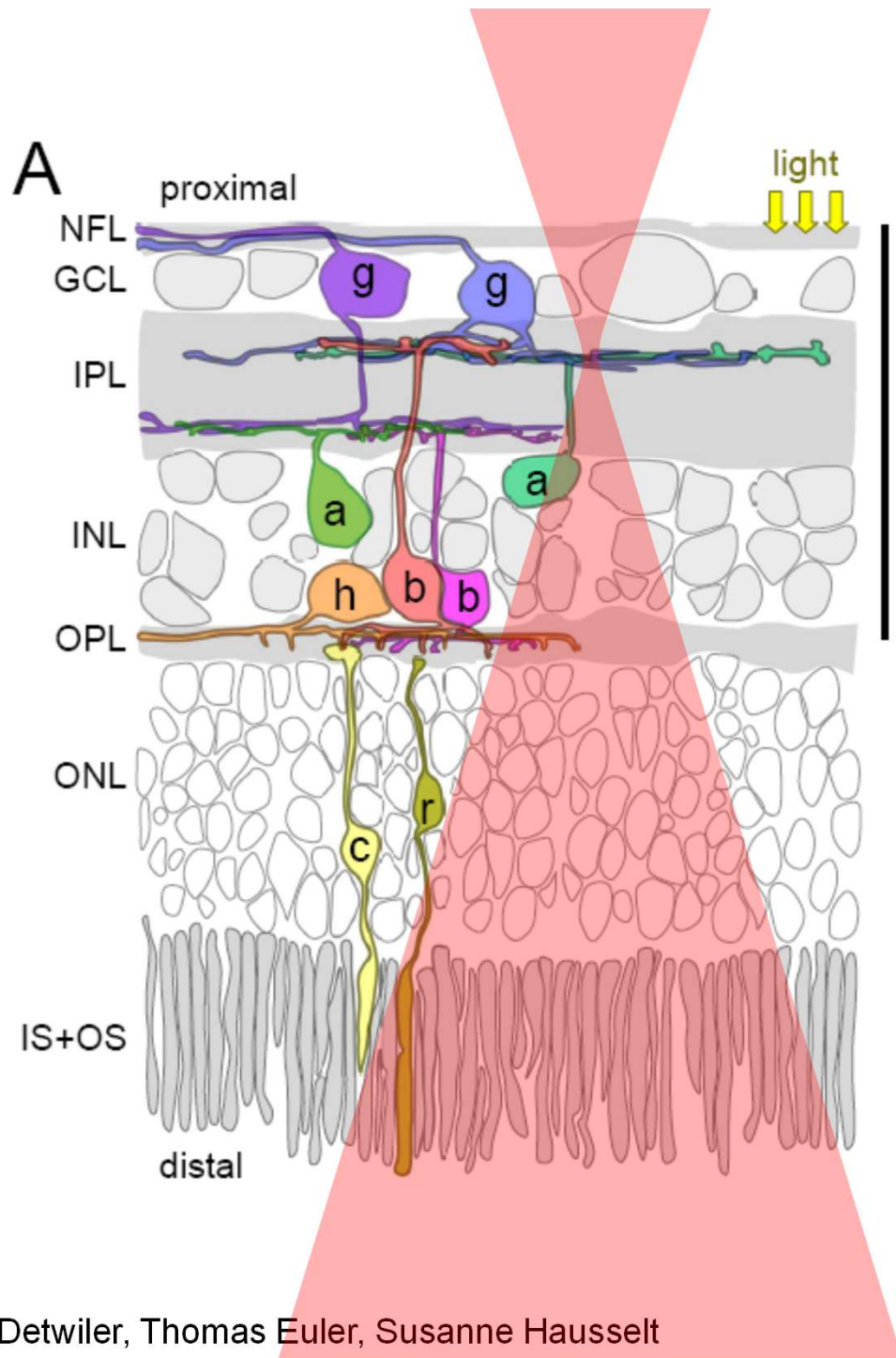
Background 10 cd/m^2
Spot 60 cd/m^2

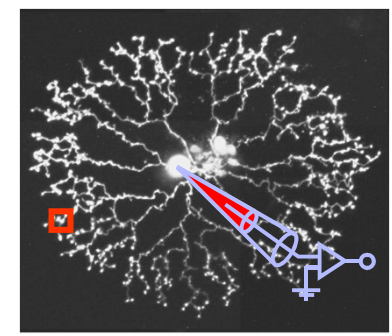
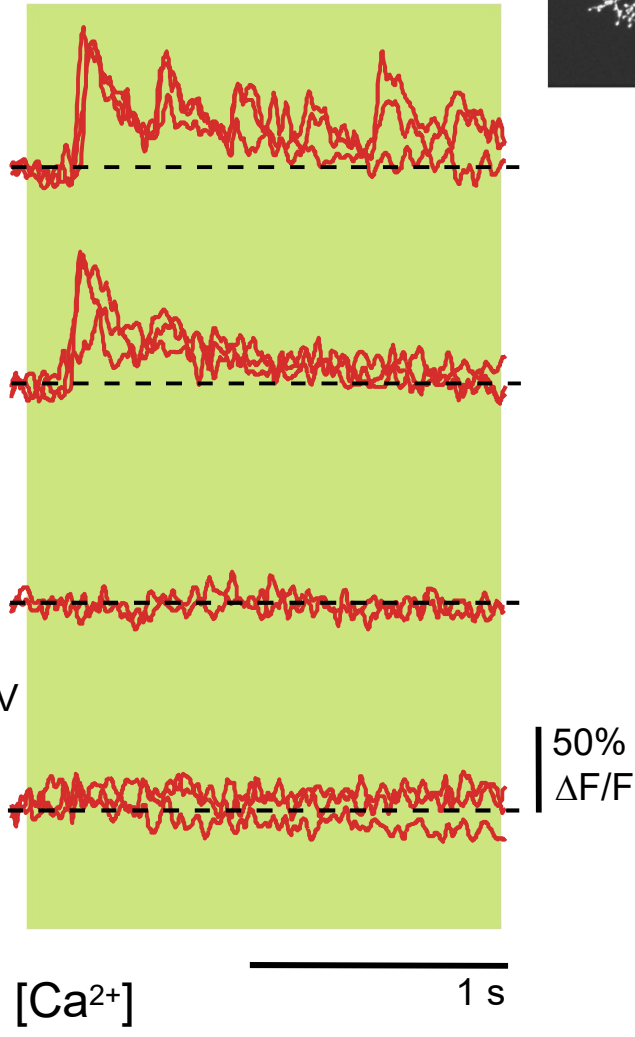
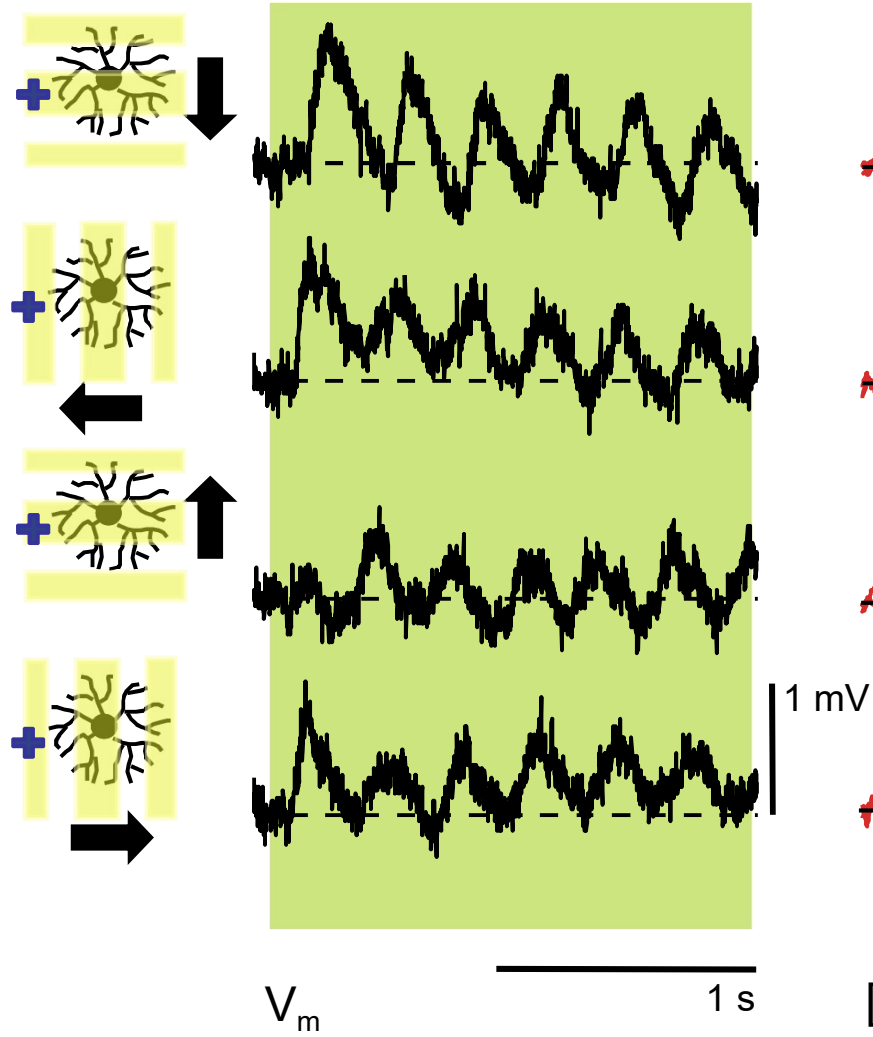
Position $5^\circ \text{ S } 10^\circ \text{ A}$
in visual field

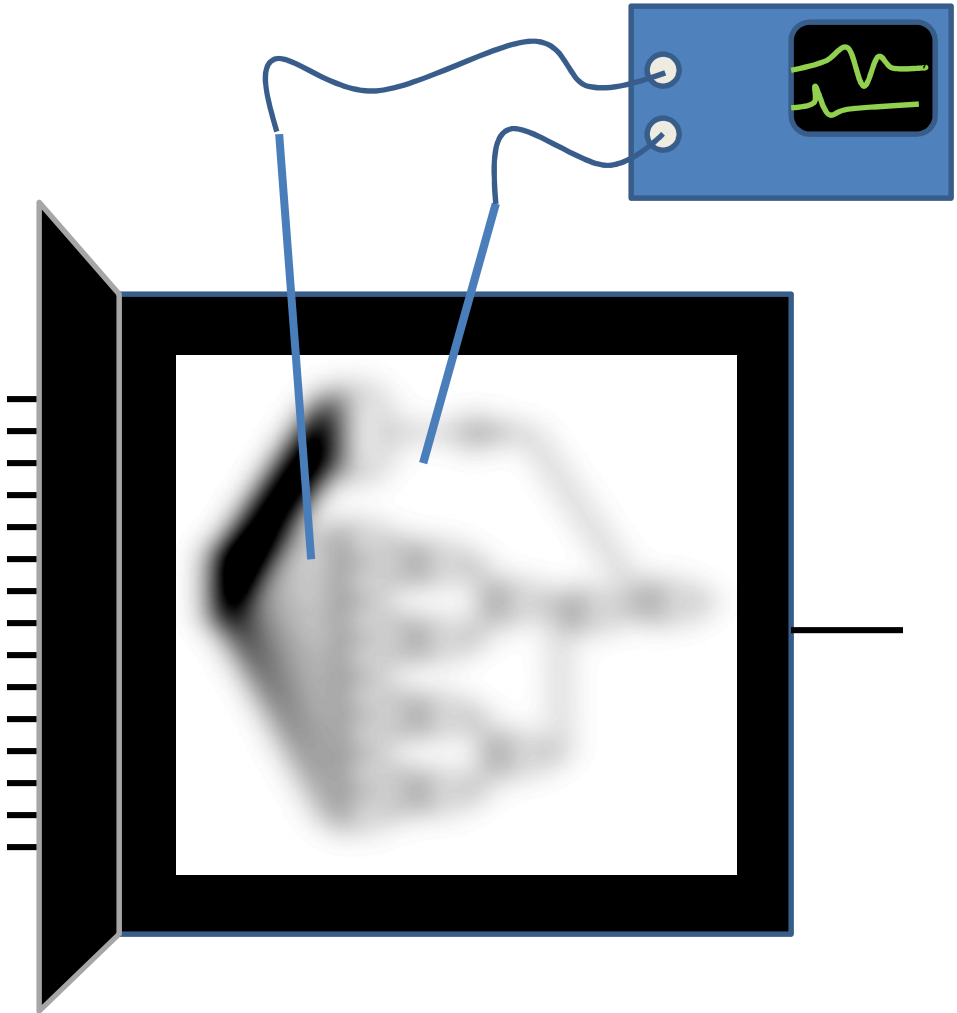


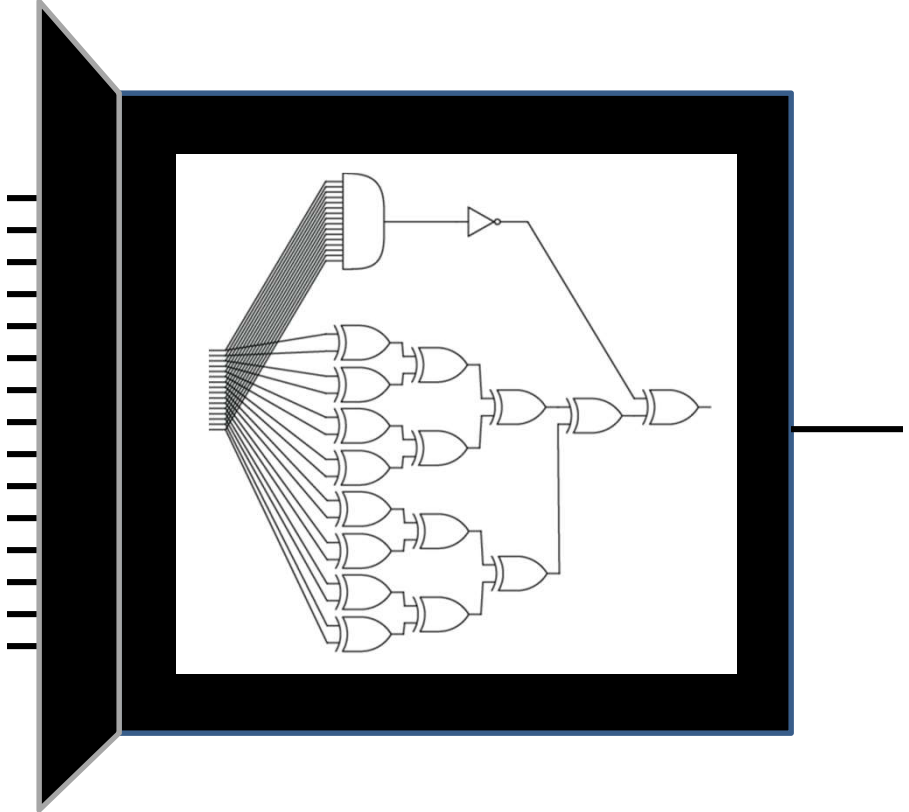
Barlow, Hill, and Levick, 1964





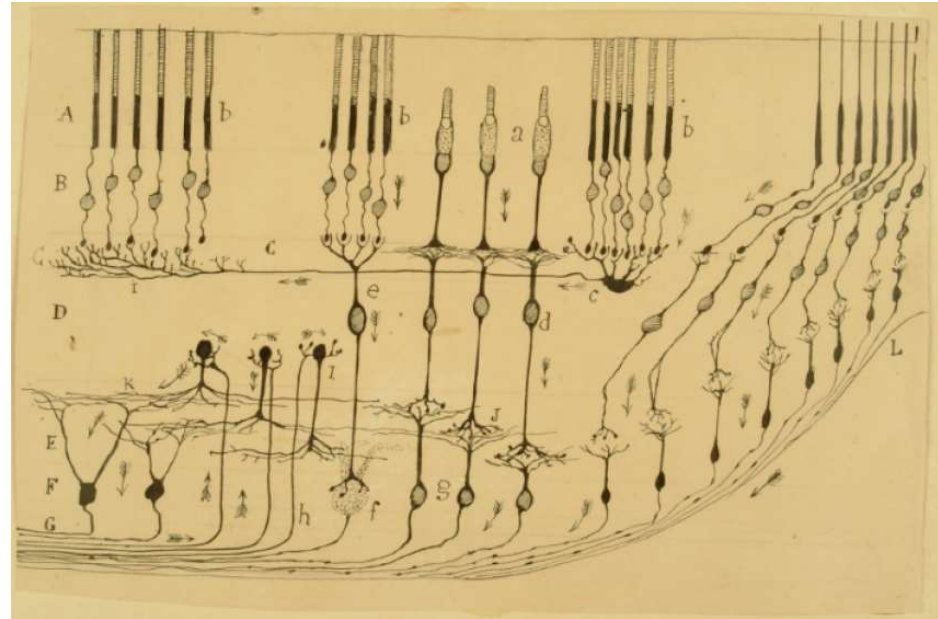




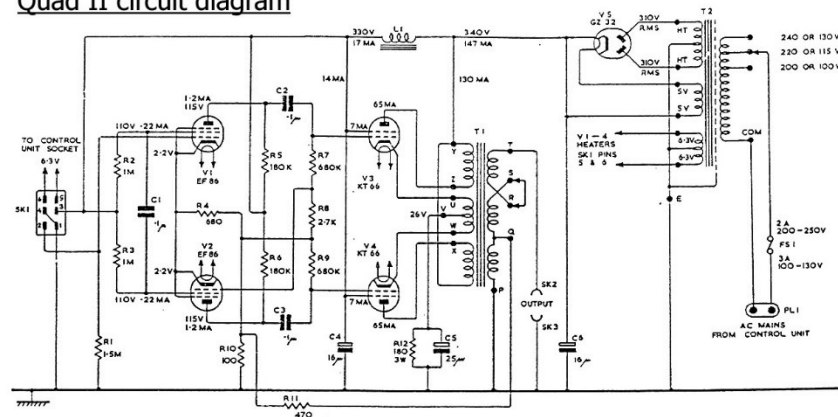


"Santiago Ramon y Cajal - arguably the most accomplished **anatomist** in the history of neuroscience - became recognized as such not only because of his incredible anatomical skills and his indefatigable working habits, but also because of his uncanny sense of the **functional implications** of his work, a sense that made him a true genius in the field of biology."

Llinas, R. R. (2003). "The contribution of Santiago Ramon y Cajal to functional neuroscience." *Nat. Rev. Neurosci.*, 4(1): 77-80.



Quad II circuit diagram

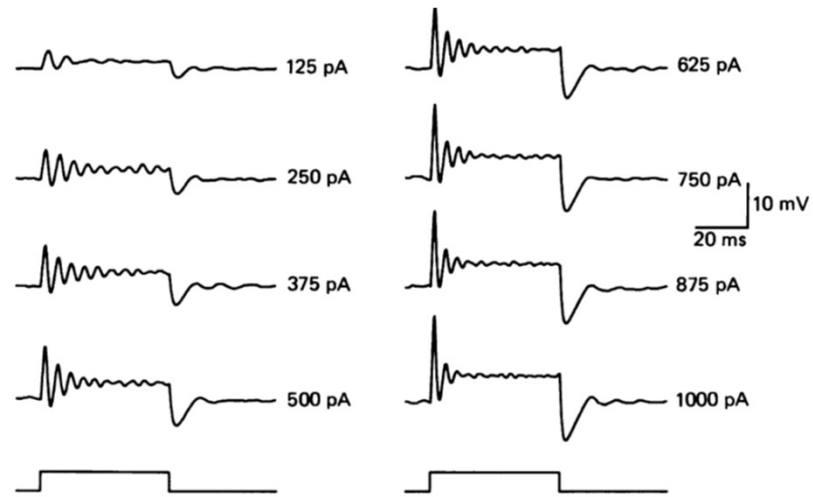
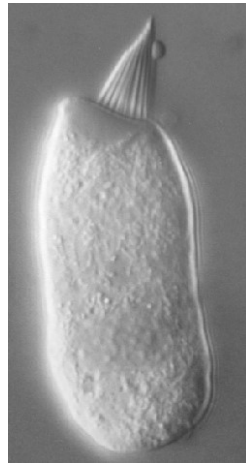


DRG 11175, ISSUE 1.

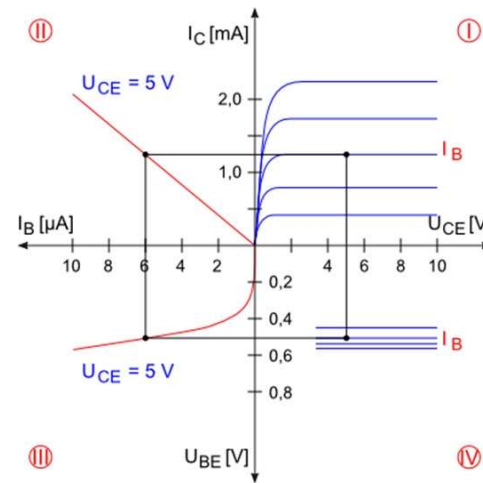
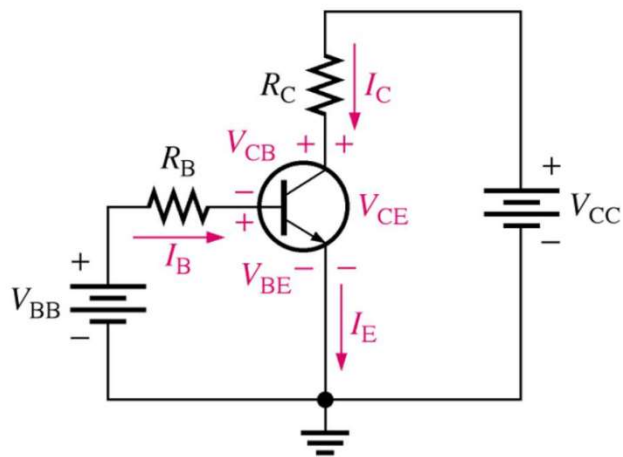
THE VOLTAGE AND CURRENT MEASUREMENTS SHOWN ARE APPROXIMATE, AND ARE ONLY PROVIDED AS A GUIDE. ALLOWANCE SHOULD BE MADE FOR THE LOADING EFFECTS OF A VOLTMETER.

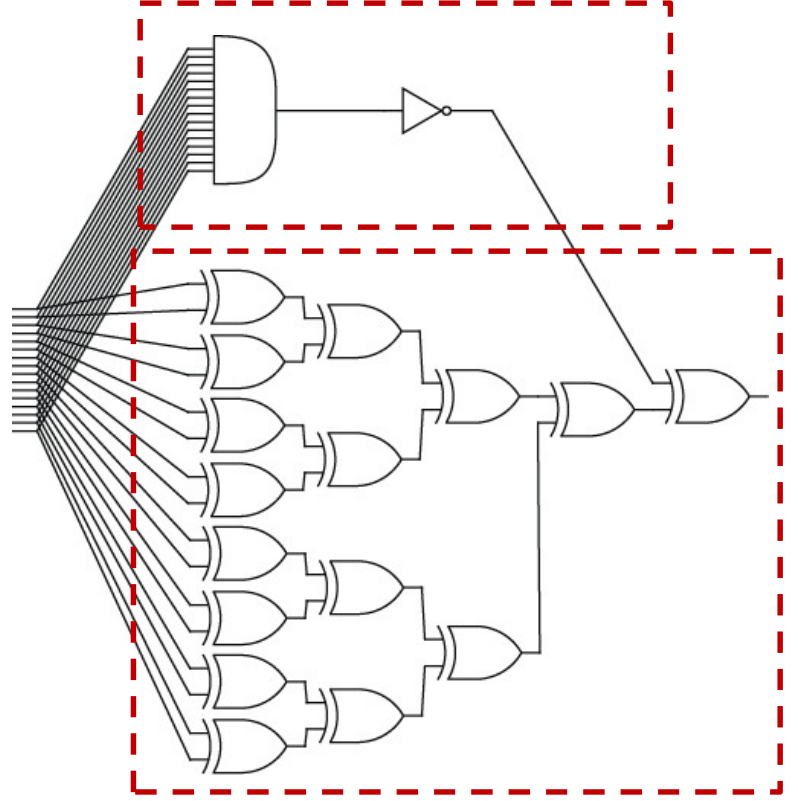
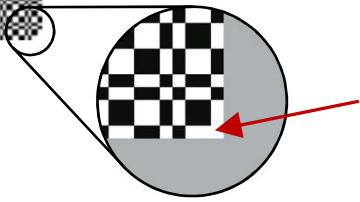
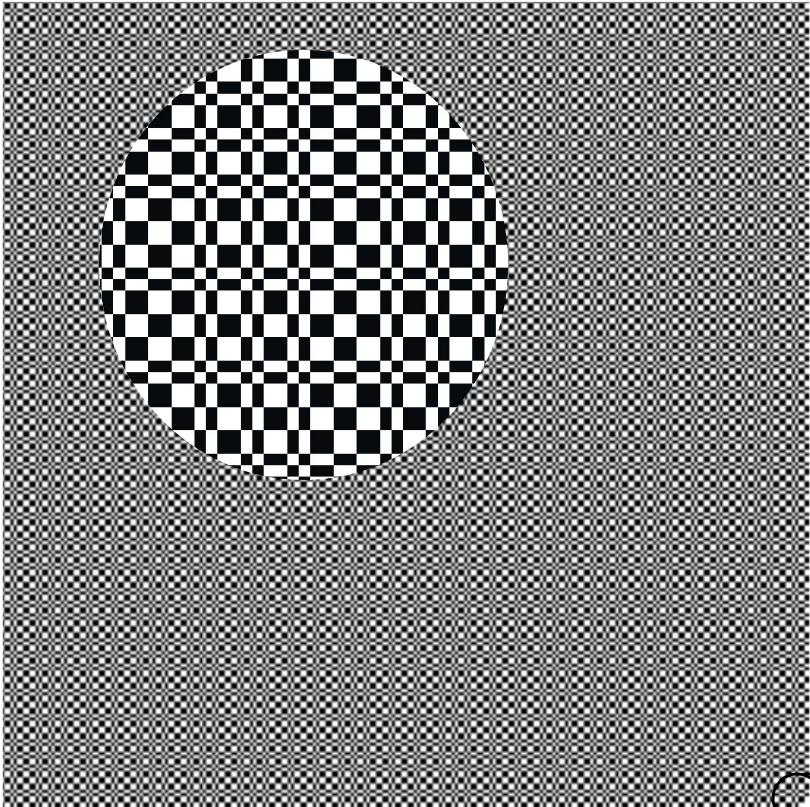
<http://www.geocities.com/ResearchTriangle/Lab/6722/quadiicrb.html>

Component properties are essential



Hudspeth and Lewis 1988





Phil. Trans. R. Soc. Lond. B 314, 1-340 (1986)
Printed in Great Britain

[1]

THE STRUCTURE OF THE NERVOUS SYSTEM OF THE NEMATODE *CAENORHABDITIS ELEGANS*

BY J. G. WHITE, E. SOUTHGATE, J. N. THOMSON
AND S. BRENNER, F.R.S.

*Laboratory of Molecular Biology, Medical Research Council Centre, Hills Road,
Cambridge CB2 2QH, U.K.*

(Received 9 August 1984 - Revised 12 November 1984)

1984

1979

THREE-DIMENSIONAL COMPUTER RECONSTRUCTION OF NEURONS AND NEURONAL ASSEMBLIES

E. R. Macagno, C. Levinthal, and I. Sobel
Department of Biological Sciences, Columbia University, New York, New York
10027

◆9136

1975

Three-Dimensional Reconstruction from Serial Sections

RANDLE W. WARE
*California Institute of Technology
Pasadena, California*

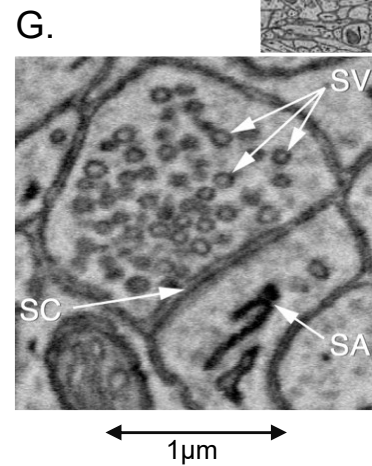
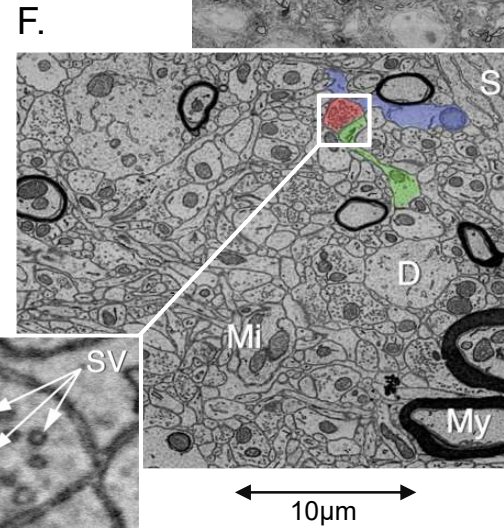
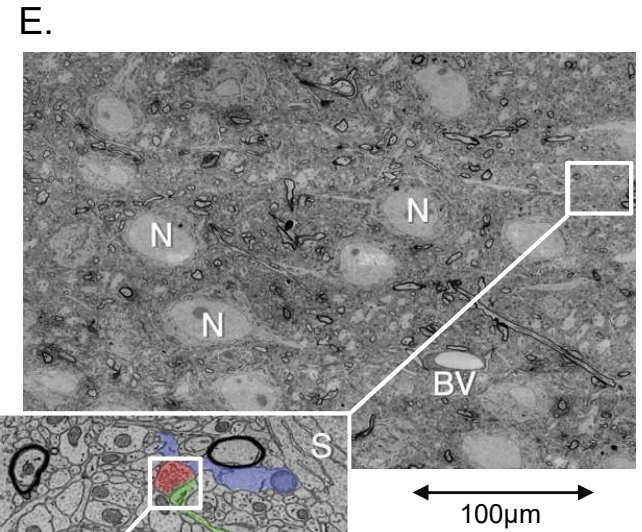
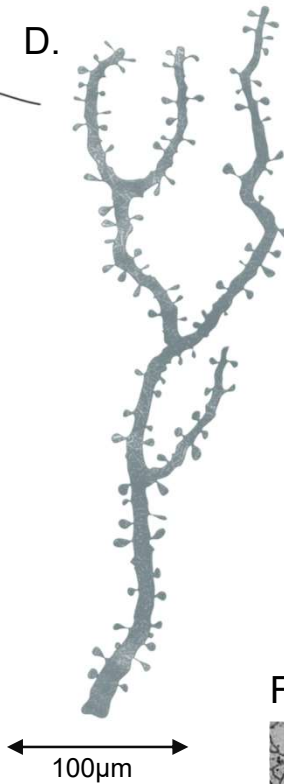
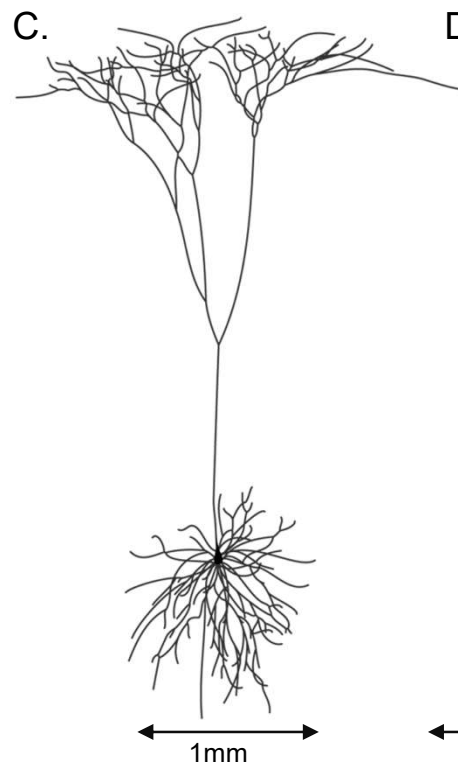
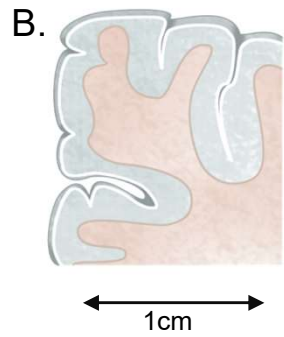
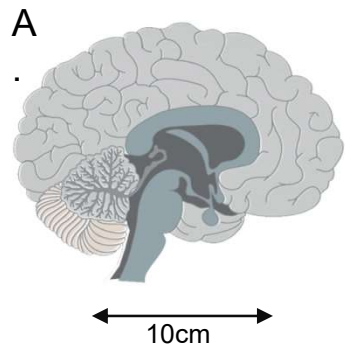
AND

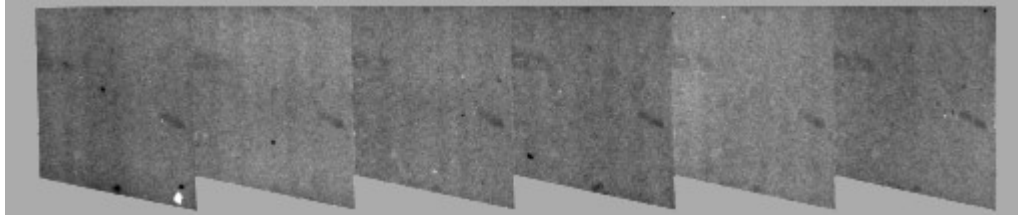
VINCENT LOPRESTI
Columbia University, New York, New York

Three Dimensional Reconstruction from Serial Sections

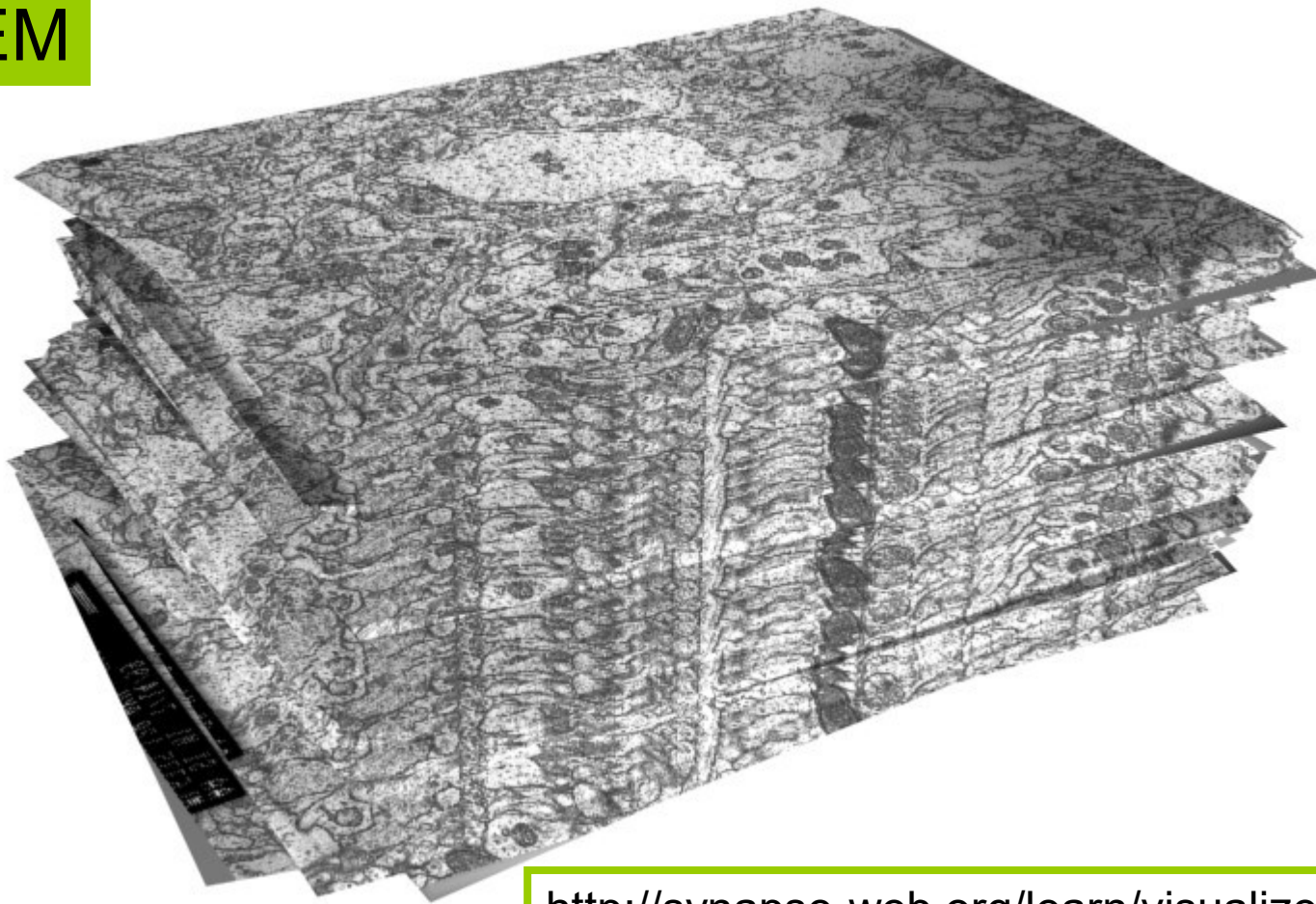
CYRUS LEVINTHAL & RANDLE WARE*
Department of Biological Sciences, Columbia University, New York, NY 10027

1972

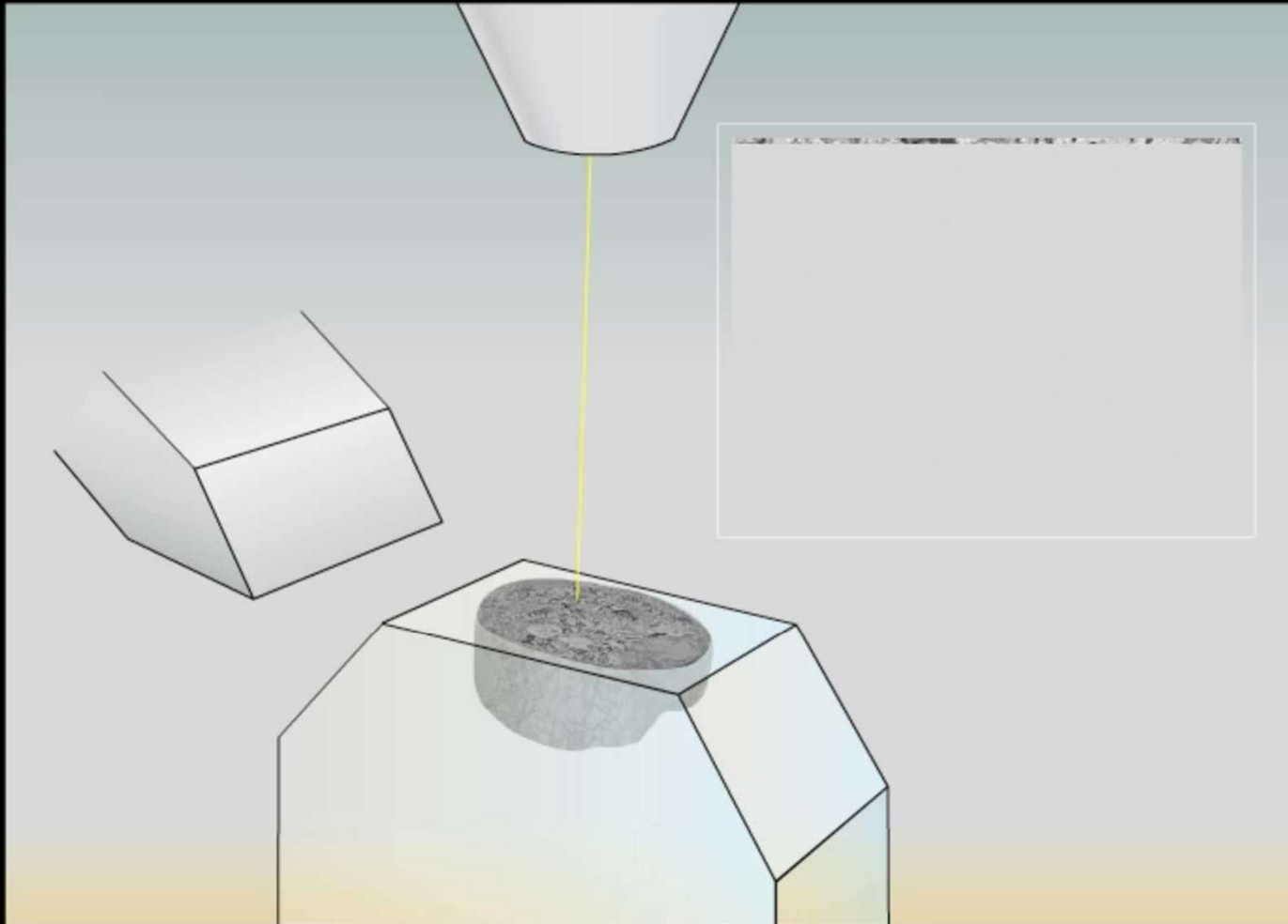




ssTEM



<http://synapse-web.org/learn/visualize/serial.stm>





EM contrast is provided by highly charged (heavy) nuclei

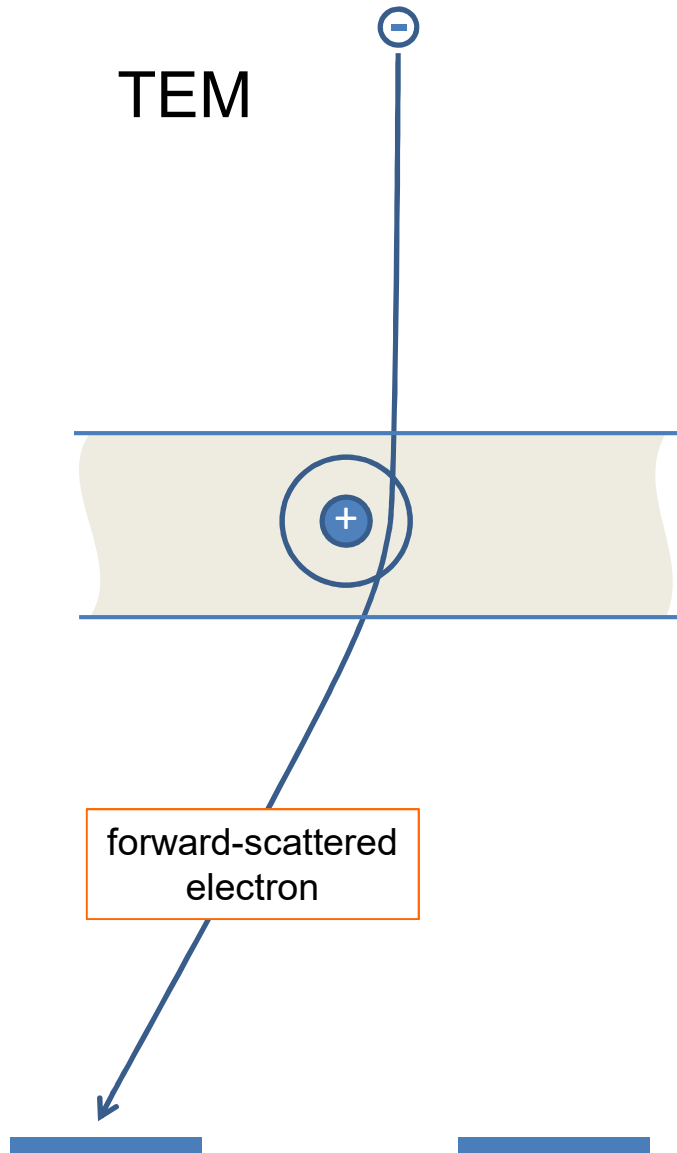
Tissue

Stains

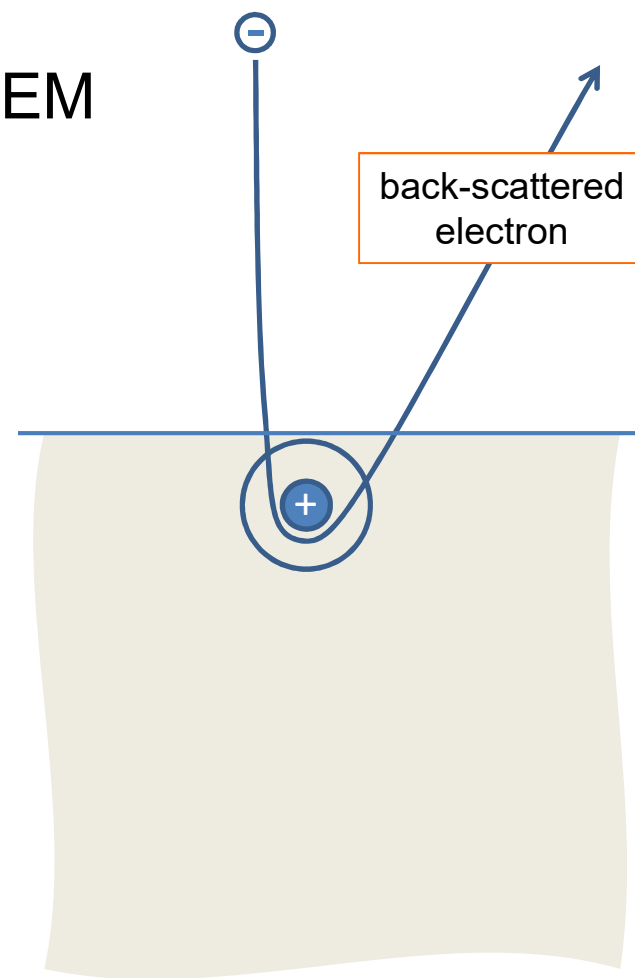
hydrogen 1 H 1.0079																	helium 2 He 4.0026						
lithium 3 Li 6.941	beryllium 4 Be 9.0122																	boron 5 B 10.81	carbon 6 C 12.011	nitrogen 7 N 14.007	oxygen 8 O 15.999	fluorine 9 F 18.998	neon 10 Ne 20.180
sodium 11 Na 22.990	magnesium 12 Mg 24.305																	aluminum 13 Al 26.982	silicon 14 Si 28.086	phosphorus 15 P 30.974	sulfur 16 S 32.065	chlorine 17 Cl 35.453	argon 18 Ar 39.948
potassium 19 K 39.098	calcium 20 Ca 40.078	scandium 21 Sc 44.956	titanium 22 Ti 47.867	vanadium 23 V 50.942	chromium 24 Cr 51.996	manganese 25 Mn 54.938	iron 26 Fe 55.845	cobalt 27 Co 58.933	nickel 28 Ni 58.693	copper 29 Cu 63.546	zinc 30 Zn 65.39	gallium 31 Ga 69.723	germanium 32 Ge 72.61	arsenic 33 As 74.922	selenium 34 Se 78.96	bromine 35 Br 79.904	krypton 36 Kr 83.80						
rubidium 37 Rb 85.468	strontium 38 Sr 87.62	yttrium 39 Y 88.906	zirconium 40 Zr 91.224	niobium 41 Nb 92.906	molybdenum 42 Mo 95.94	technetium 43 Tc [98]	ruthenium 44 Ru 101.07	rhodium 45 Rh 102.91	palladium 46 Pd 106.42	silver 47 Ag 107.87	cadmium 48 Cd 112.41	indium 49 In 114.82	tin 50 Sn 118.71	antimony 51 Sb 121.76	tellurium 52 Te 127.60	iodine 53 I 126.90	xenon 54 Xe 131.29						
caesium 55 Cs 132.91	barium 56 Ba 137.33	* 57-70 lanthanide series	lutetium 71 Lu 174.97	hafnium 72 Hf 178.49	tantalum 73 Ta 180.95	tungsten 74 W 183.84	rhenium 75 Re 186.21	osmium 76 Os 190.23	iridium 77 Ir 192.22	platinum 78 Pt 195.08	gold 79 Au 196.97	mercury 80 Hg 200.59	thallium 81 Tl 204.38	lead 82 Pb 207.2	bismuth 83 Bi 208.98	polonium 84 Po [209]	astatine 85 At [210]	radon 86 Rn [222]					
francium 87 Fr [223]	radium 88 Ra [226]	** 89-102 actinide series	lawrencium 103 Lr [262]	rutherfordium 104 Rf [261]	dubnium 105 Db [262]	seaborgium 106 Sg [263]	bohrium 107 Bh [264]	hassium 108 Hs [269]	meitnerium 109 Mt [268]	ununnium 110 Uun [271]	ununium 111 Uuu [272]	unubium 112 Uub [277]	ununtrium 113 Uuq [289]	unquadrium 114 Uuq [289]									

lanthanum 57 La 138.91	cerium 58 Ce 140.12	praseodymium 59 Pr 140.91	neodymium 60 Nd 144.24	promethium 61 Pm [145]	samarium 62 Sm 150.36	europium 63 Eu 151.96	gadolinium 64 Gd 157.25	terbium 65 Tb 158.93	dysprosium 66 Dy 162.50	holmium 67 Ho 164.93	erbium 68 Er 167.26	thulium 69 Tm 168.93	ytterbium 70 Yb 173.04
actinium 89 Ac [227]	thorium 90 Th 232.04	protactinium 91 Pa 231.04	uranium 92 U 238.03	neptunium 93 Np [237]	plutonium 94 Pu [244]	americium 95 Am [243]	curium 96 Cm [247]	berkelium 97 Bk [247]	californium 98 Cf [251]	einsteinium 99 Es [252]	fermium 100 Fm [257]	mendelevium 101 Md [258]	nobelium 102 No [259]

TEM

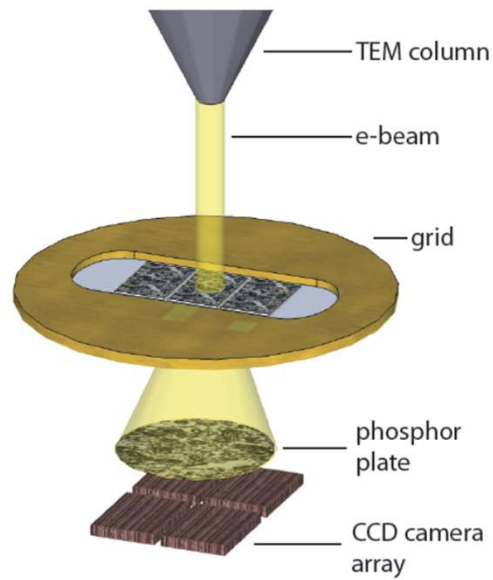
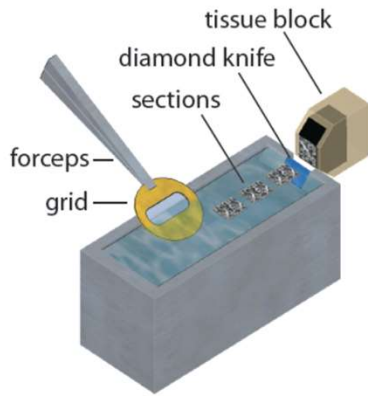


SEM

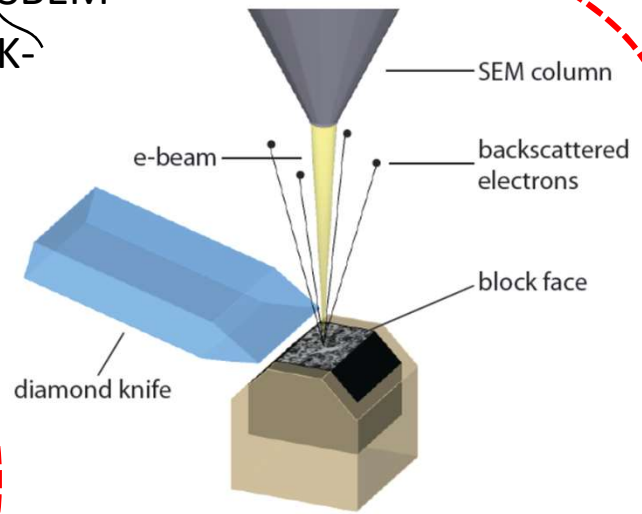


3D-EM Techniques

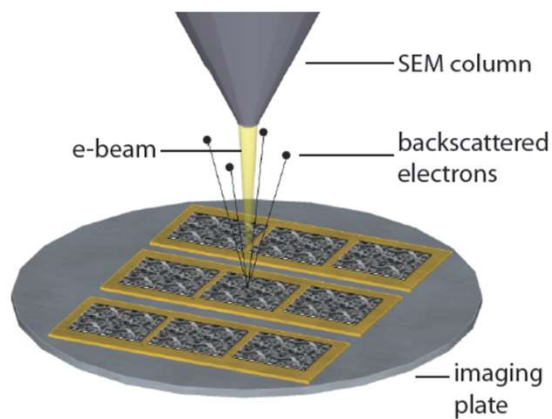
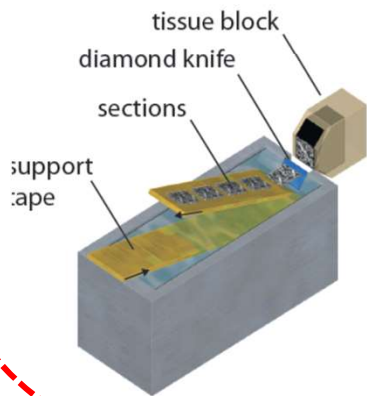
ssSTEMCA



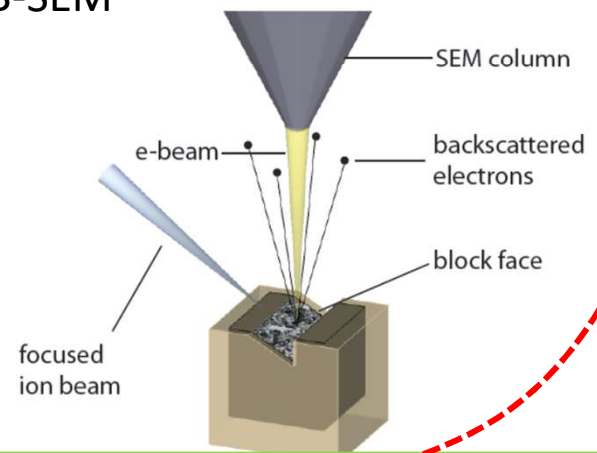
SBEM DiK-

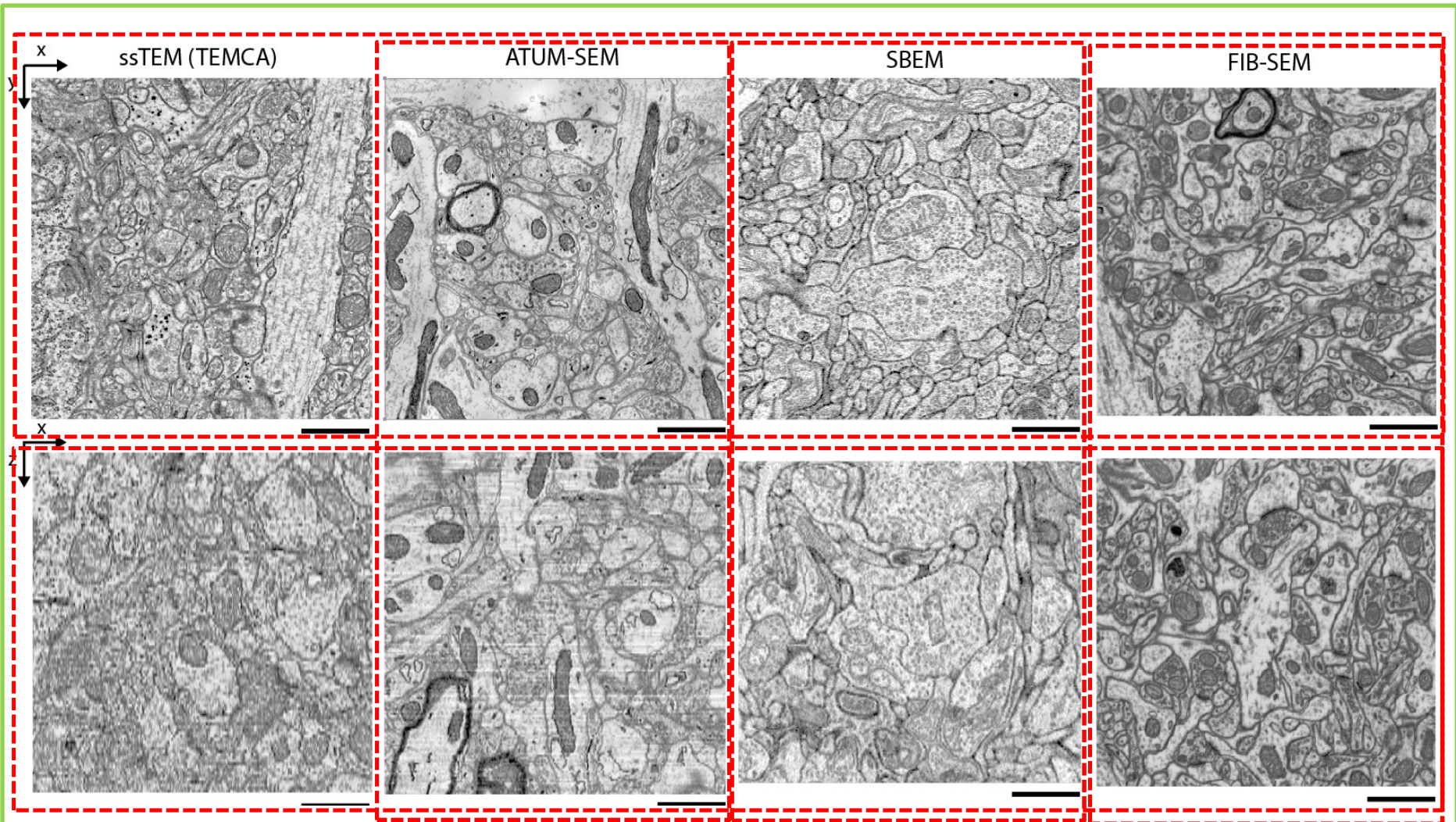


AT(L)UM



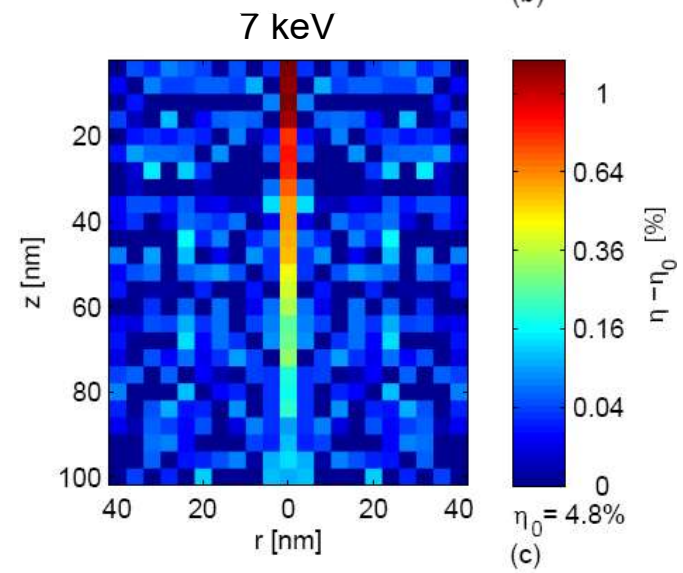
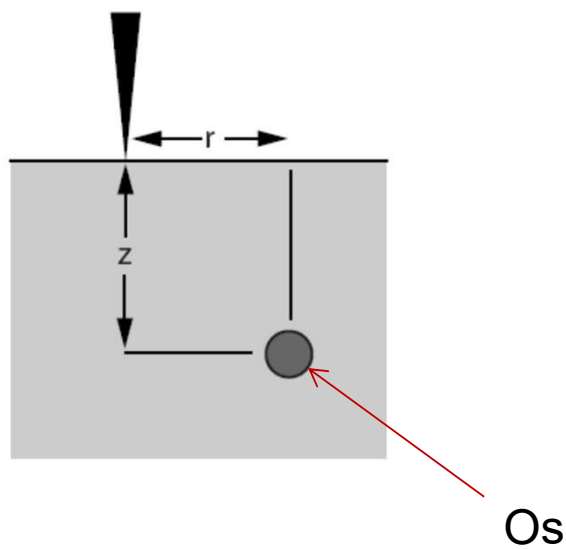
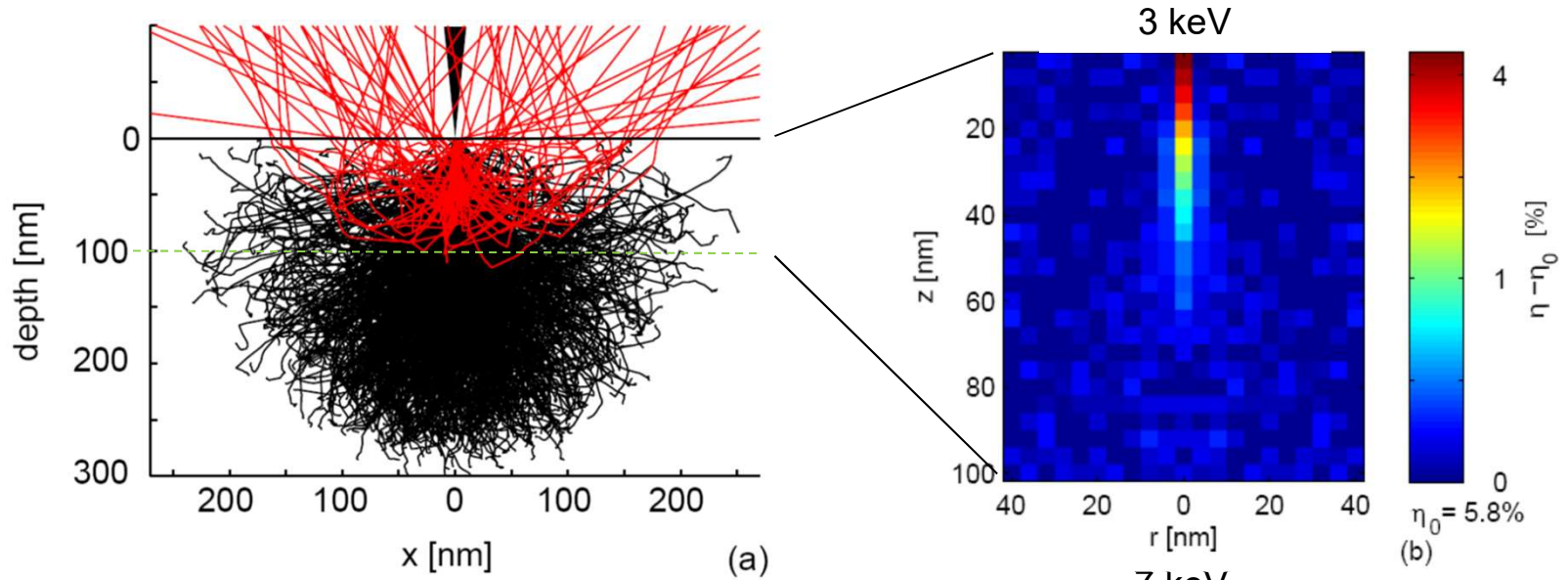
FIB-SEM





A) ssTEMCA: mouse visual cortex at $4 \times 4 \times 45 \text{ nm}^3$. B) ATUM-SEM: Mouse cortex at $3 \times 3 \times 29 \text{ nm}^3$. C) SBEM: mouse retina at $12 \times 12 \times 25 \text{ nm}^3$. D) FIB-SEM: cortex at $5 \times 5 \times 5 \text{ nm}^3$.
 Images by: D. Bock (A), K. Hayworth, J. Lichtman (B), K. Briggman (C), and G. Knott (D).

Monte-Carlo simulations yield point-spread functions for block-face imaging



BACKSCATTERING COEFFICIENTS FOR LOW ENERGY ELECTRONS

A.M.D. Assa'd and M.M. El Gomati*

The Department of Electronics, University of York, York YO1 5DD, U.K.

(Received for publication August 6, 1996 and in revised form December 9, 1996)

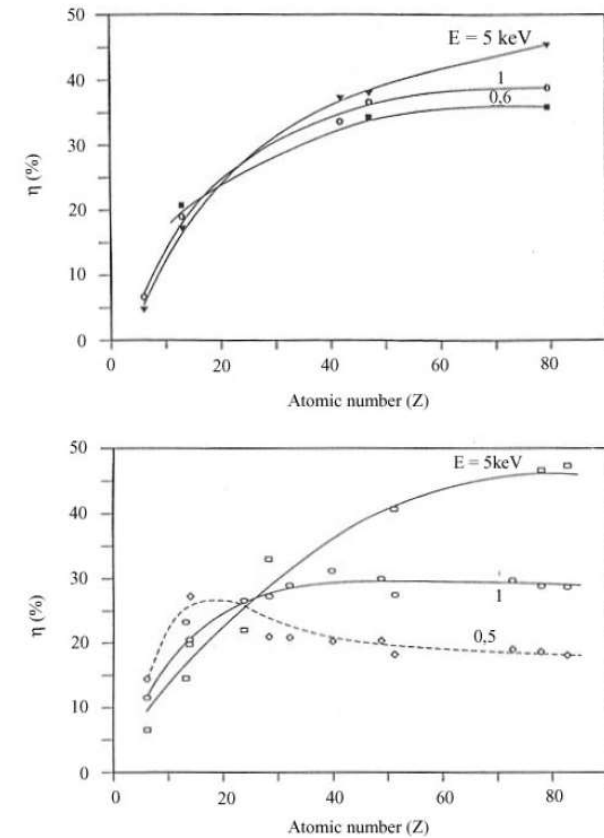
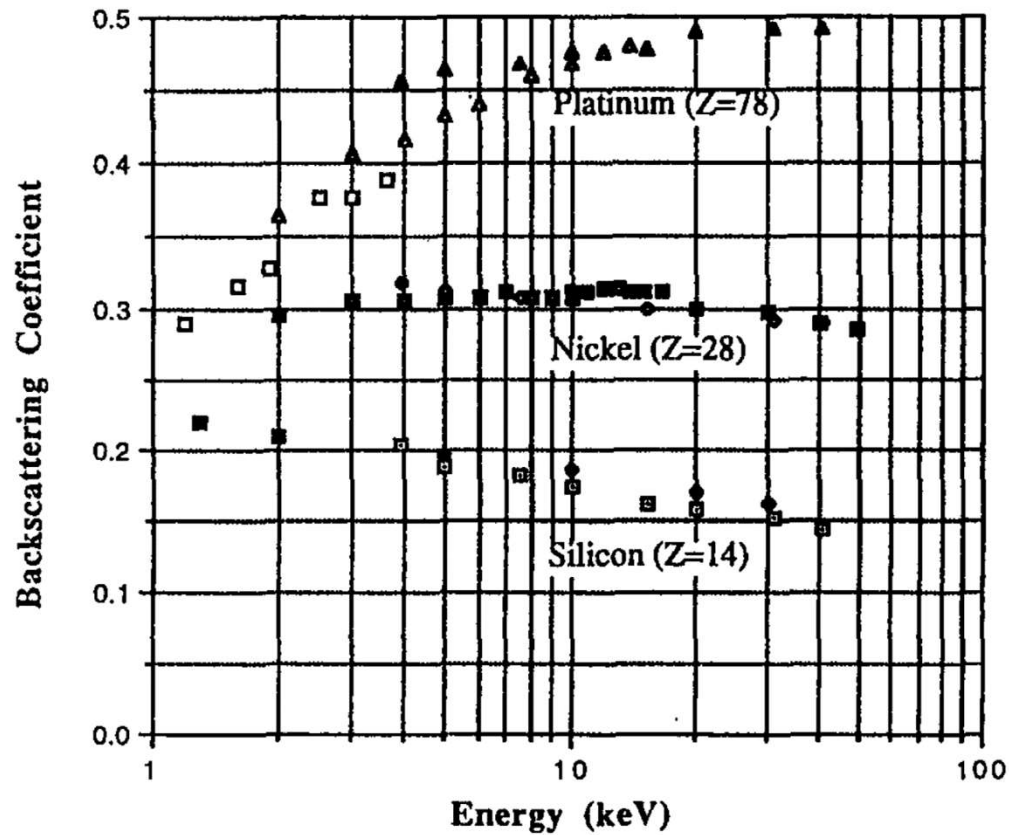
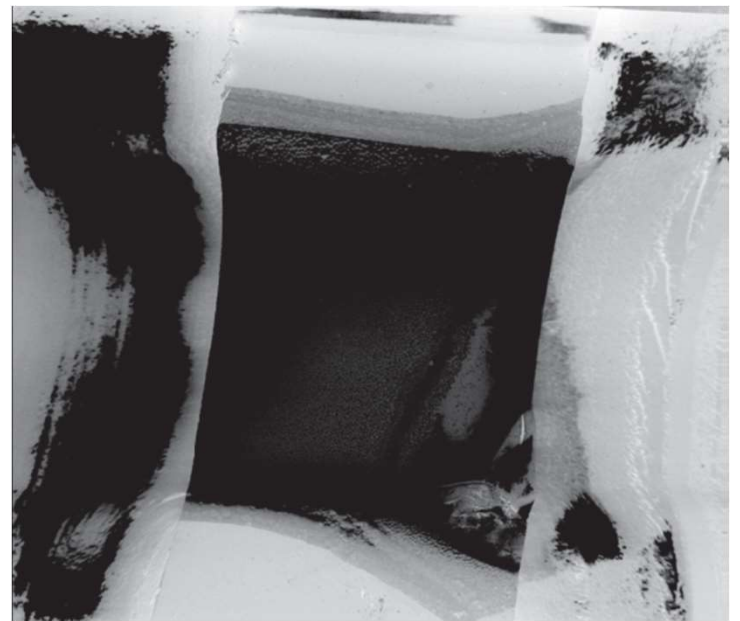
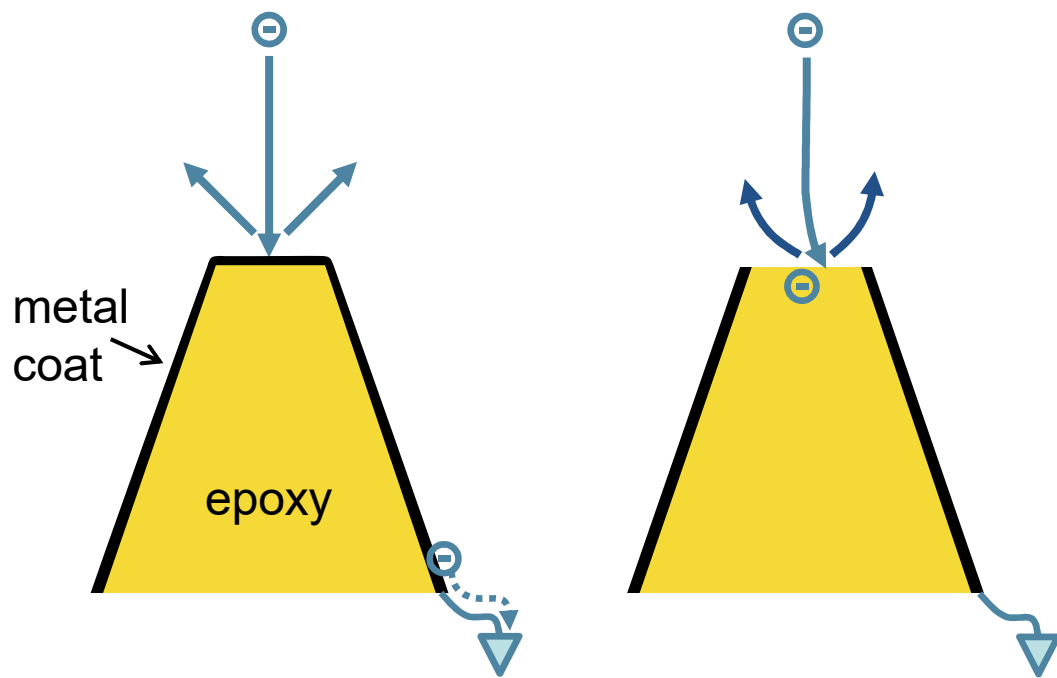


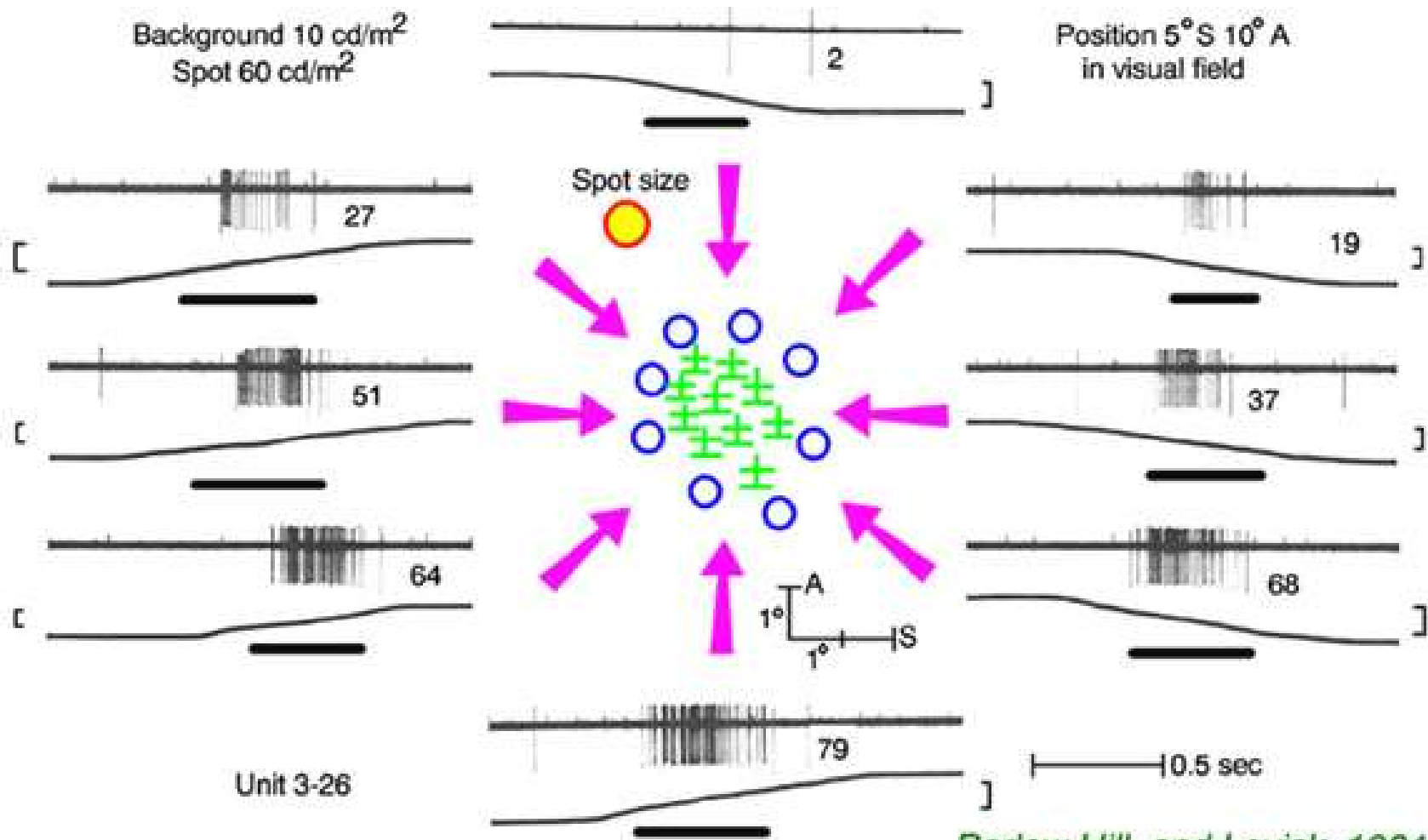
Figure 4. The backscattered electron coefficient as a function of the atomic number for different electron beam energies (a) for Ar ion cleaned surfaces, (b) as inserted from Bongeler *et al.* (1993).



~100 μ m

Background 10 cd/m^2
Spot 60 cd/m^2

Position $5^\circ \text{ S } 10^\circ \text{ A}$
in visual field

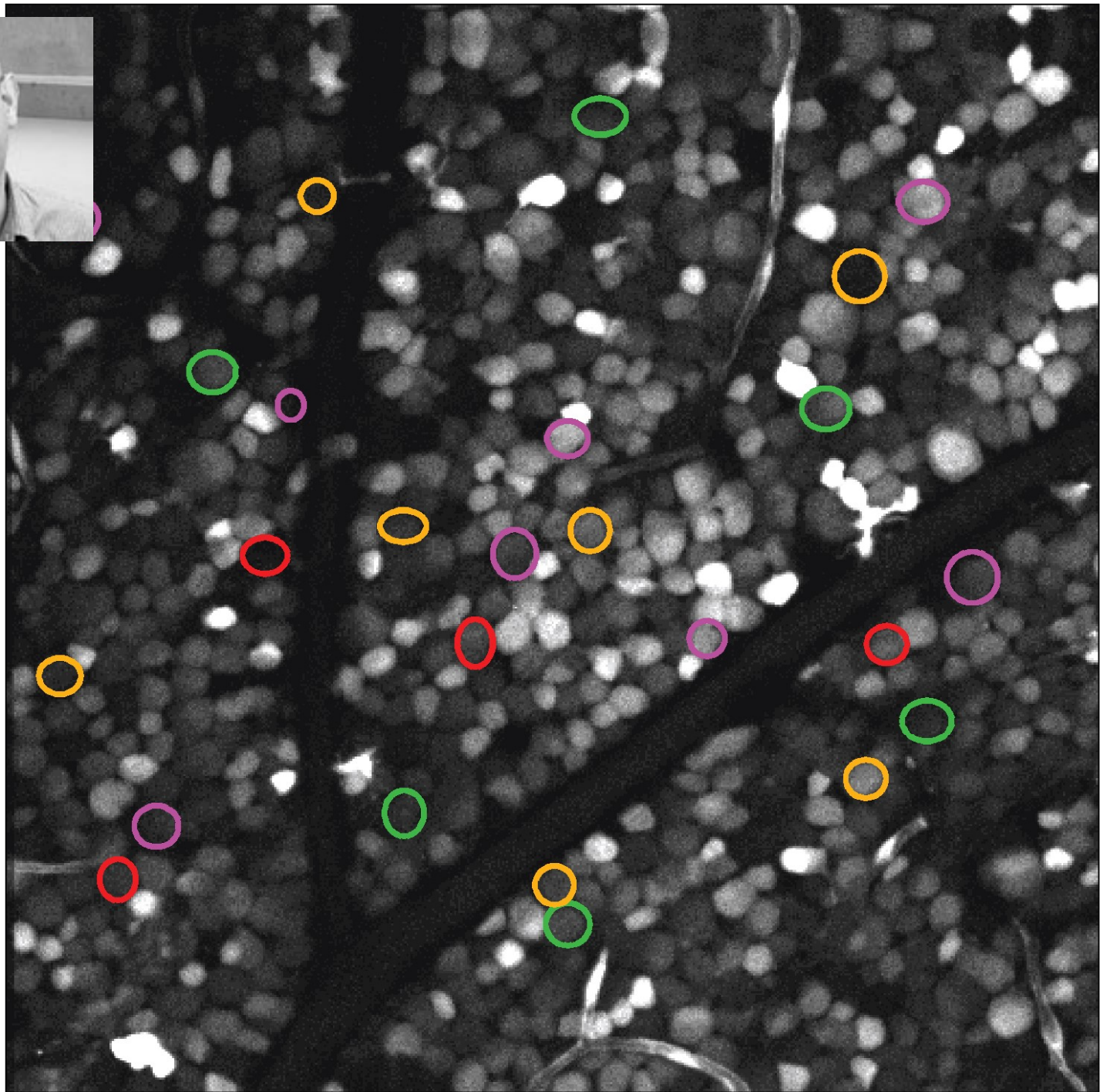


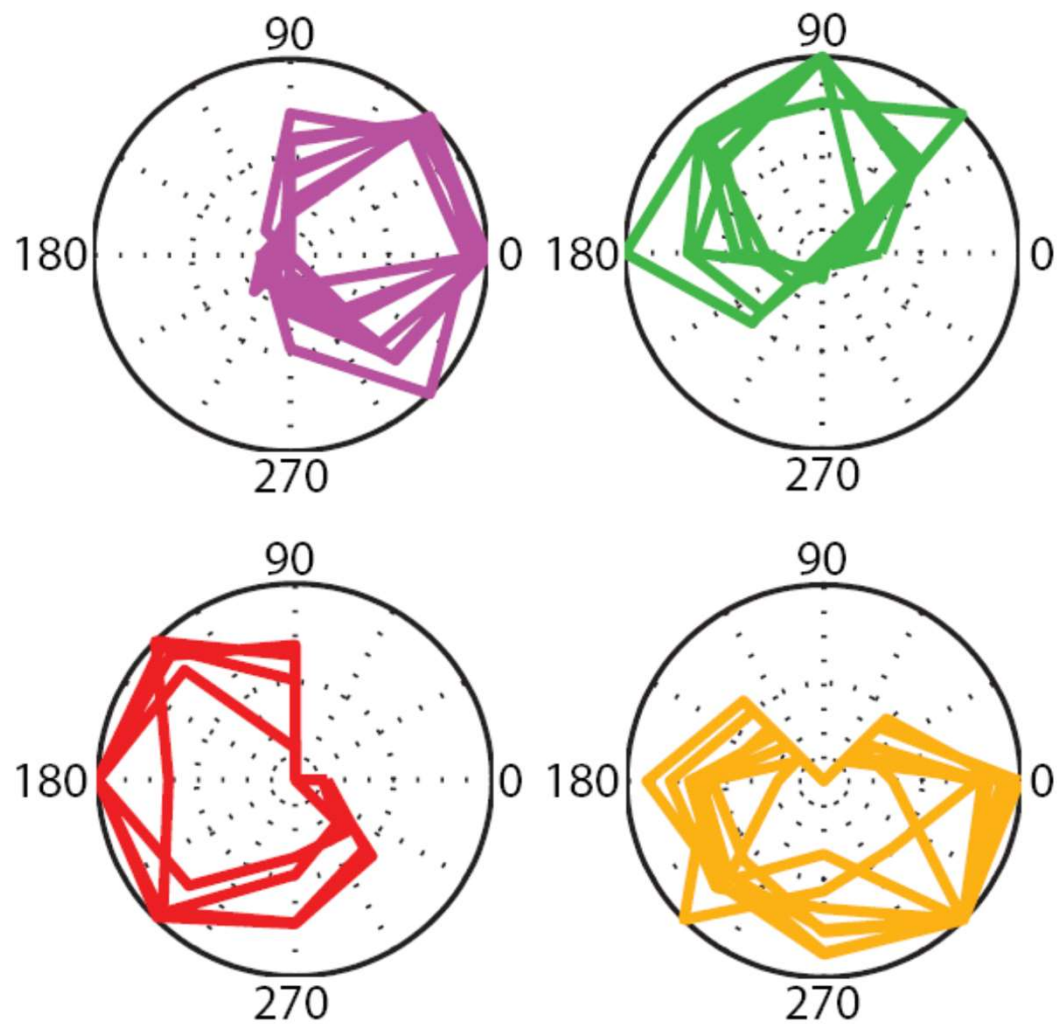
Unit 3-26

Barlow, Hill, and Levick, 1964

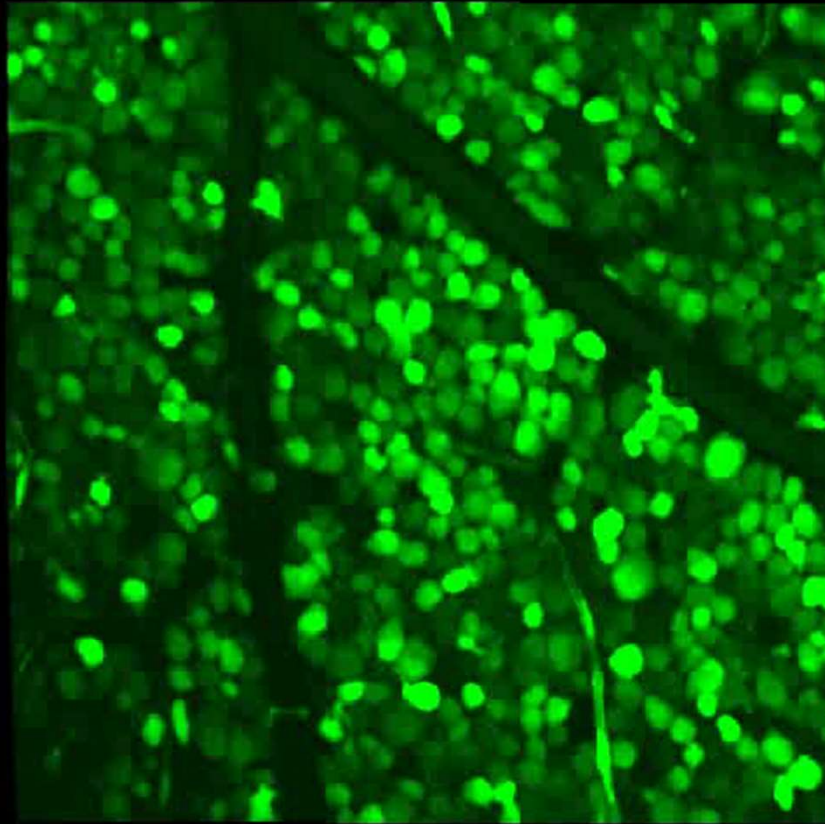


Kevin
Briggman

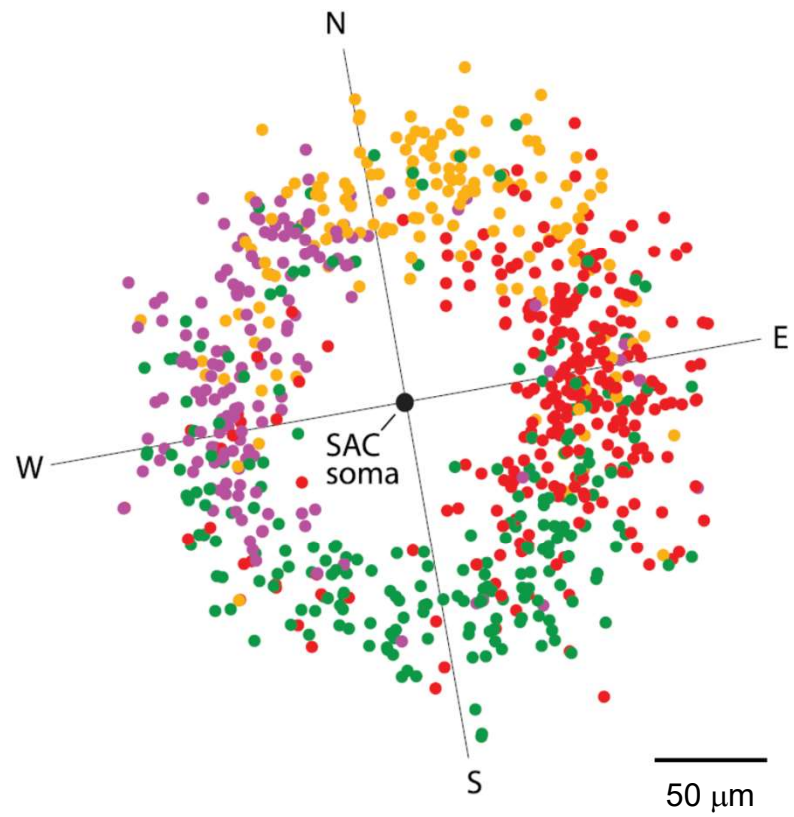
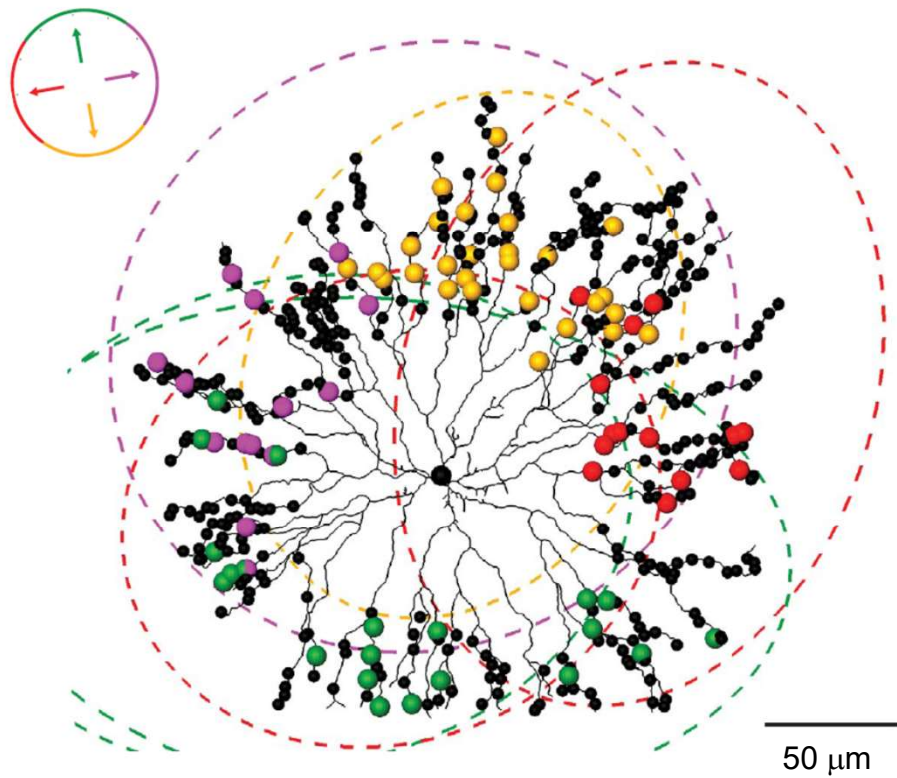




Kevin Briggman

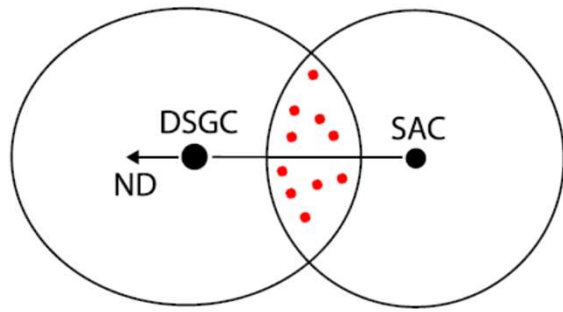


Kevin Briggman

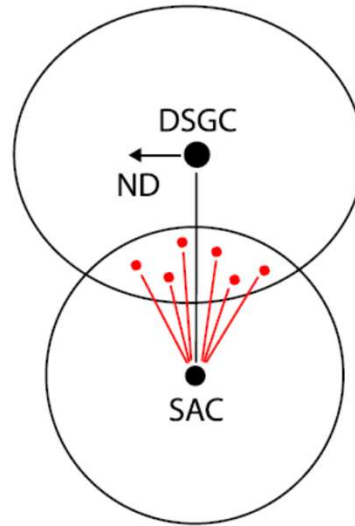


Briggman et al. 2011

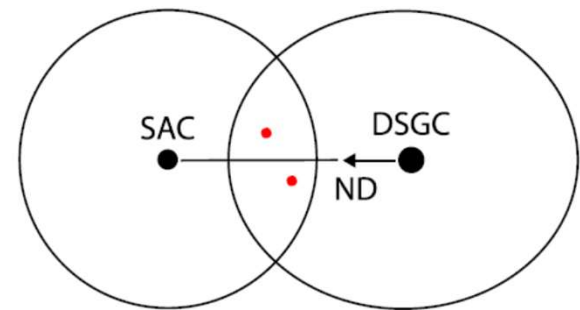
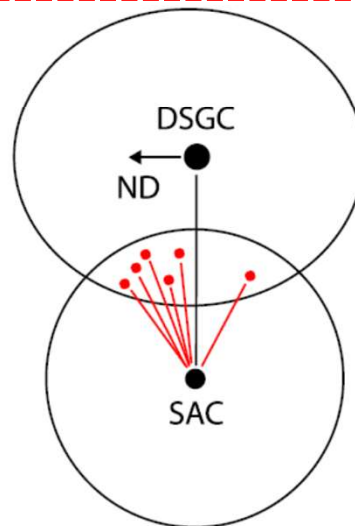
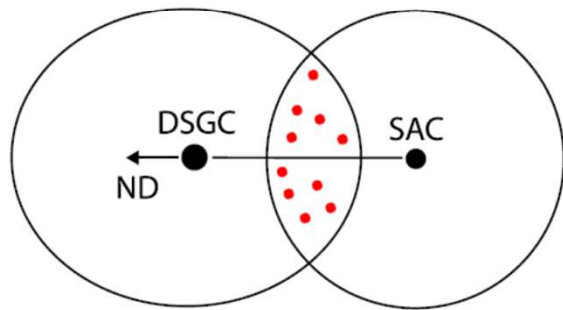
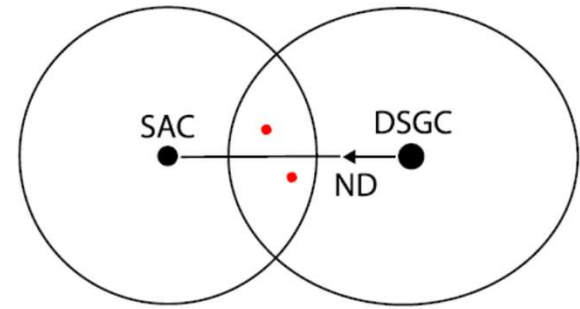
$$(\theta_{\text{soma}} - \theta_{\text{ND}}) = 0^\circ$$

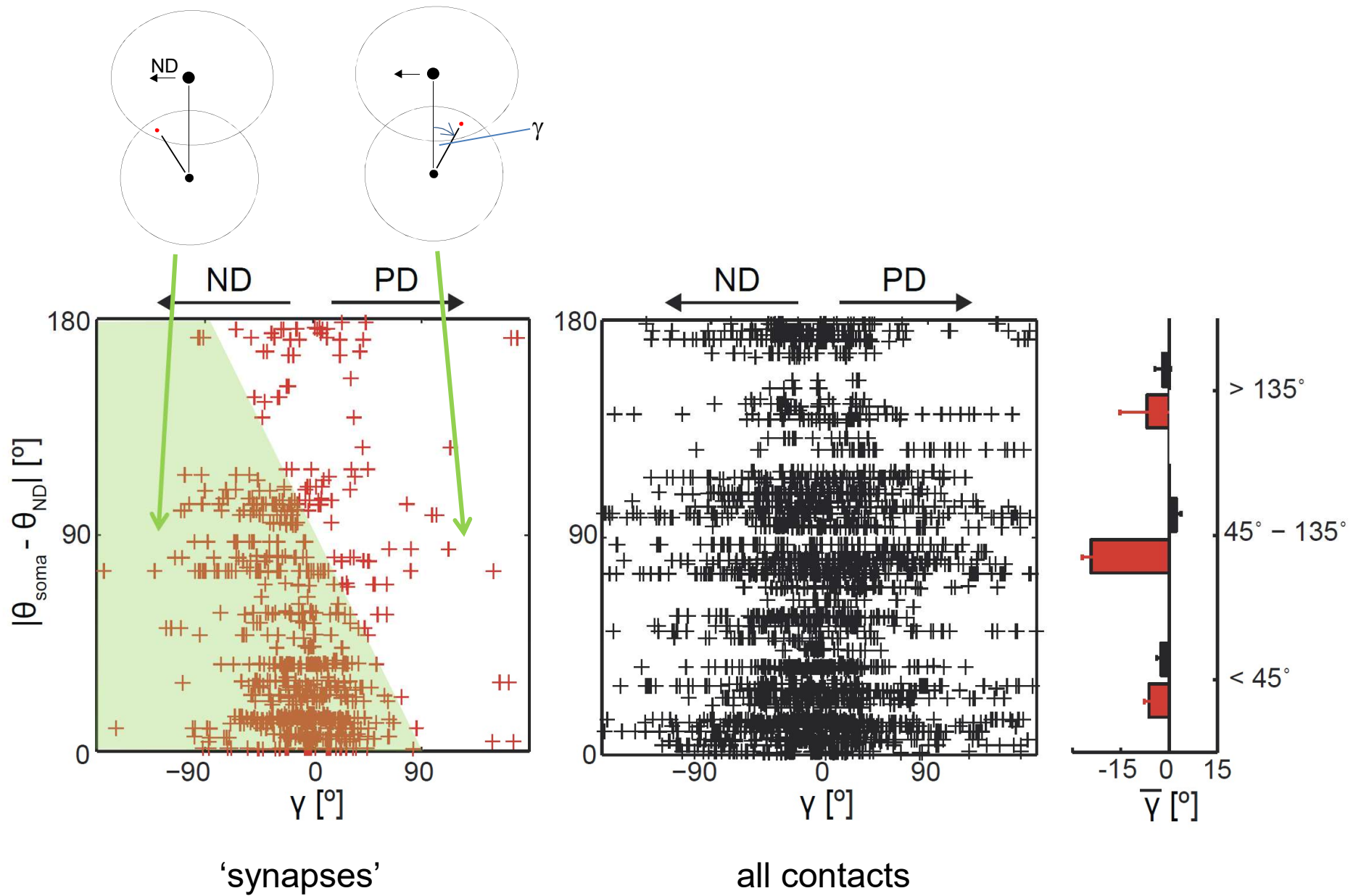


$$(\theta_{\text{soma}} - \theta_{\text{ND}}) = 90^\circ$$



$$(\theta_{\text{soma}} - \theta_{\text{ND}}) = 180^\circ$$



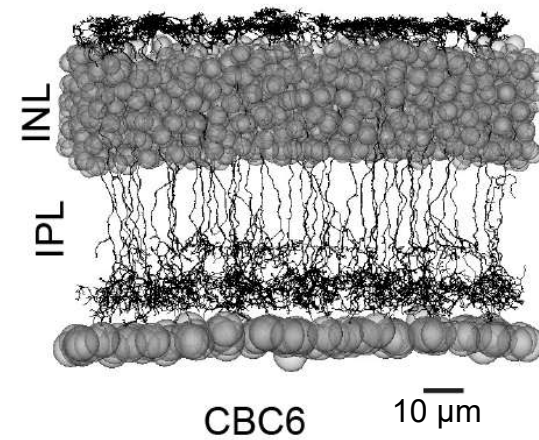
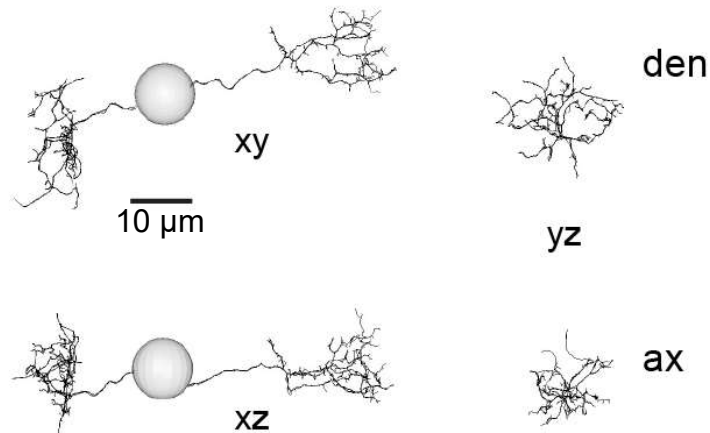
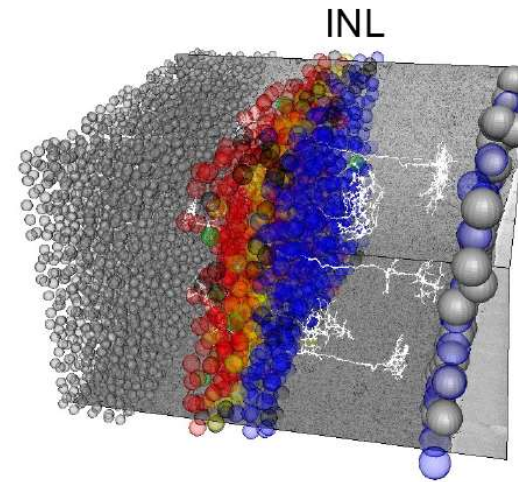
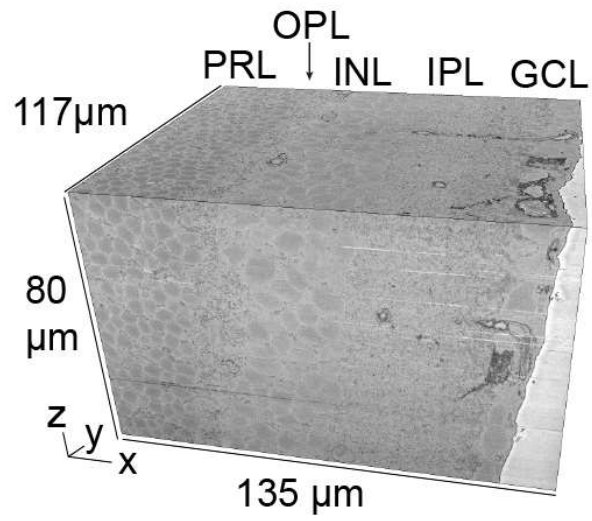


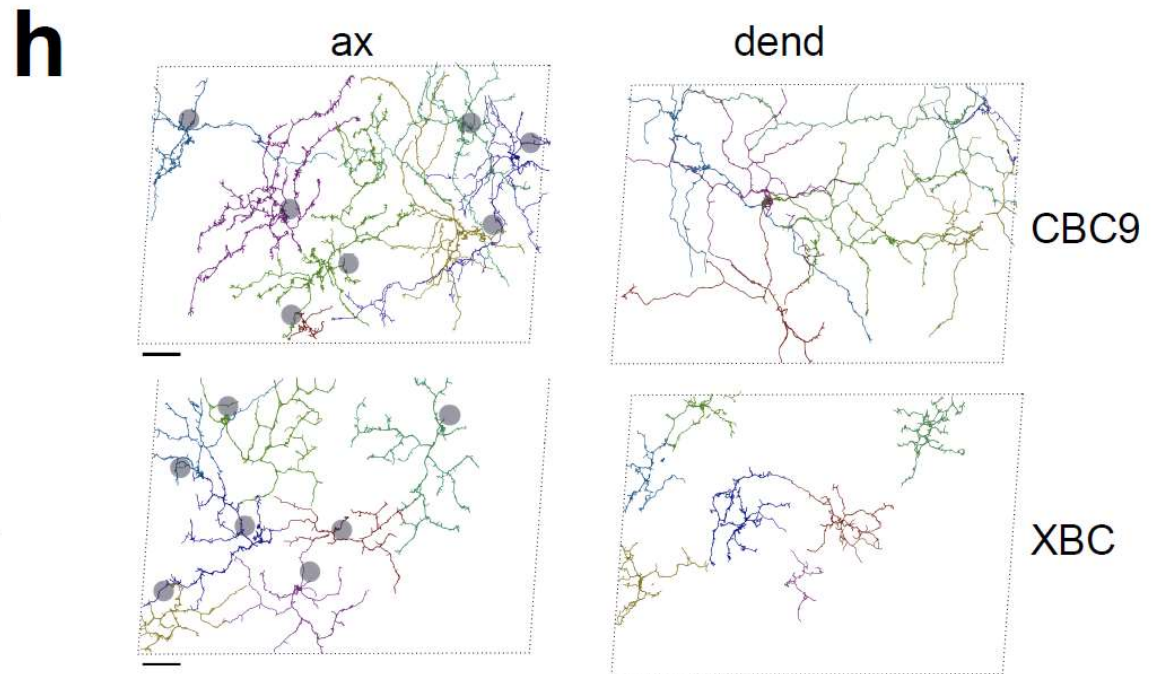
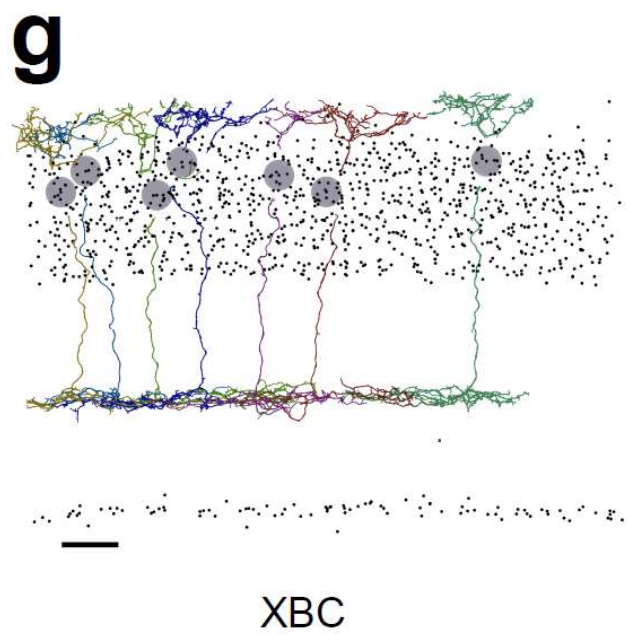
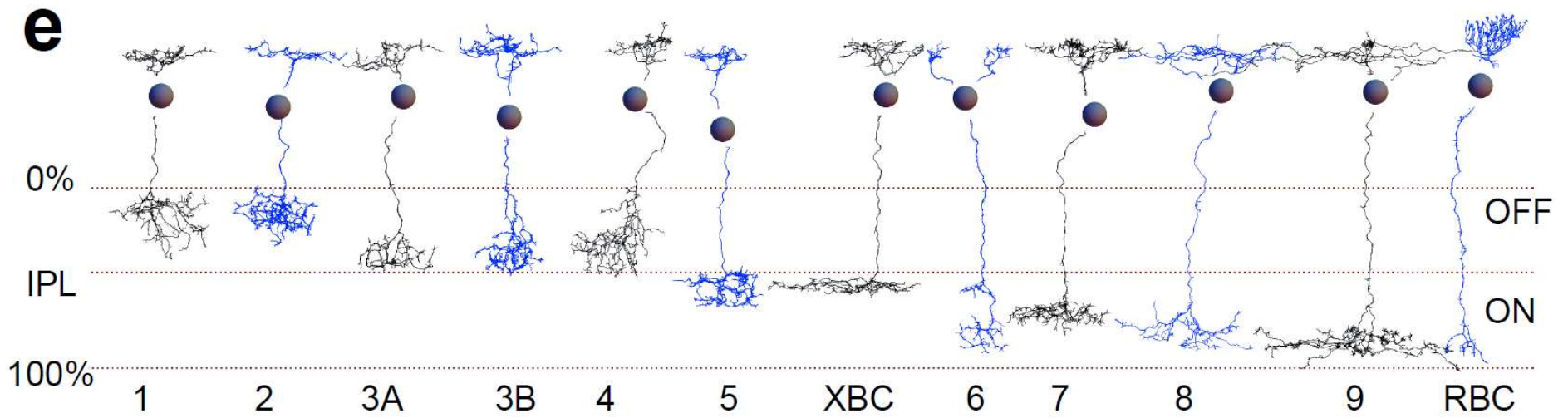
Briggman et al. 2011

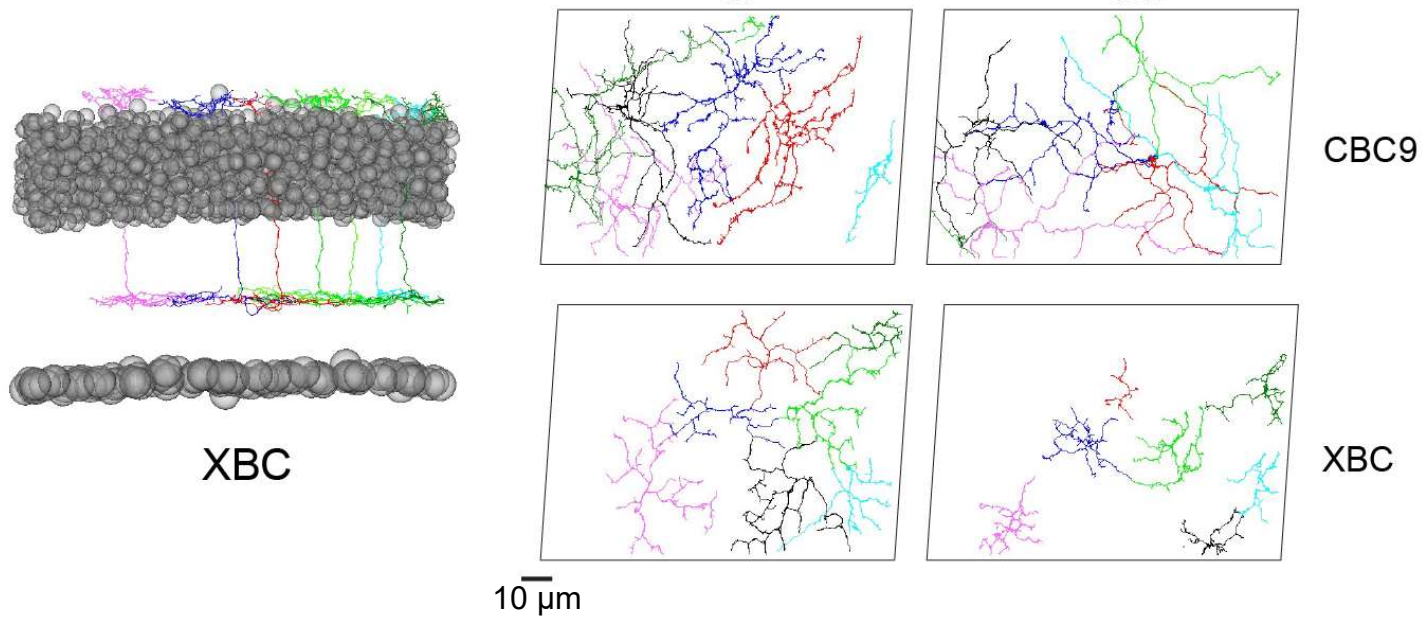
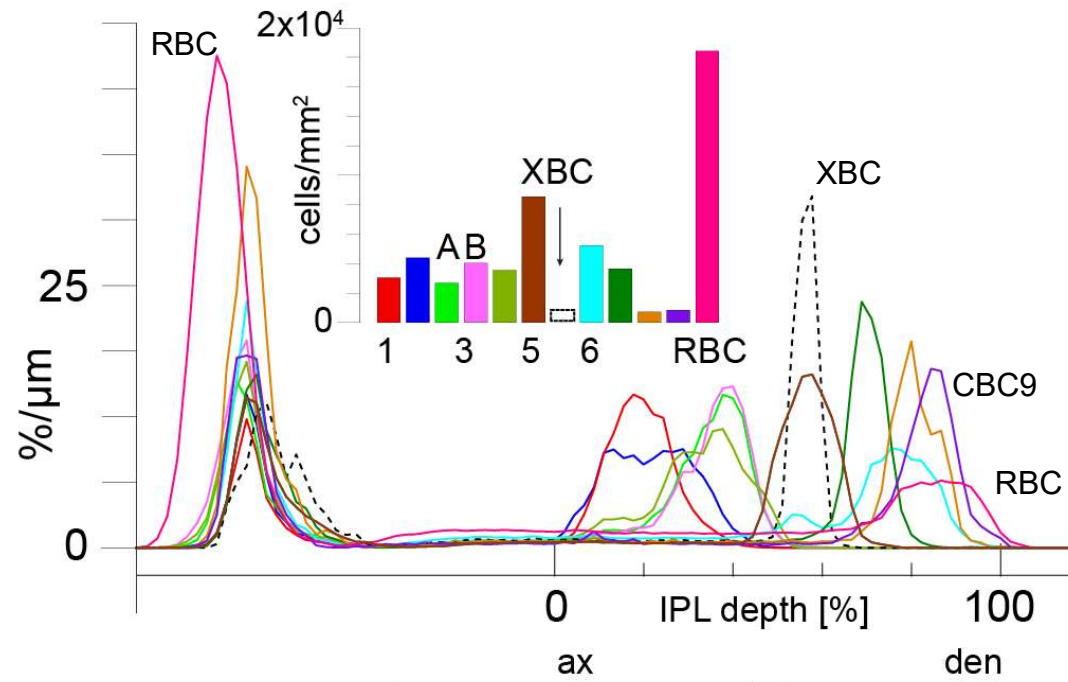
“Connectomics”...



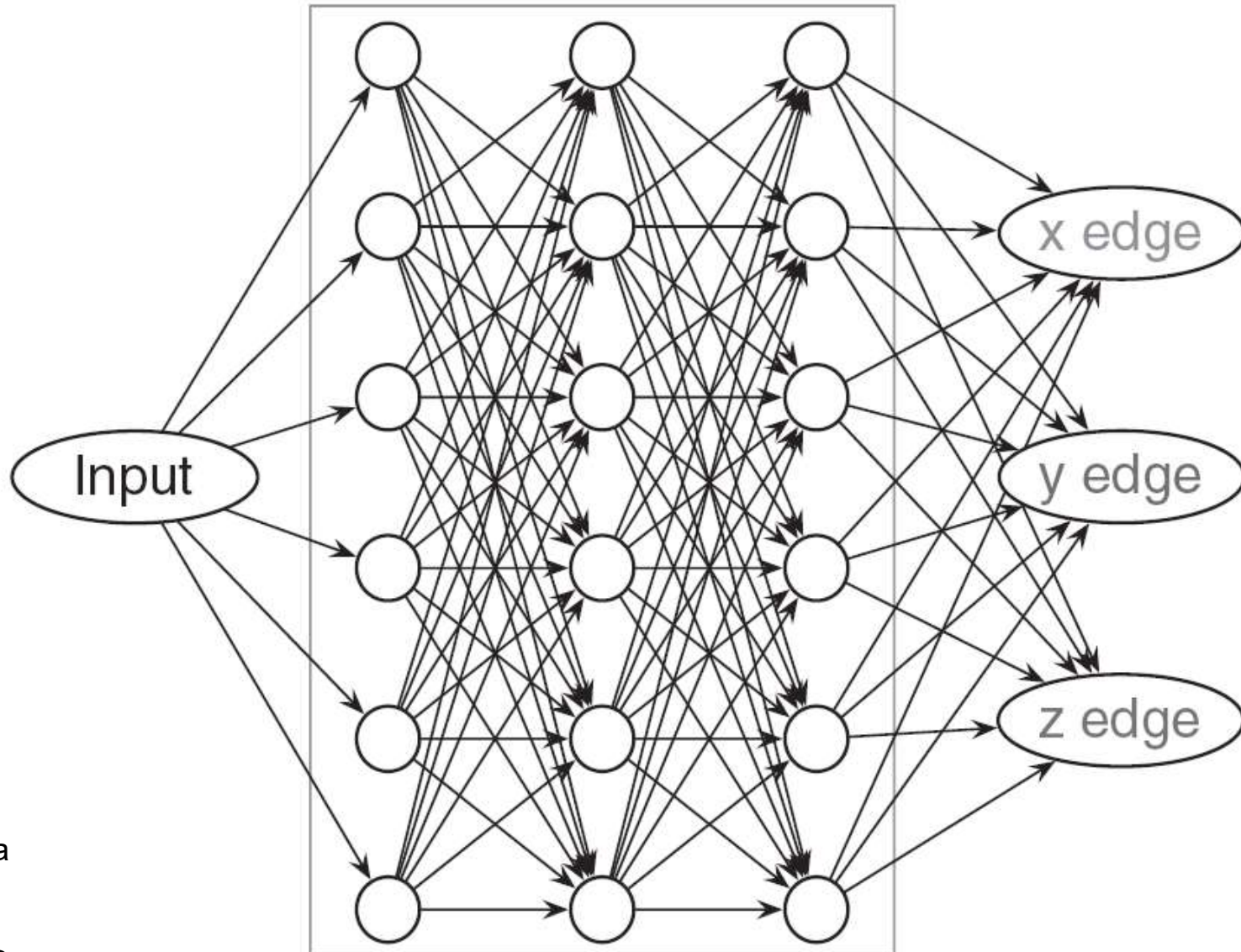
Moritz
Helmstaedter



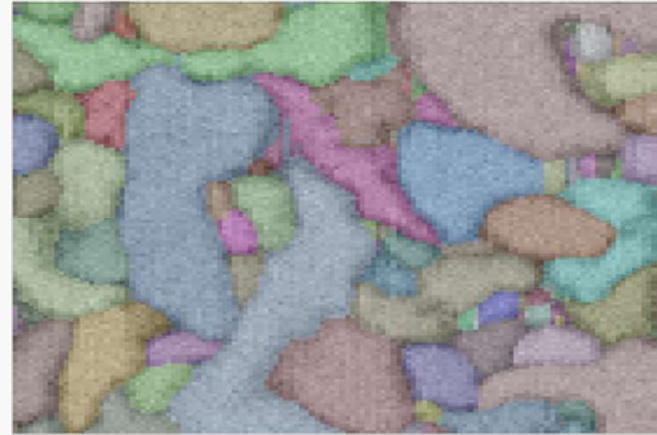
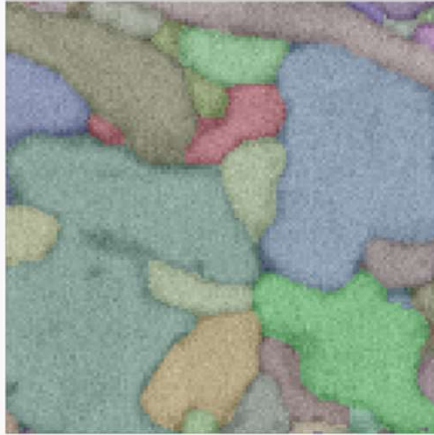




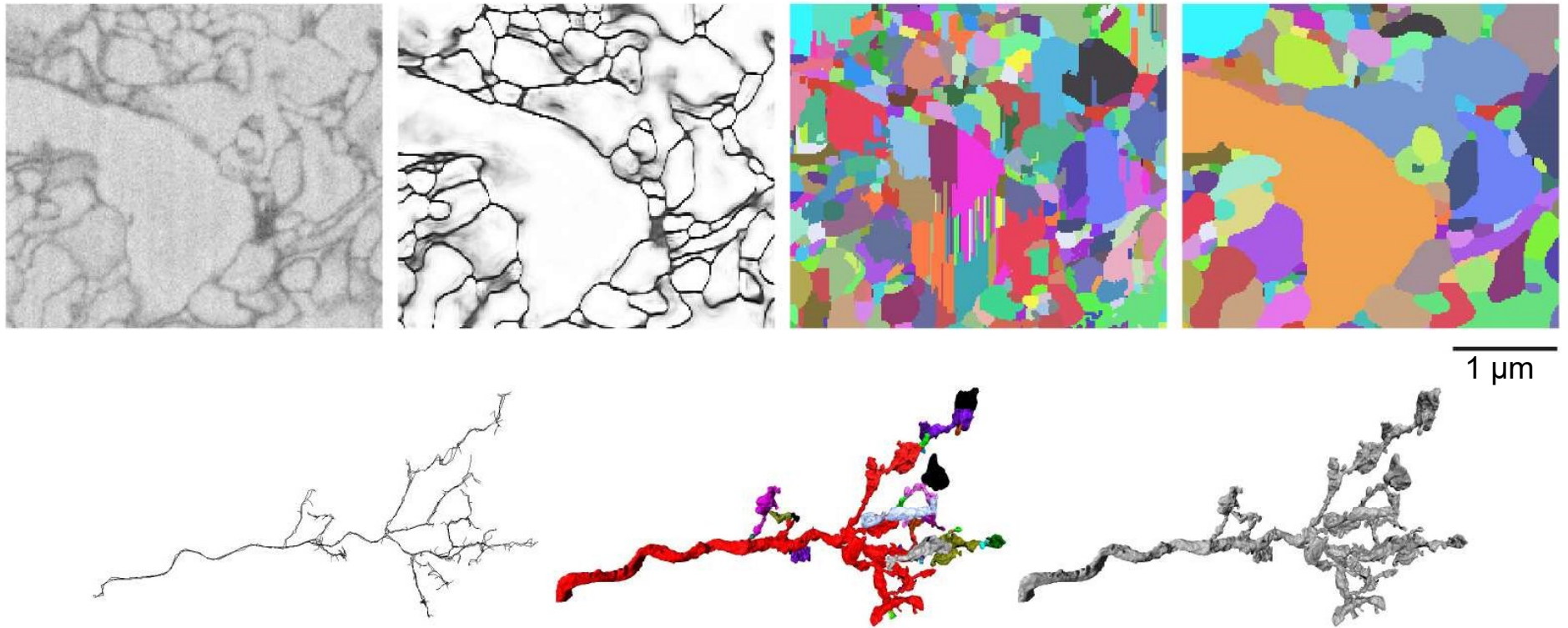
3 Hidden Layers
all nodes shown



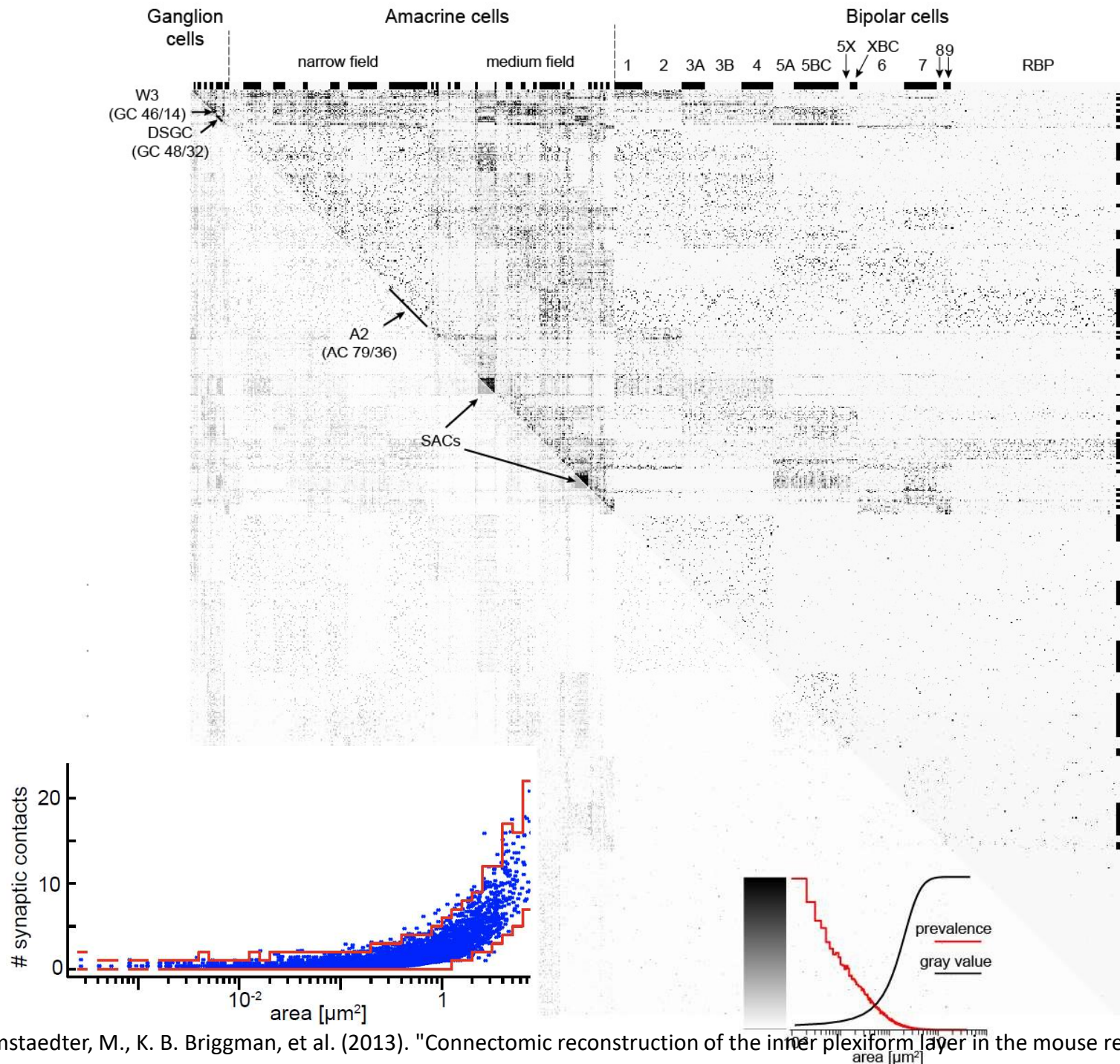
Srini Turaga
Viren Jain
...
Sebastian Seung
MIT



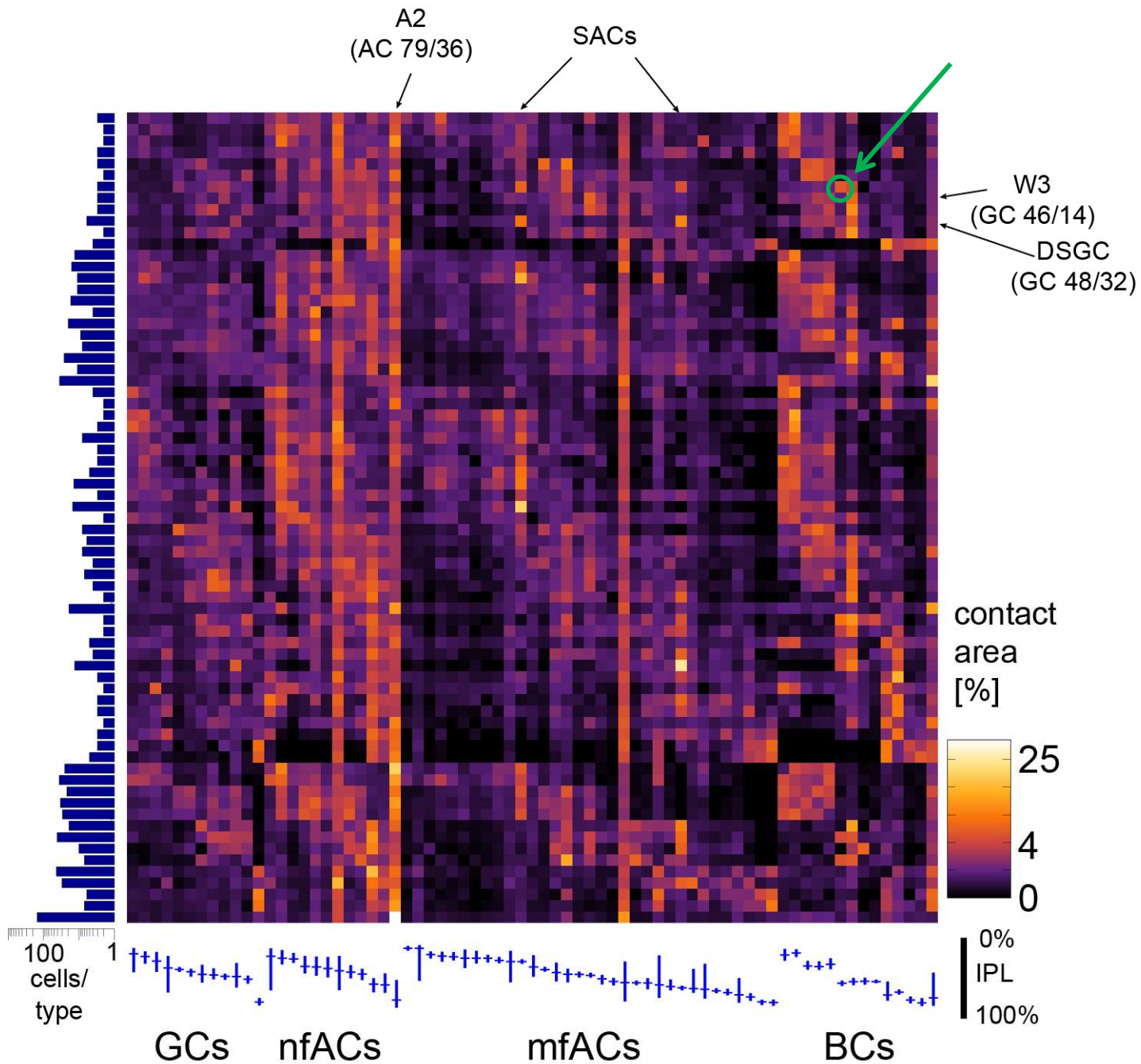
Helmstaedter, M., K. B. Briggman, et al. (2013). "Connectomic reconstruction of the inner plexiform layer in the mouse retina." [Nature: \(in press\)](#).



Helmstaedter, M., K. B. Briggman, et al. (2013). "Connectomic reconstruction of the inner plexiform layer in the mouse retina." [Nature: \(in press\)](#).



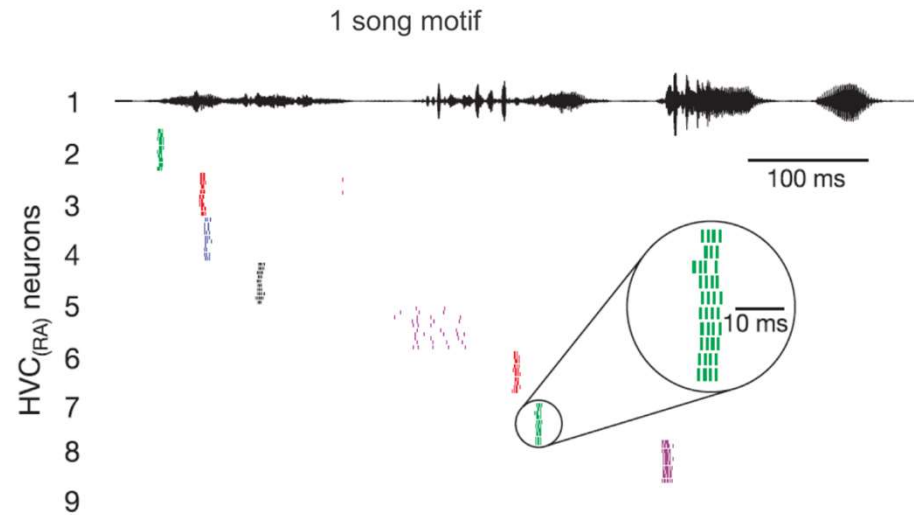
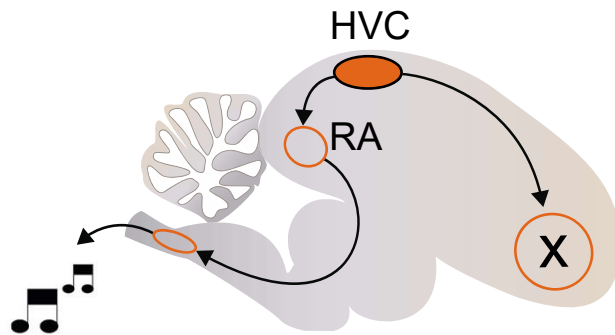
Helmstaedter, M., K. B. Briggman, et al. (2013). "Connectomic reconstruction of the inner plexiform layer in the mouse retina." Nature: (in press).



Helmstaedter, M., K. B. Briggman, et al. (2013). "Connectomic reconstruction of the inner plexiform layer in the mouse retina." [Nature: \(in press\)](#).

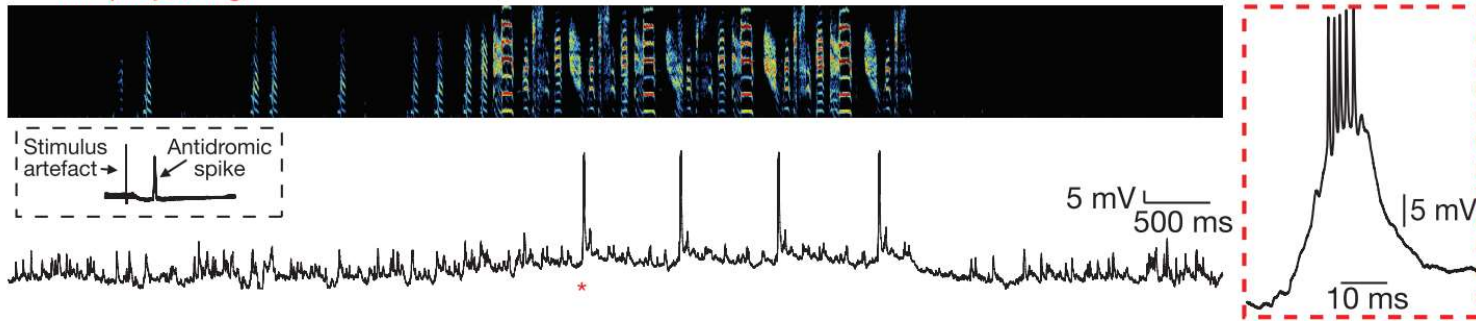


Joergen Kornfeld

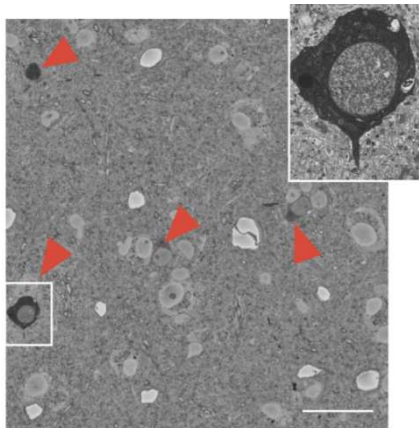
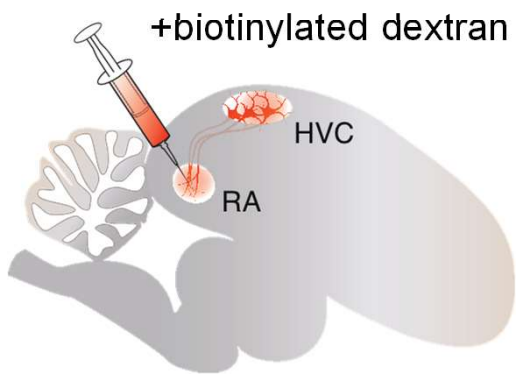


Hahnloser et al., 2002: Sparse time code

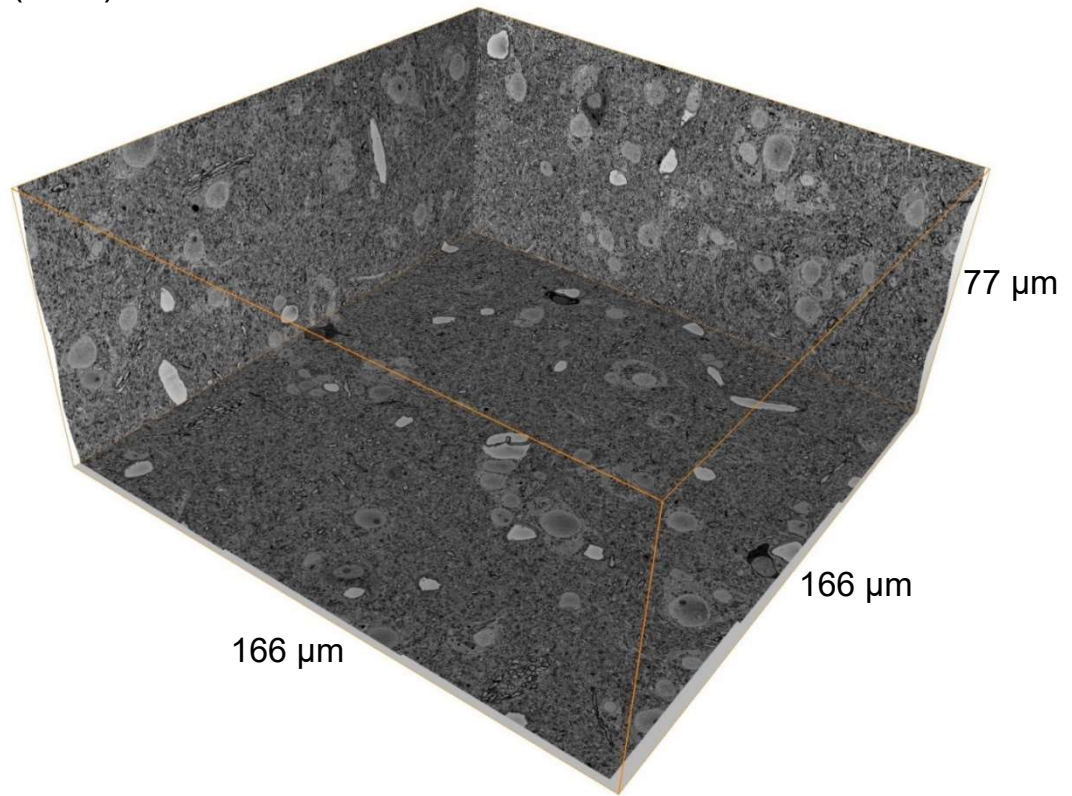
e RA-projecting



Long et al., 2010: Rapid depolarization underlies the burst

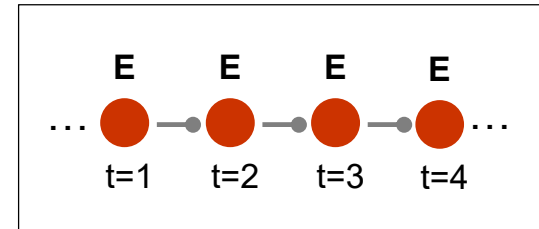
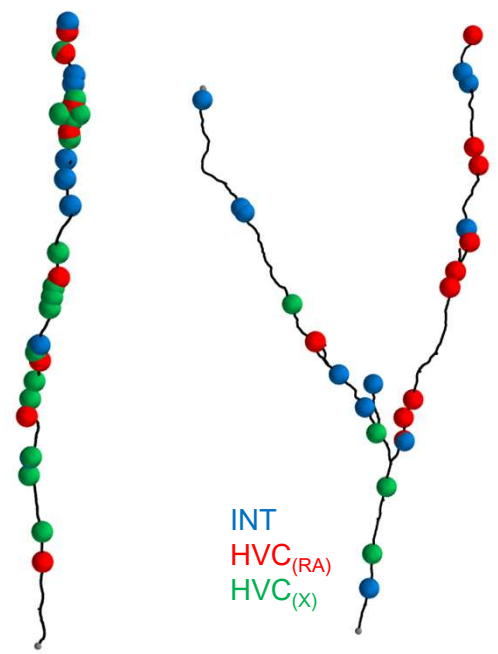
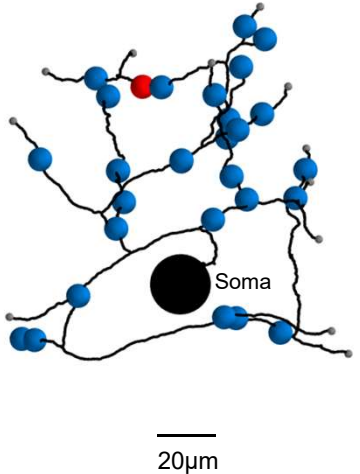


BDA labeled
HVC(RA) neurons

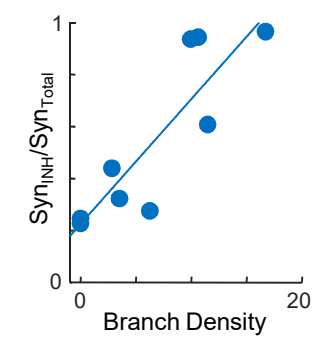
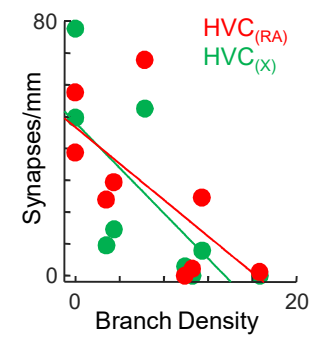
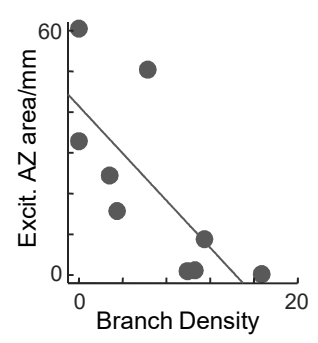


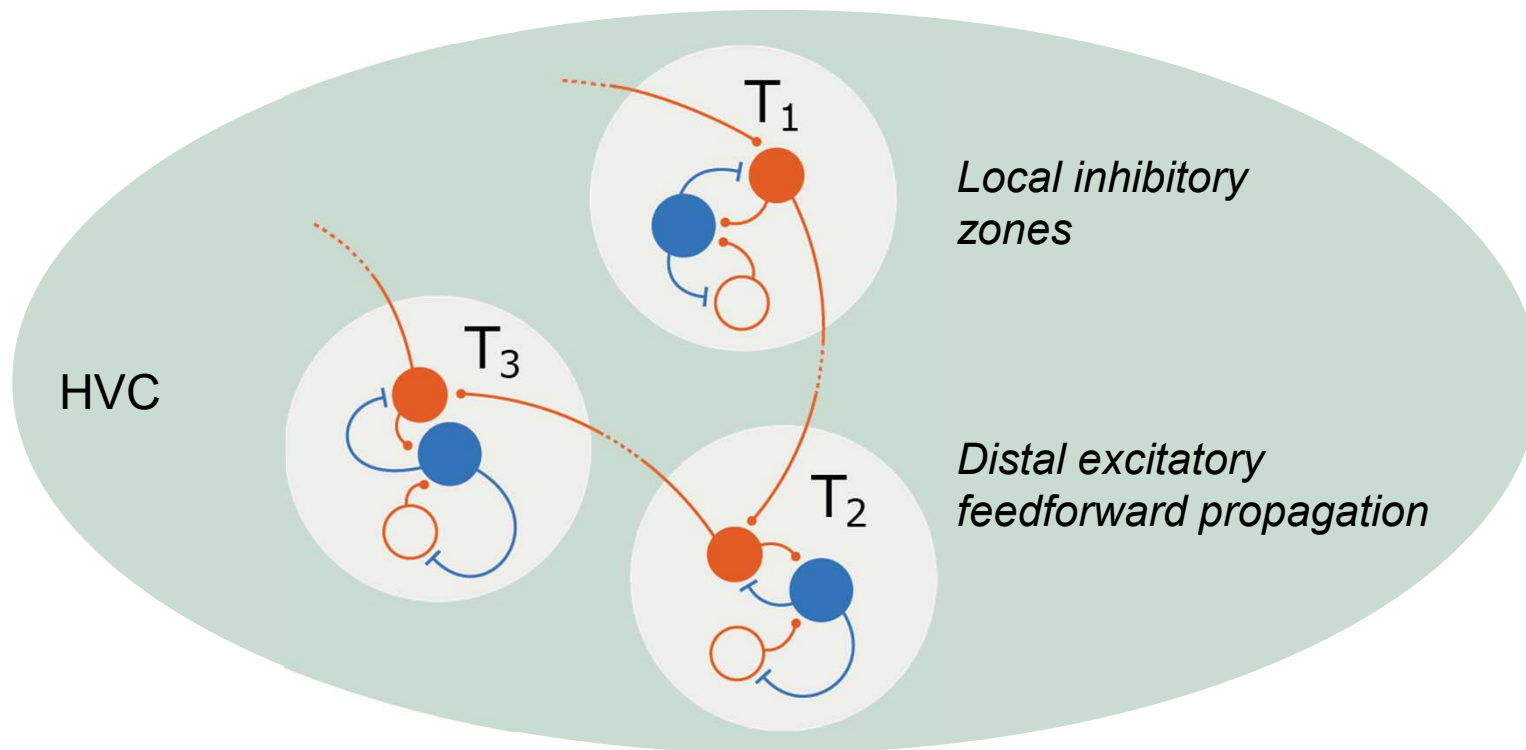
11x11x29 nm, ROTO stain combined with
HRP-DAB protocol for labeling, ECS
preservation

HVC_(RA) axons with synapses colored by postsynaptic type

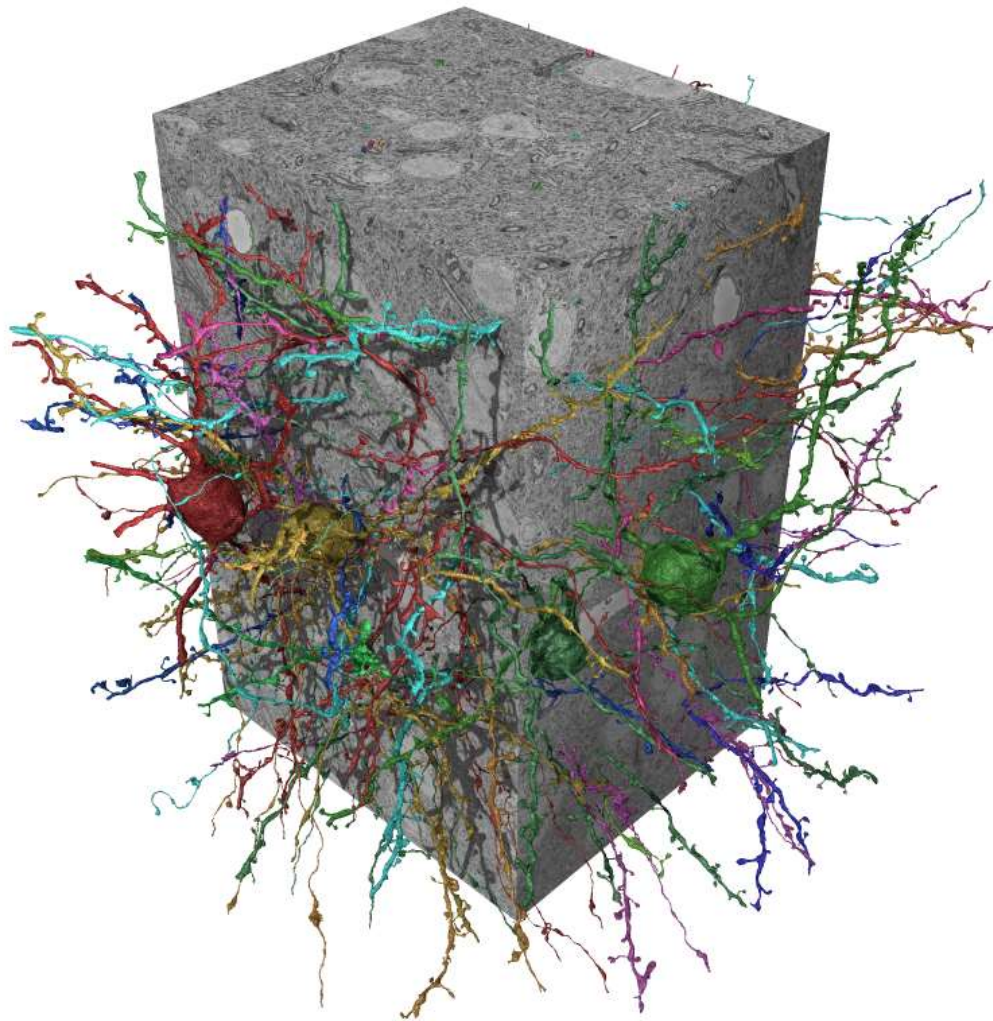


Quantified for 9 axons,
504 postsynaptic dendrites

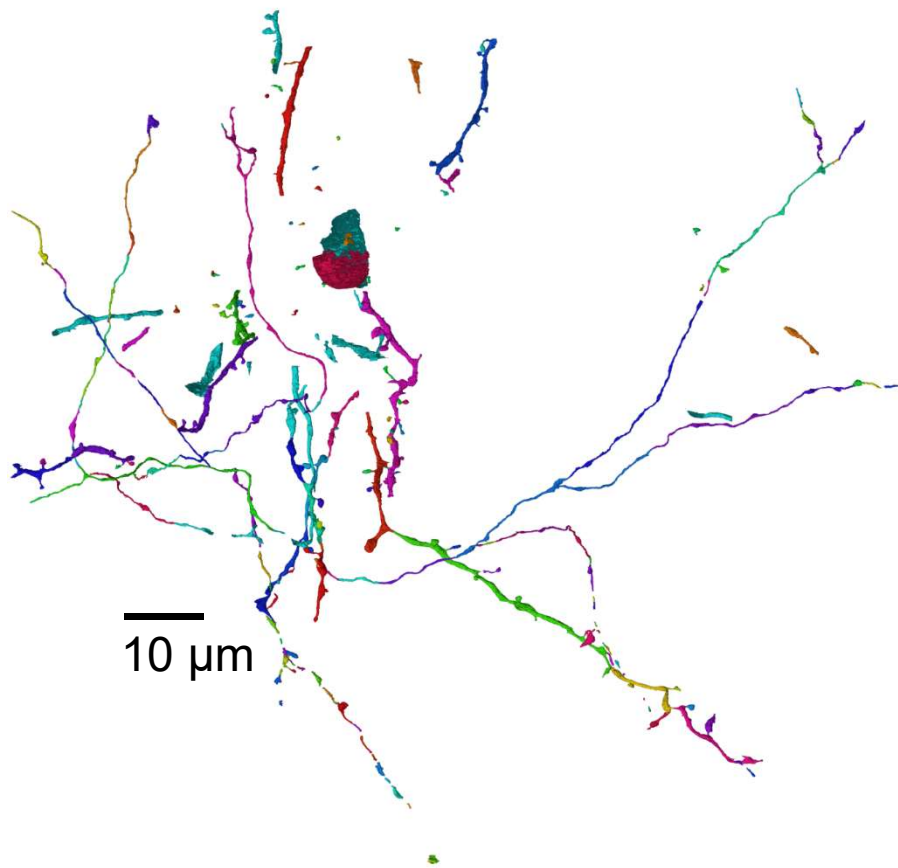




Similar network architecture proposed by Binas et al., 2014
for cortical sequence generation (coupled winner-take-all)



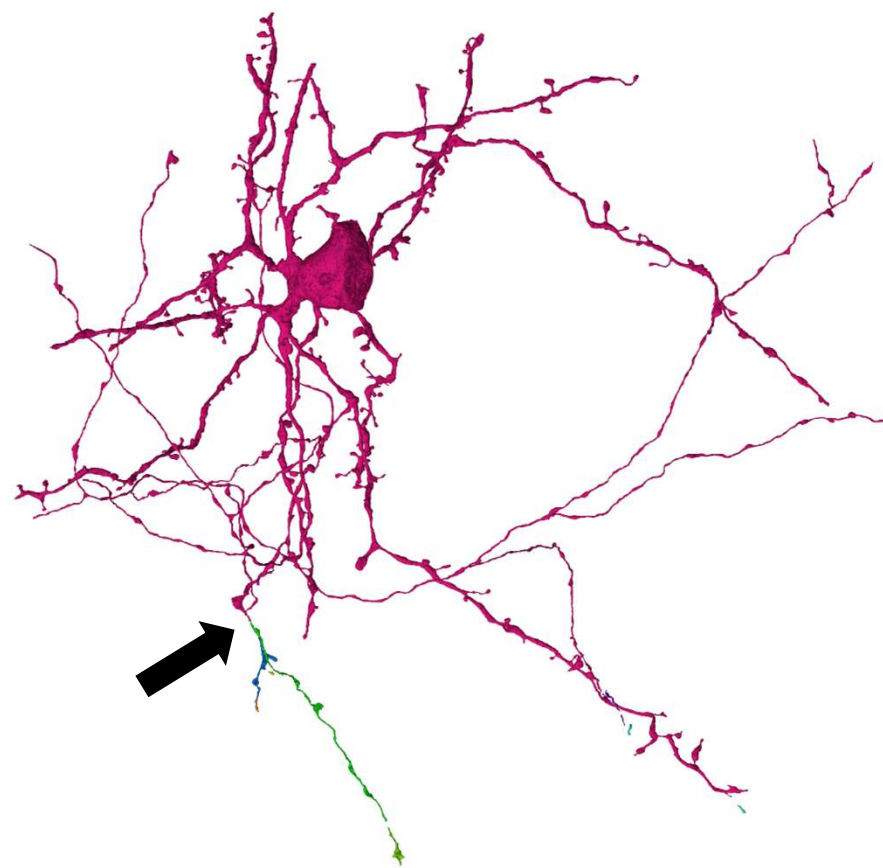
2015



10 μm

~0.01 mm error free path length

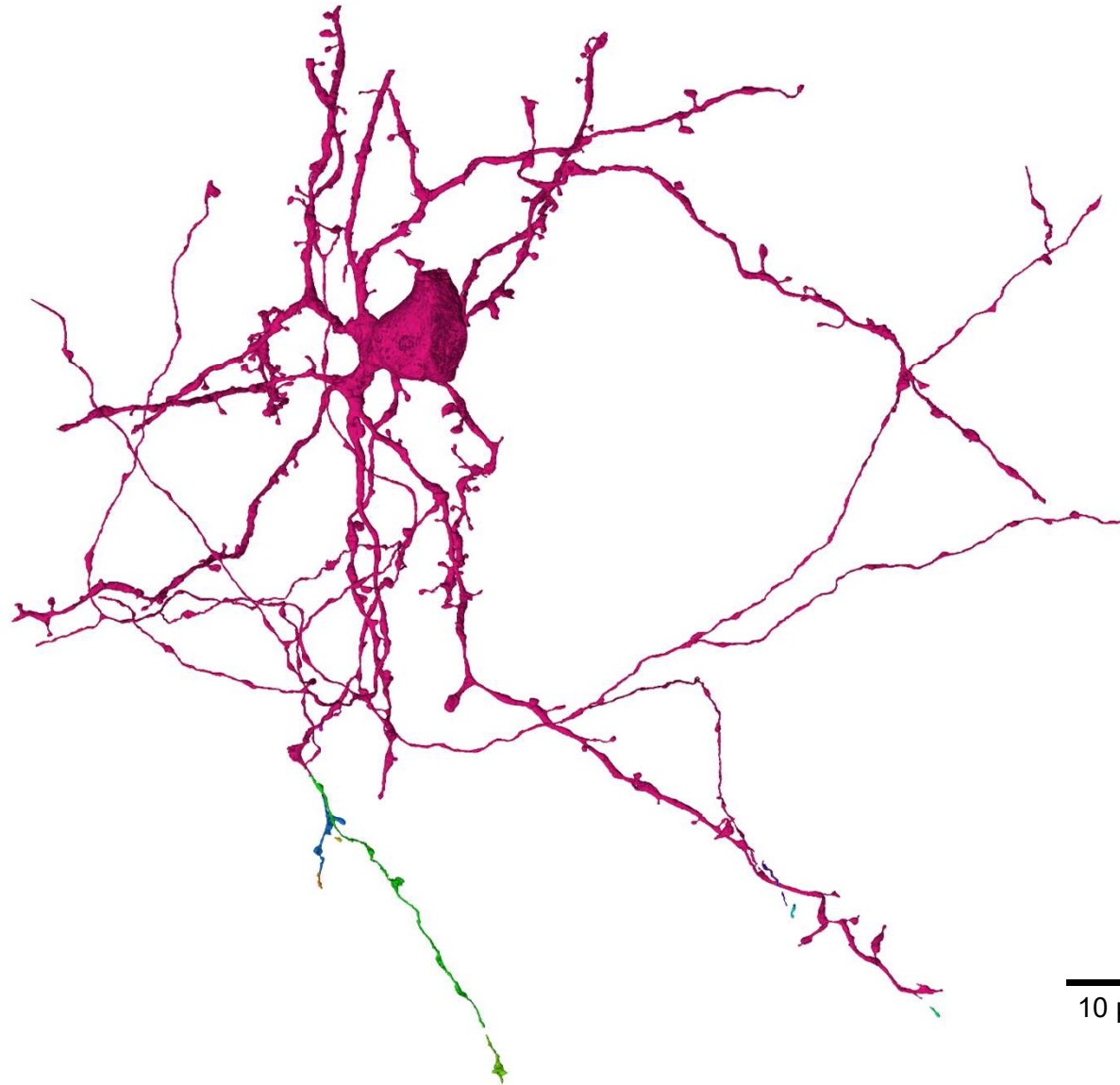
2017



> 1 mm error free path length



Michal Januszewski (Google), Jeremy Maitin-Shepard (Google), Peter Li (Google), Joergen Kornfeld (MPINB), Viren Jain (Google)

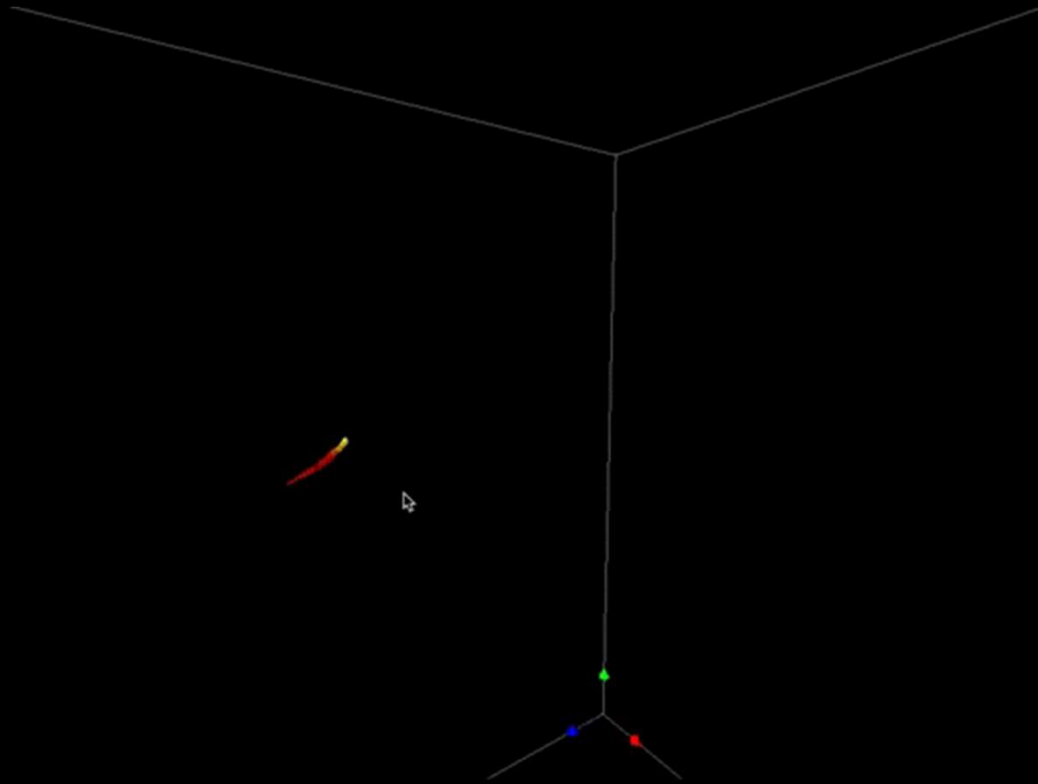


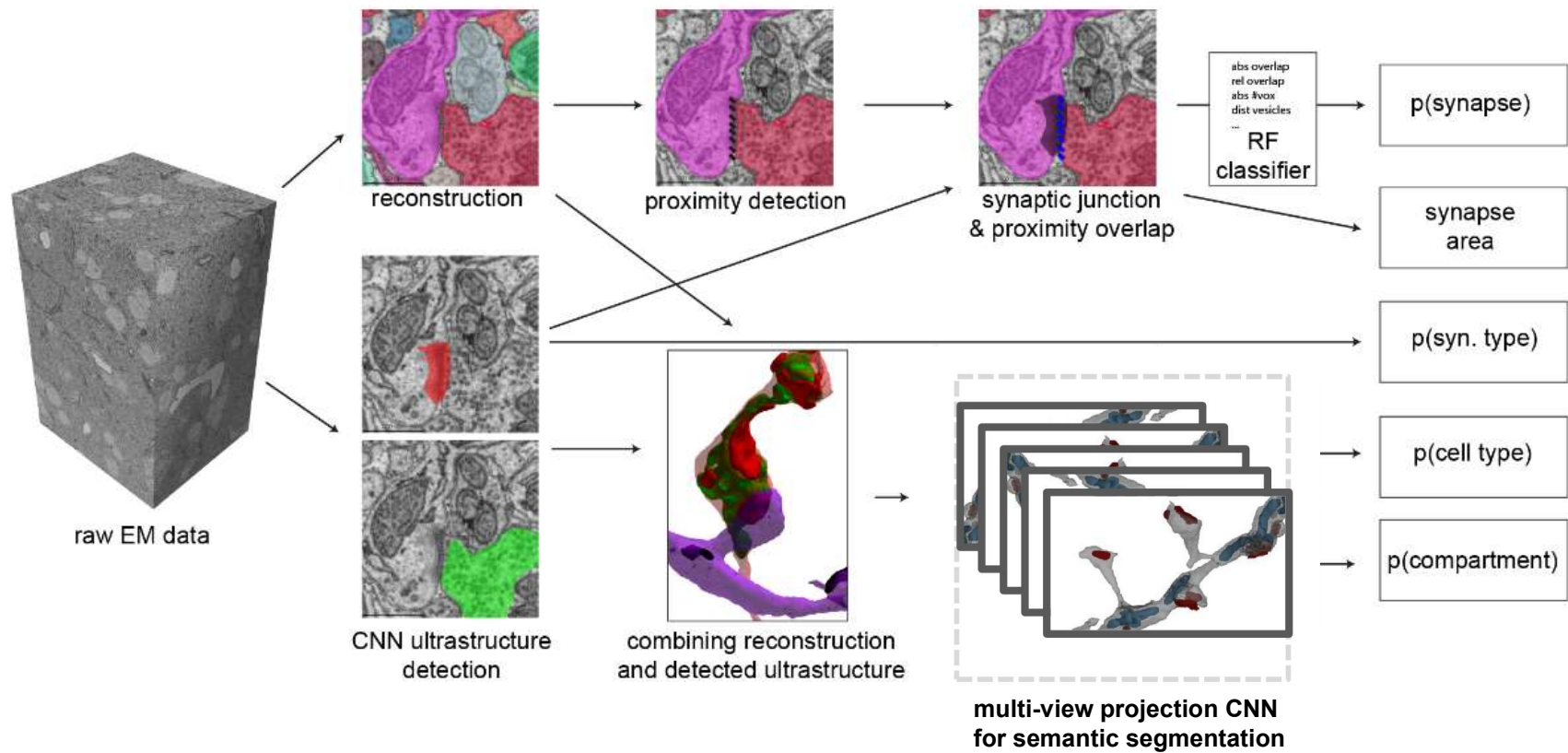
M. Januszewski



V. Jain

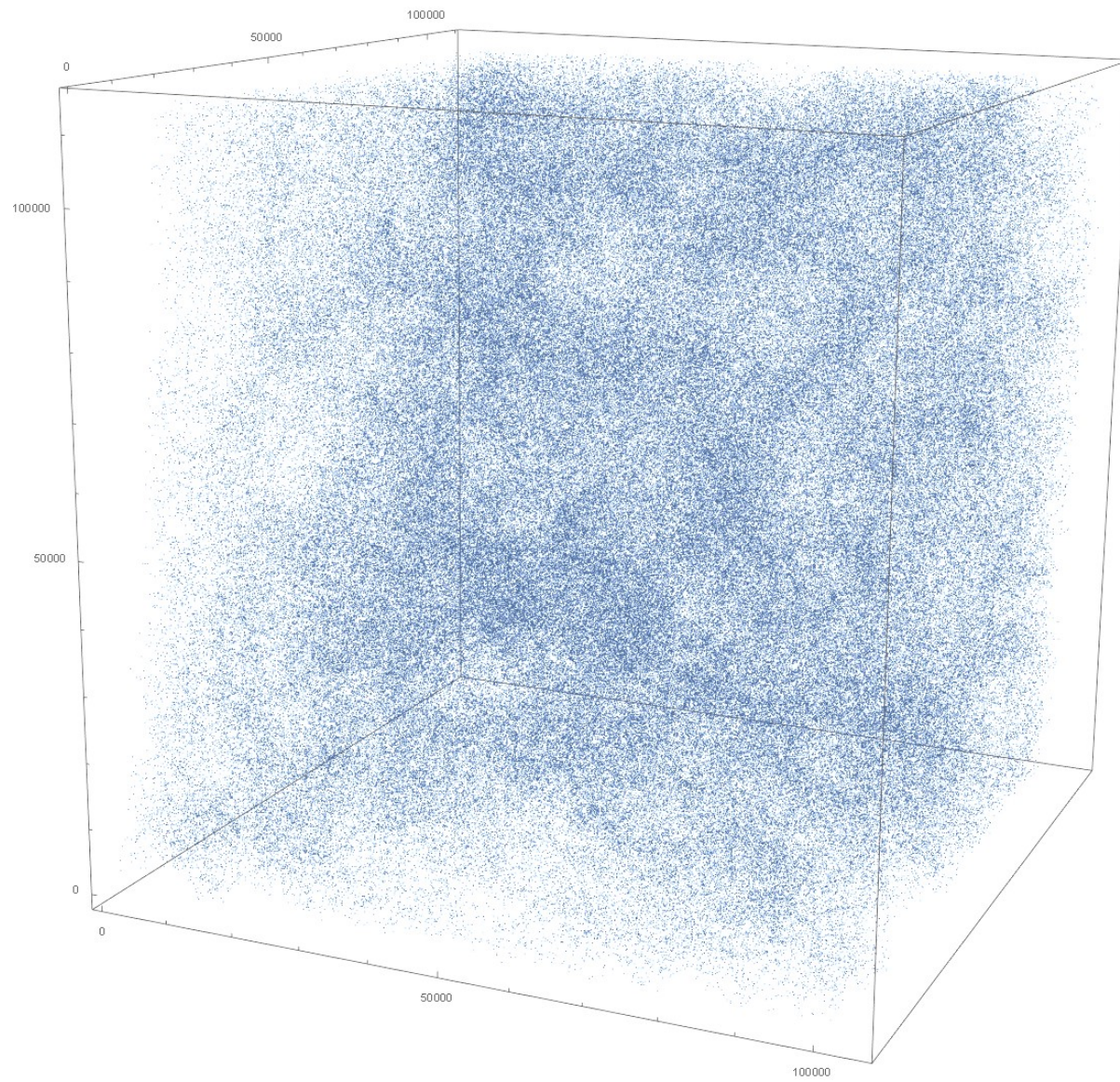
Completed reconstruction through targeted tracing with KNOSSOS
Total workload for small data set: ~900 hours





Automated synaptic connectivity inference for volume electron microscopy

Sven Dorkenwald, Philipp J Schubert, Marius F Killinger, Gregor Urban, Shawn Mikula, Fabian Svava & Joergen Kornfeld



16384000

100000

50000

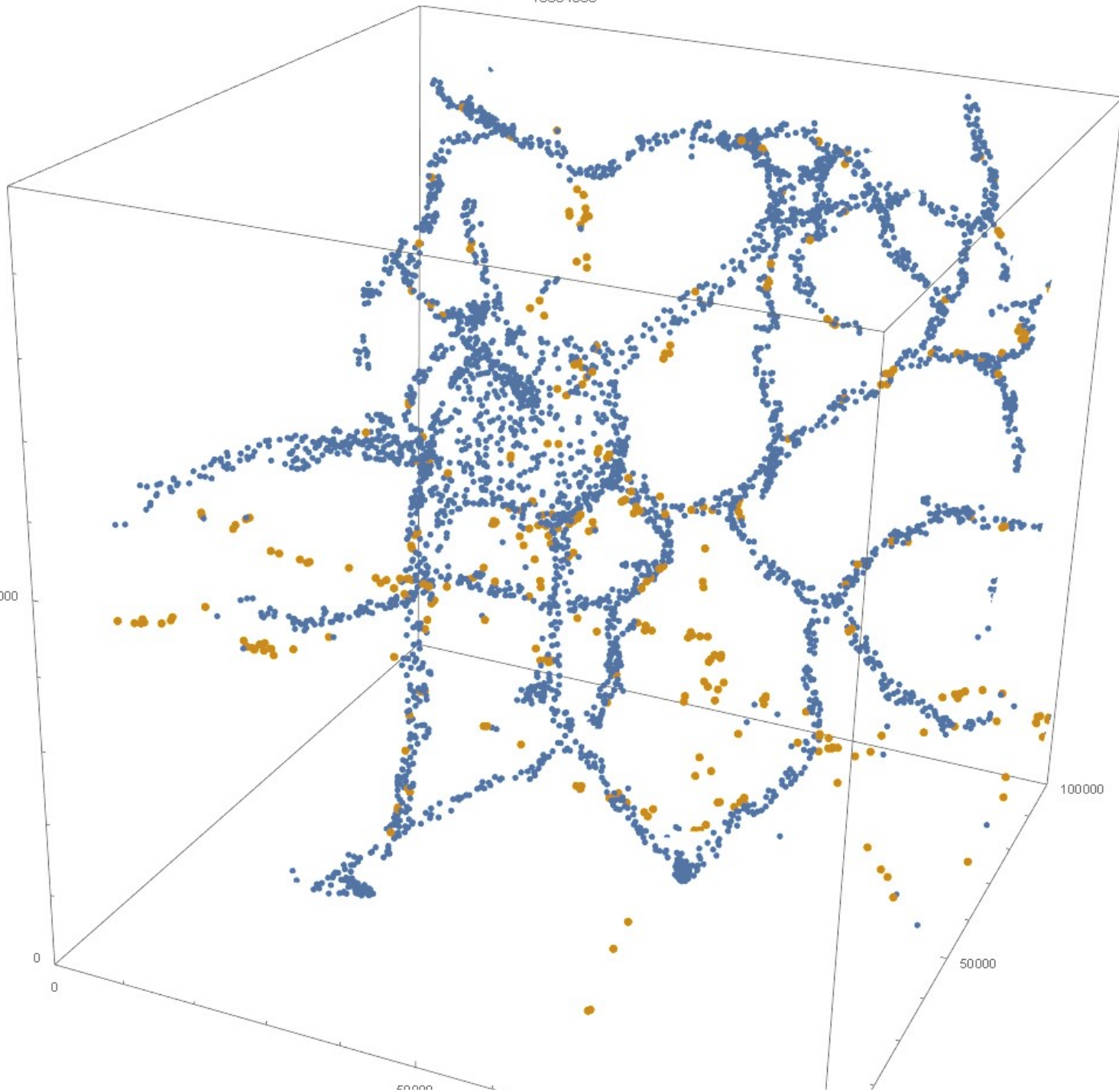
0

0

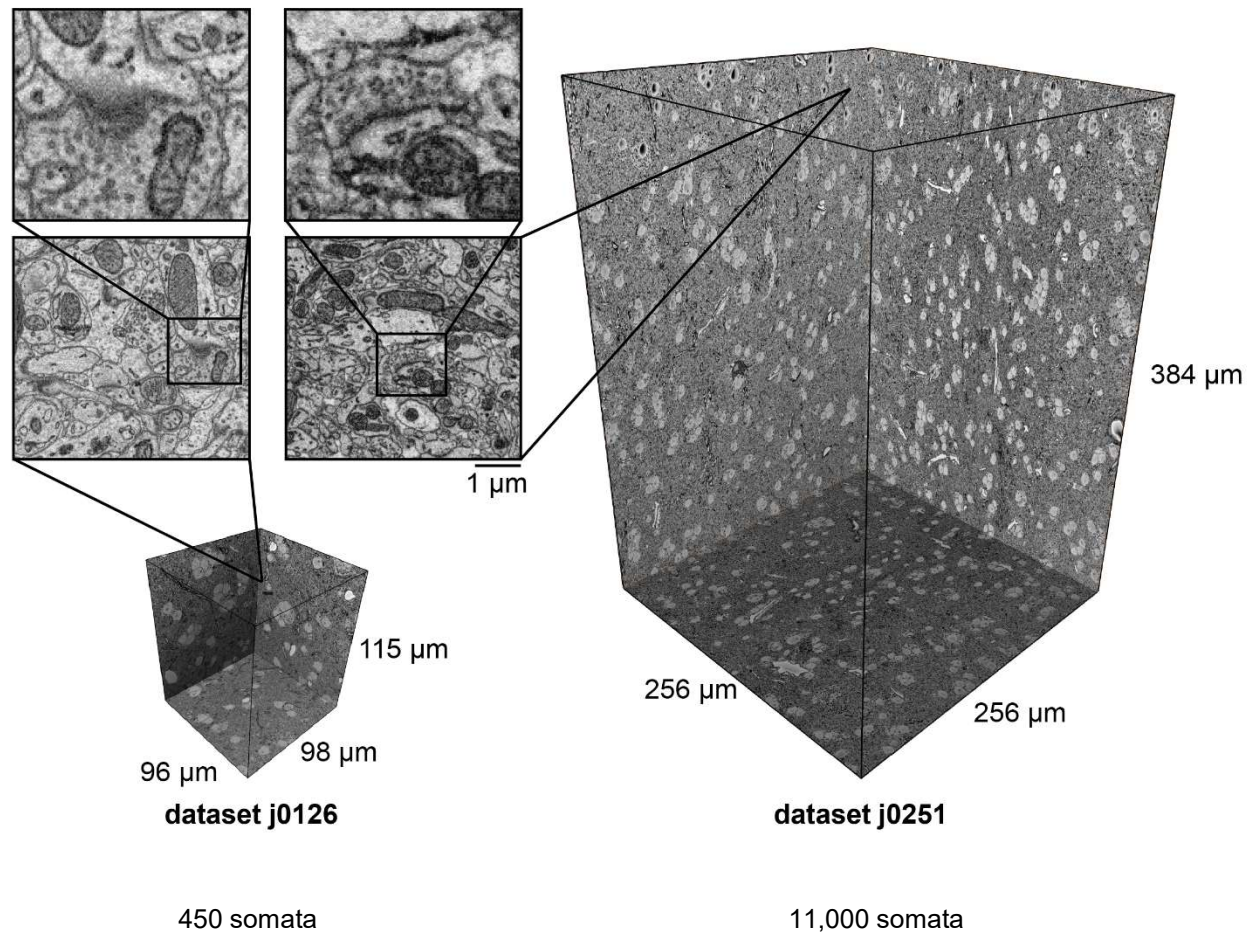
50000

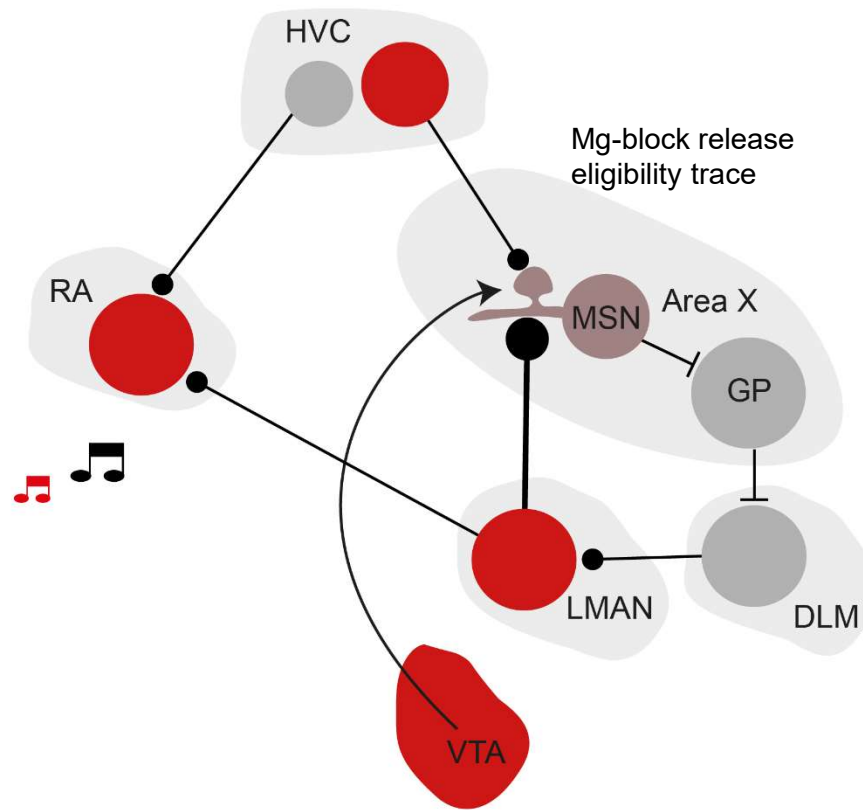
100000

50000



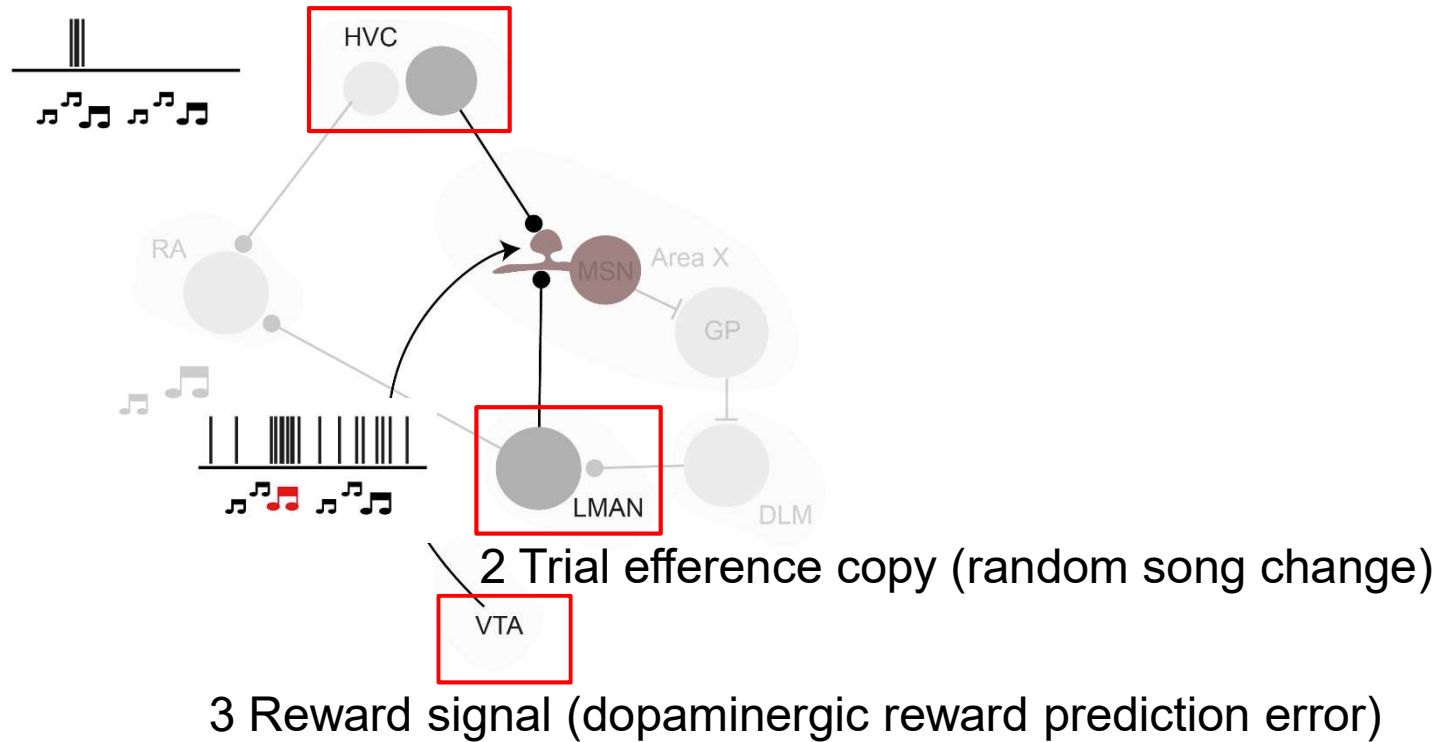
Songbird basal ganglia datasets



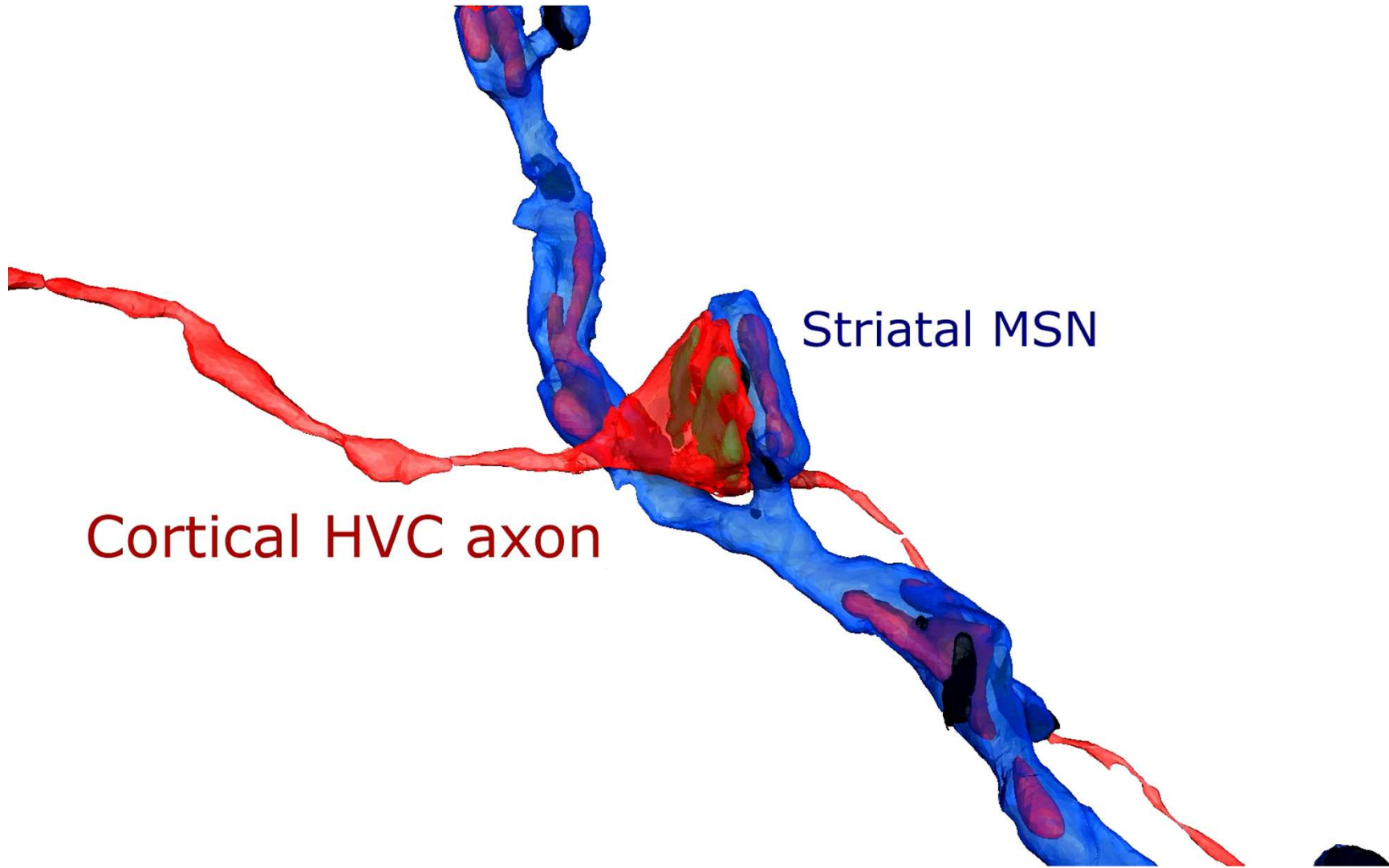


The three ingredients for reinforcement learning

1 Behavioral context (relative song time)

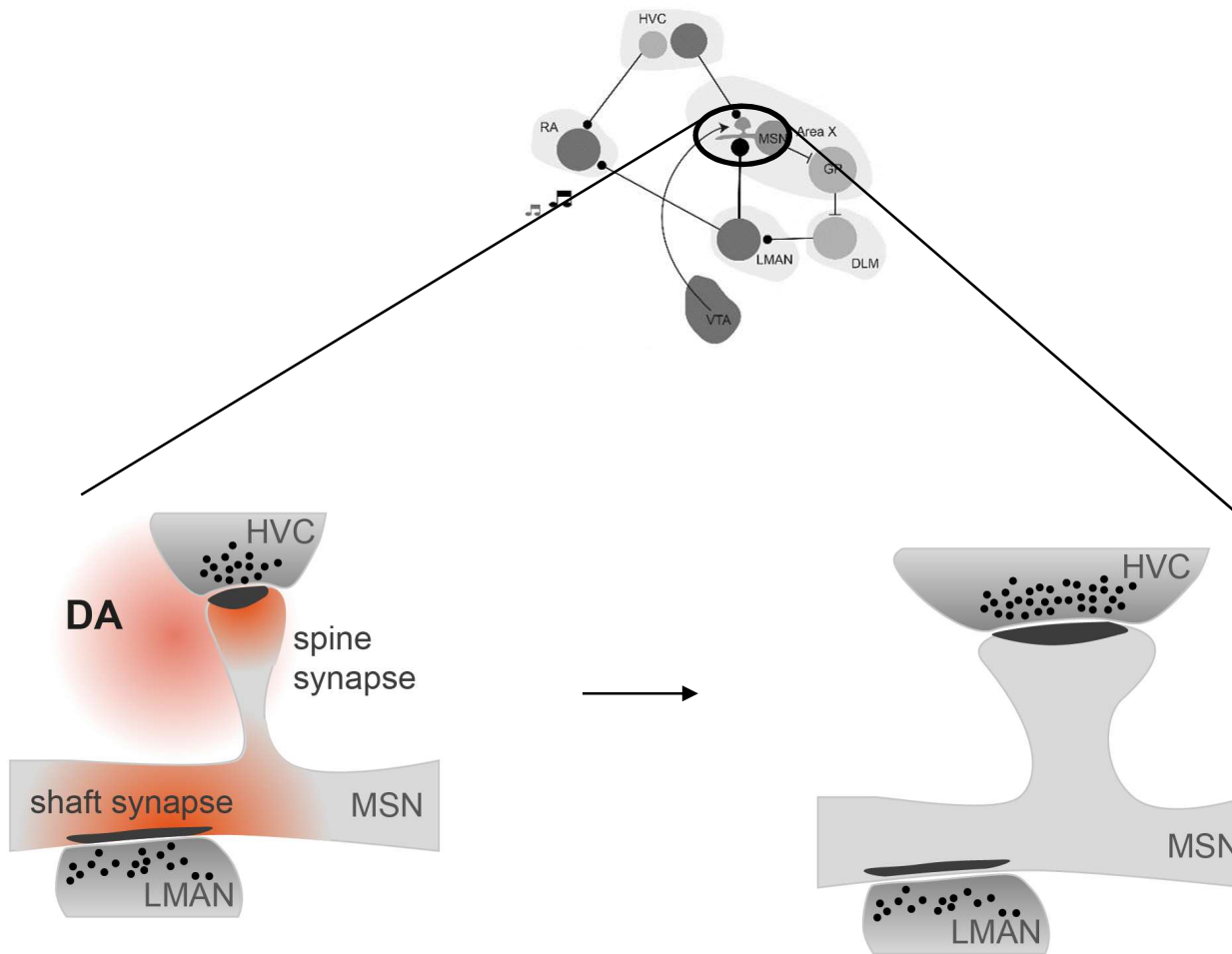


M. Fee

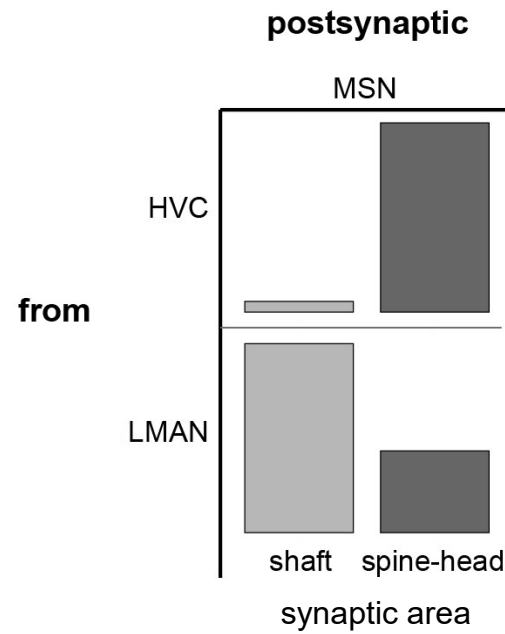
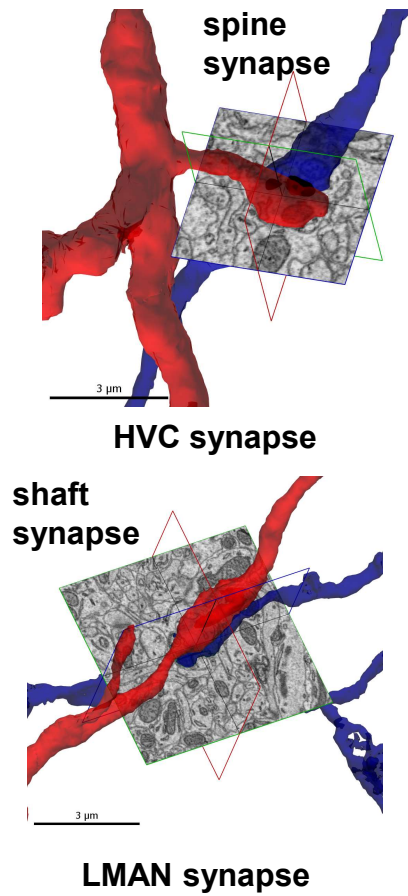


Striatal MSN

Cortical HVC axon



Links between plasticity and spines e.g. Yuste and Bonhoefer. Ann. Rev. Neuroscience 2001



Preliminary analysis with manually identified cells
 11-fold higher synaptic area of LMAN shaft
 synapses in comparison to HVC synapses

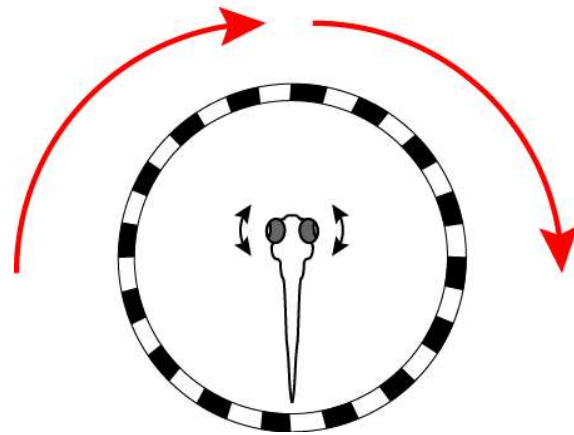


Fumi
Kubo



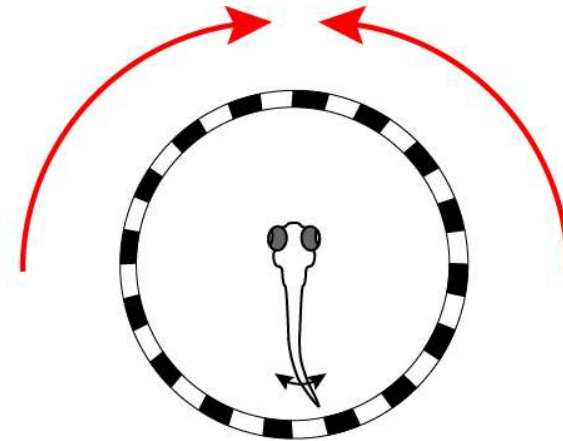
Fabian
Svara

Rotation
(clockwise)

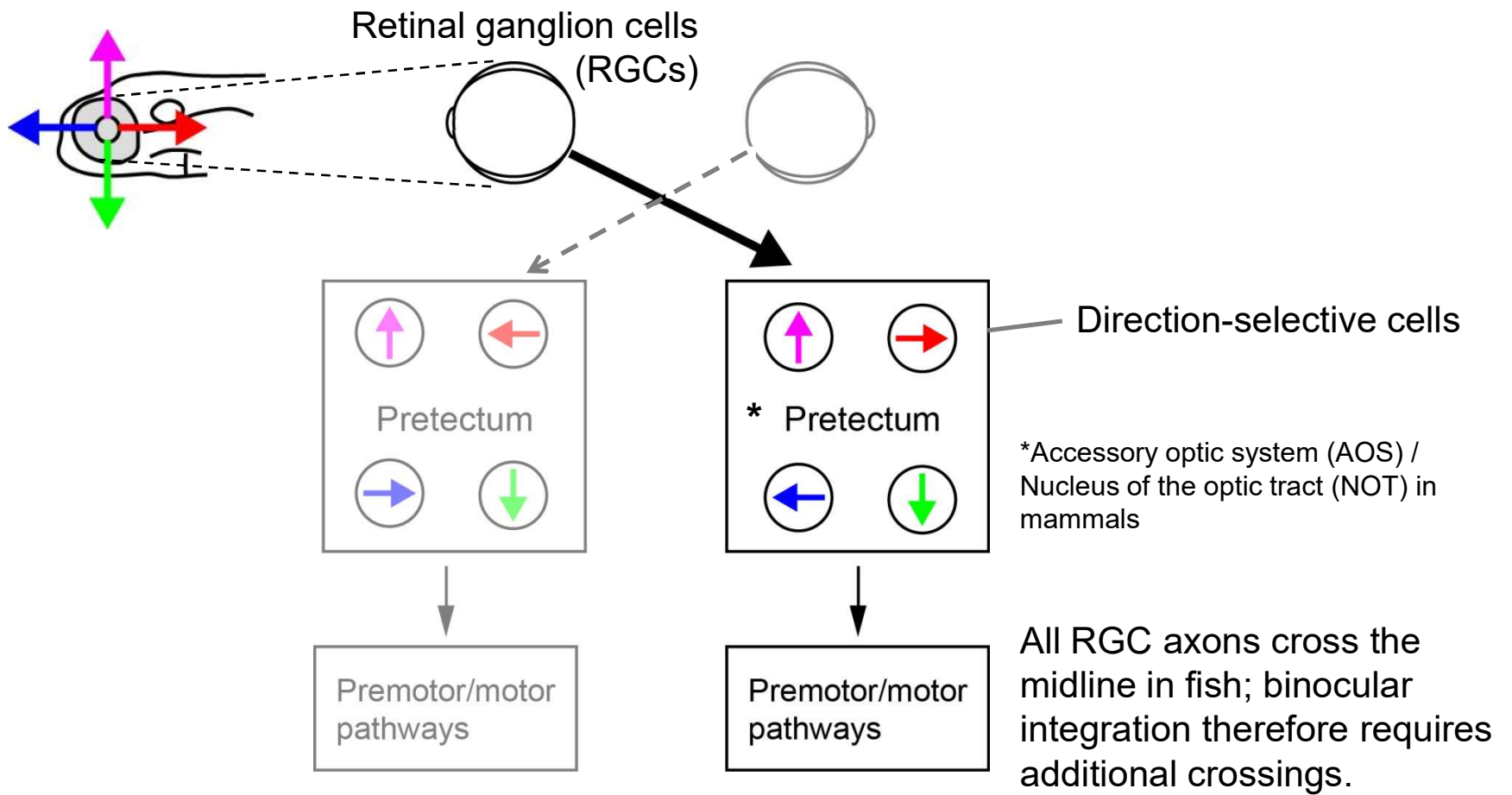


Optokinetic response (OKR)
(Eye movements)

Translation
(forward)

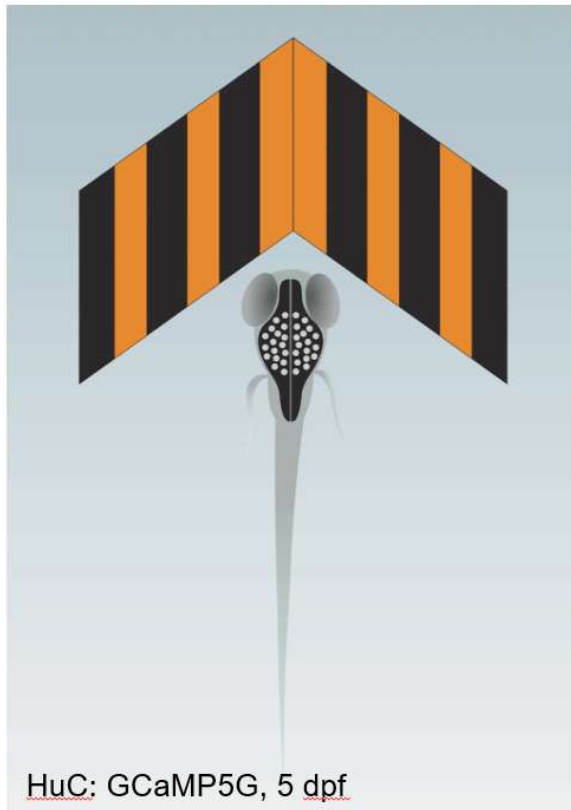


Optomotor response (OMR)
(Swimming)



From functional imaging to electron microscopy (EM) reconstruction

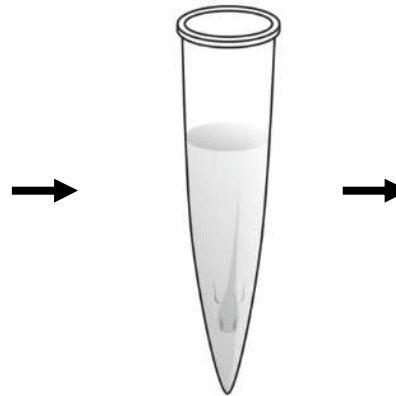
Pretectal Ca^{2+} imaging



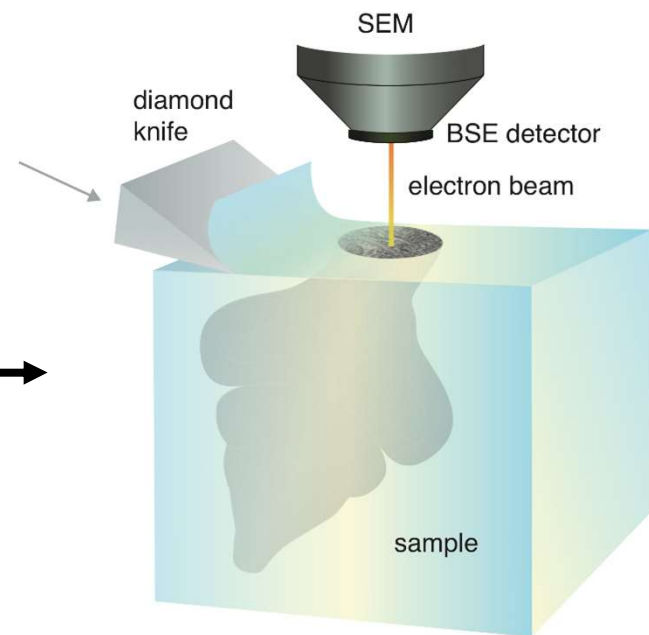
HuC: GCaMP5G, 5 dpf

approx. 4-30 neurons per each type
(approx. 200 neurons in total)

Fixation and staining

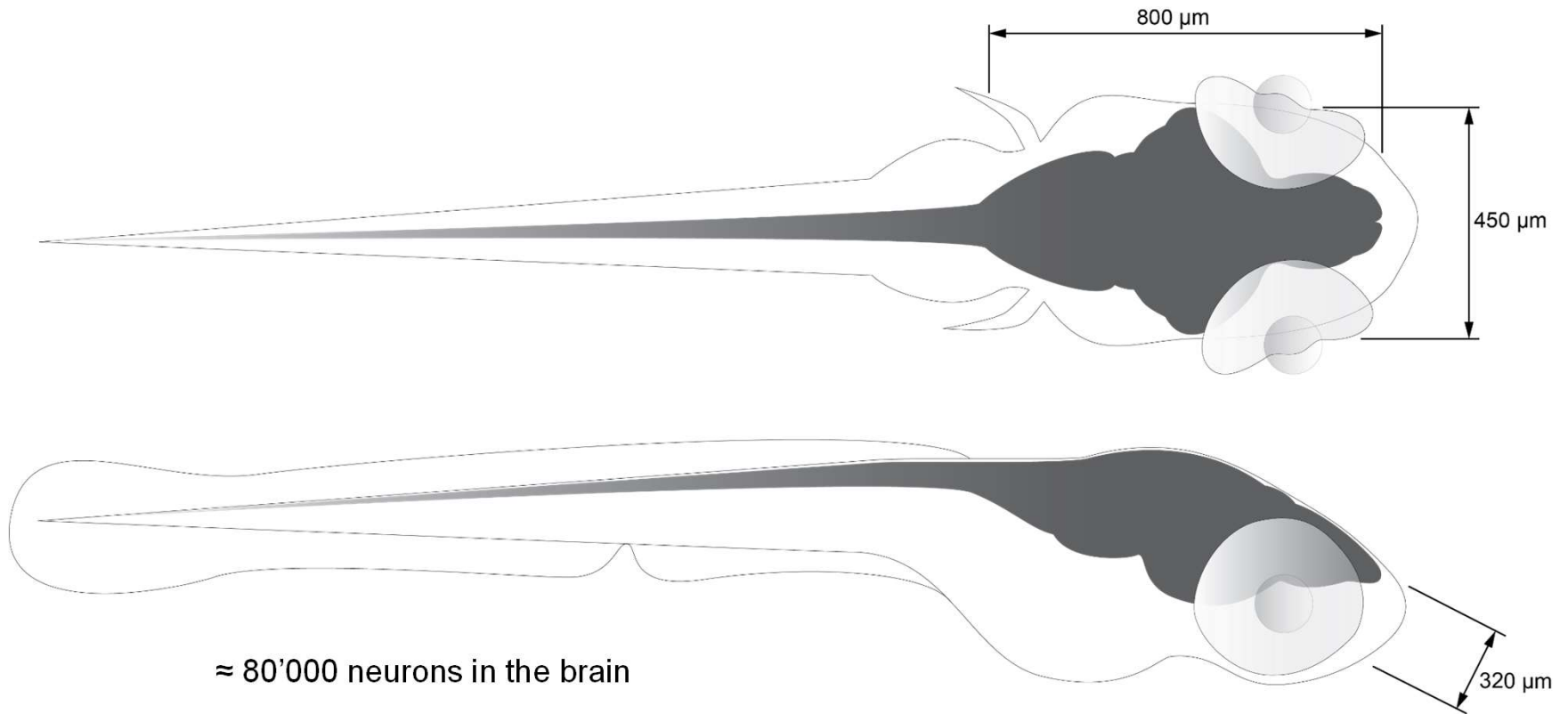


Serial block-face EM of whole larval brain



14 x 14 x 25 nm in x,y,z axis
Data size: ~12 TB

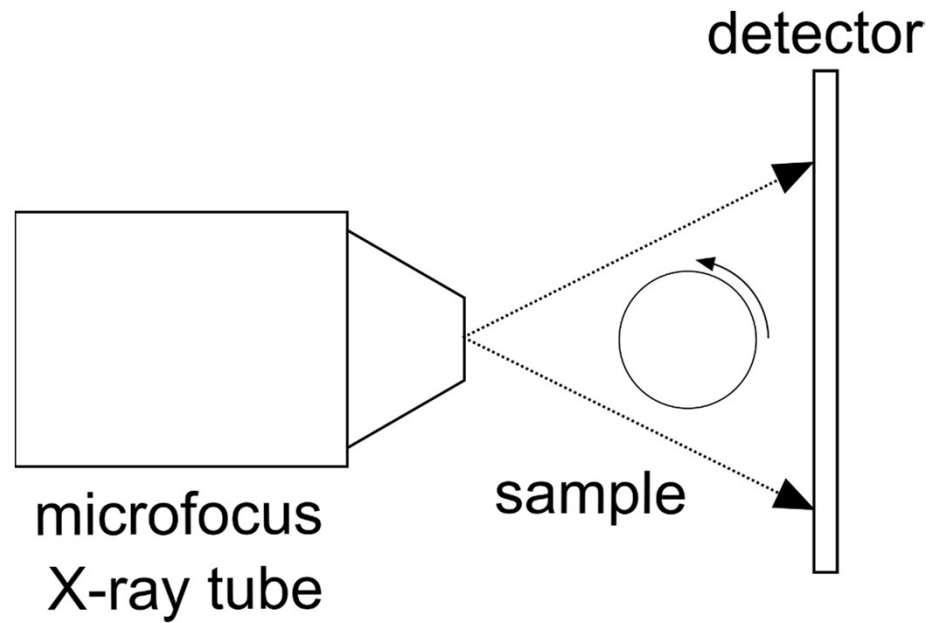
Larval Zebrafish Whole-Brain EM



≈ 80'000 neurons in the brain

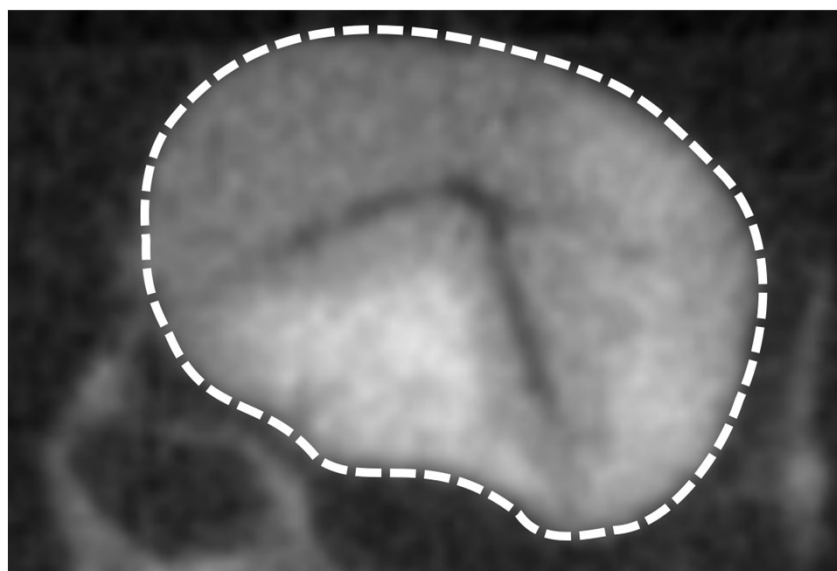
≈ **7 months, 28000 sections** at 25 nm
(at 14 x 14 nm resolution, with standard SBEM setup)

X-ray microCT

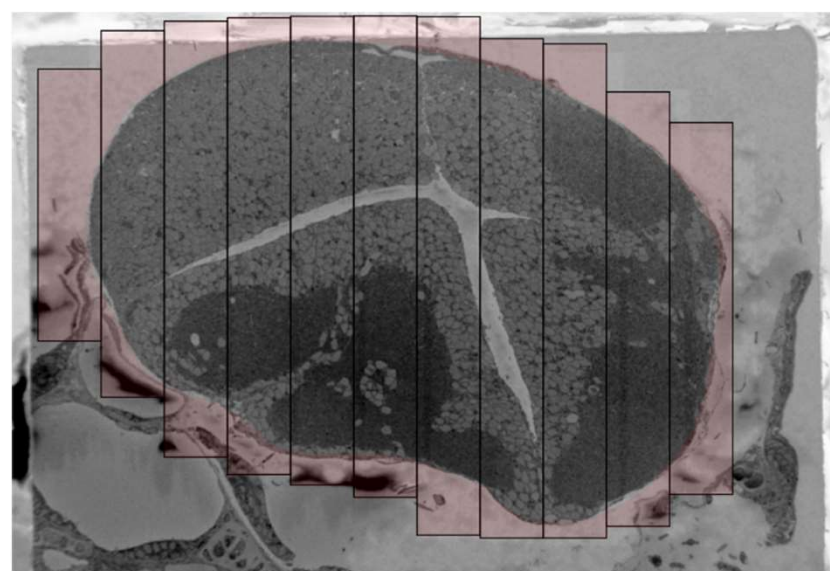


Allows exact measurement of sample geometry after embedding,
even in opaque epoxy

microCT



Linescanning + dynamic mosaic

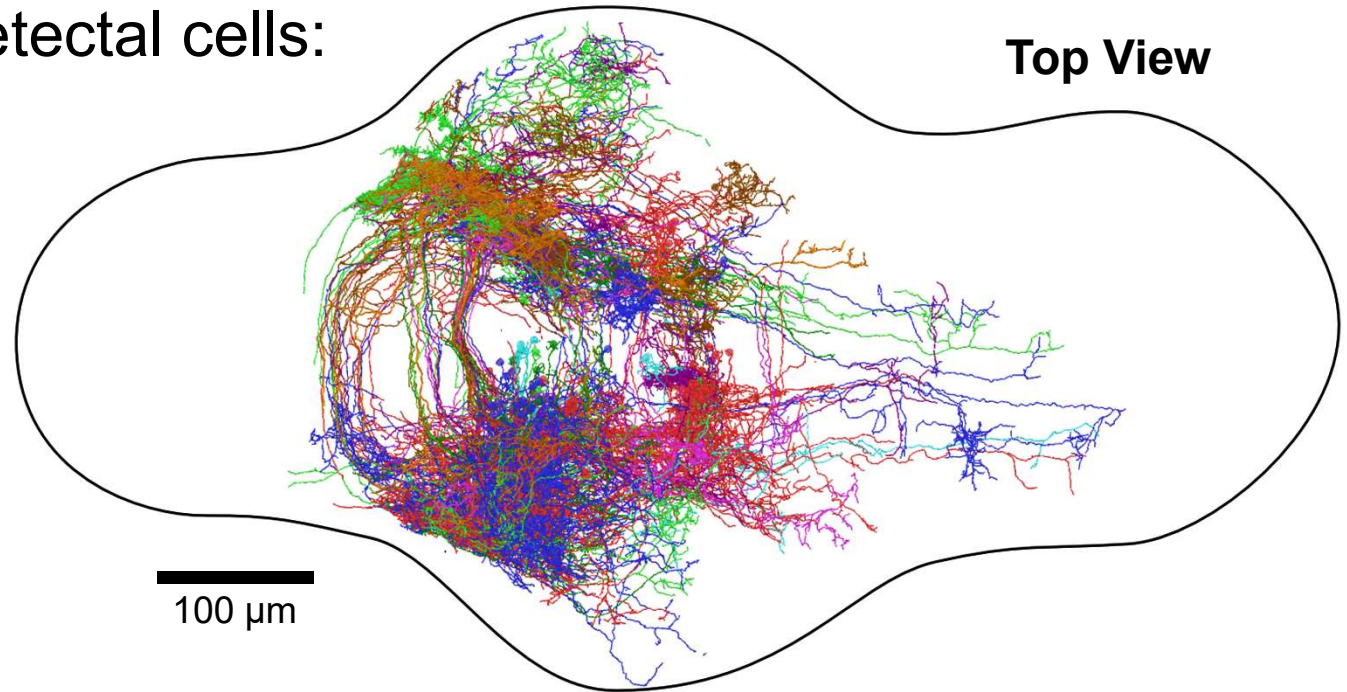


50 μ m

Reconstruction of functionally characterized pretecal cells: Current status

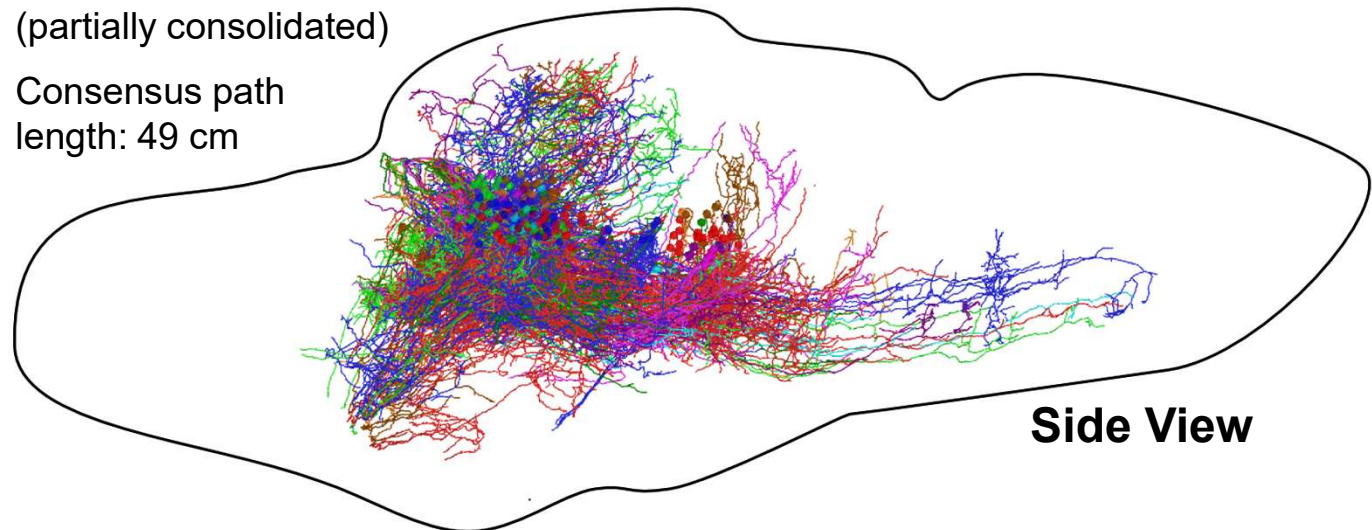
Simple Complex

MoNL	■	FEL	■
MoNR	■	FER	■
MoNL	■	BEL	■
MoTR	■	BER	■
		FELR	■
		BSP	■
		FSP	■

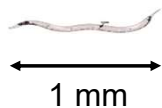


195 cells traced
(partially consolidated)

Consensus path
length: 49 cm



C. elegans



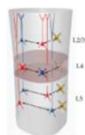
10^{-3} mm^3
 10^2 neurons

Fly brain

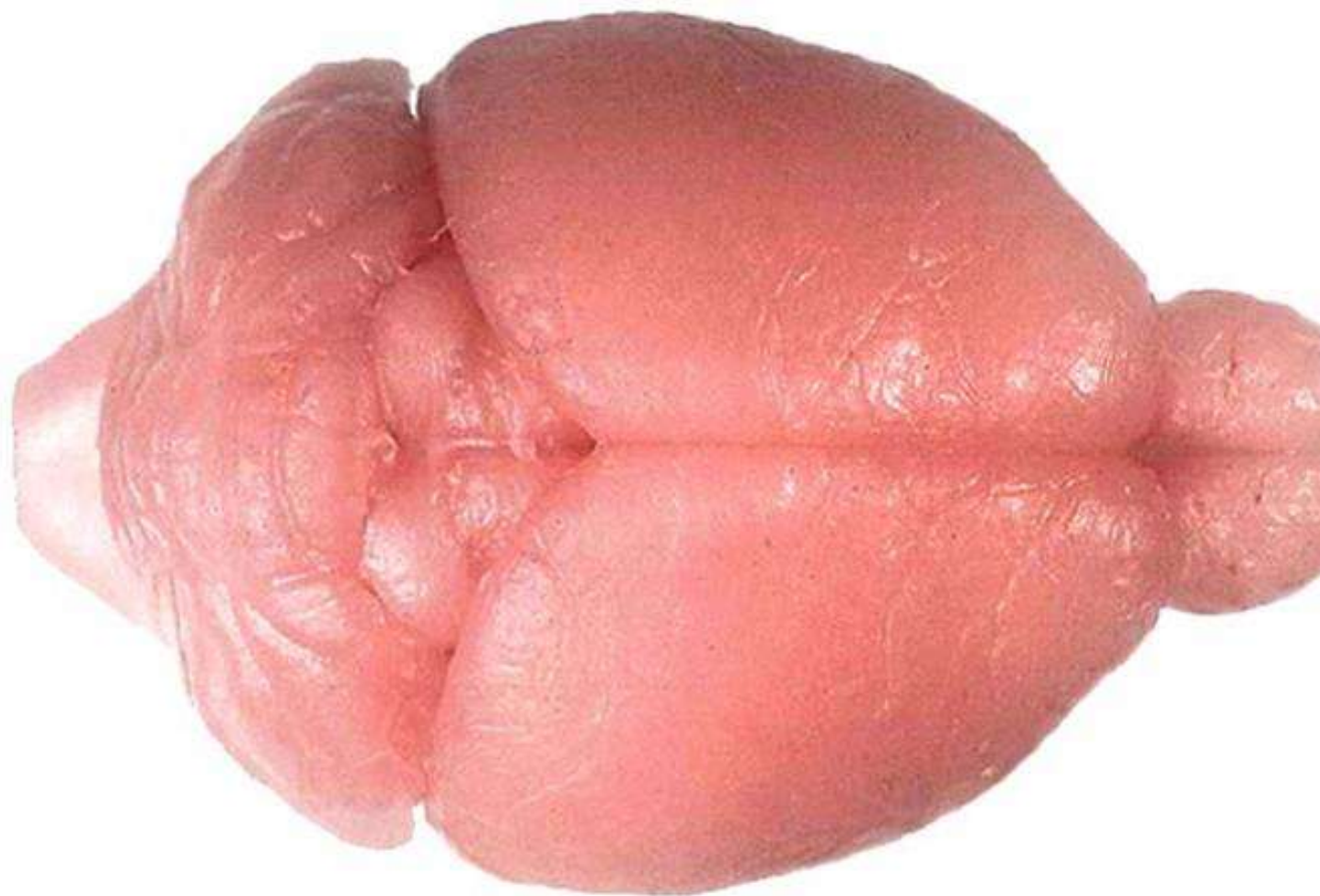


10^{-1} mm^3
 10^5 neurons

Mouse cortical column

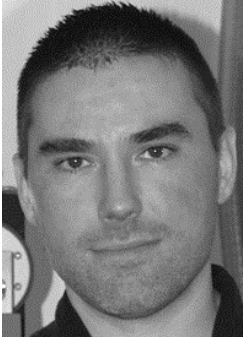


10^{-2} mm^3
 10^4 neurons

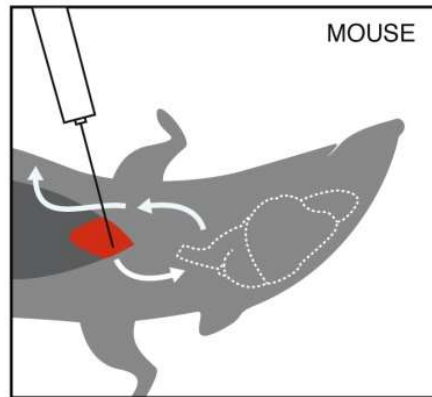


Mouse brain

10^3 mm^3
 10^8 neurons



Shawn Mikula



aldehyde perfusion



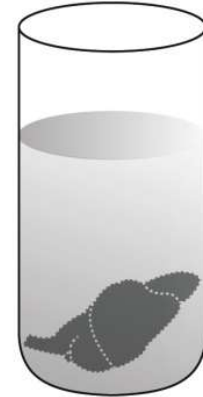
postfix with aldehyde (48h)
3 rinses (8h each)



periodate (48h)
3-4 rinses (8h each)



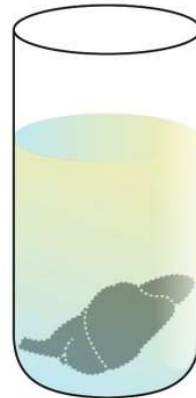
thiocarbohydrazide (48h)
3-4 rinses (8h each)



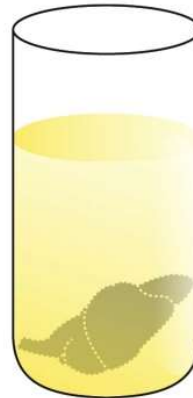
osmium tetroxide (48h)
distilled water wash (8h)



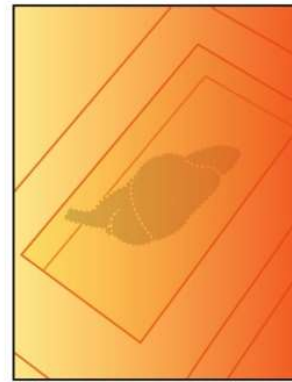
acetone:
50% (8h)
75% (8h)
100% (8h)
100% (8h)



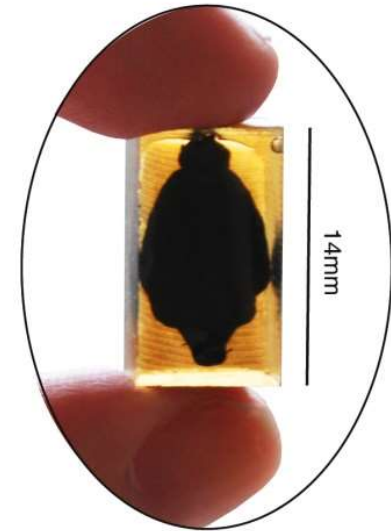
50% acetone/
50% epoxy (16h)



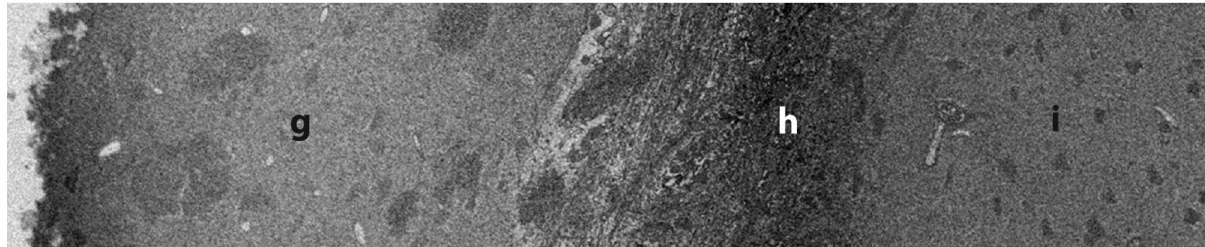
100% epoxy (16h)



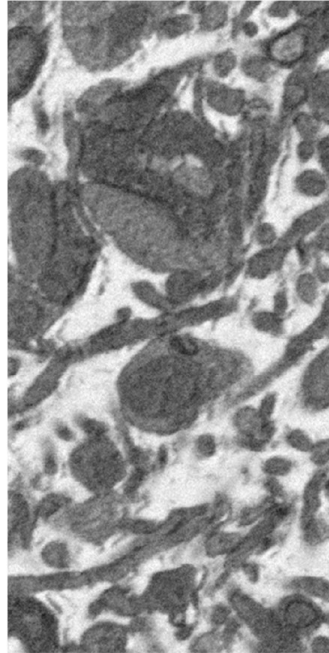
polymerize
(24h at 70 degrees)



f



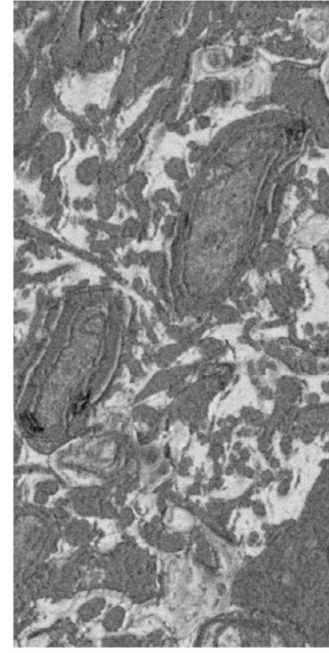
g



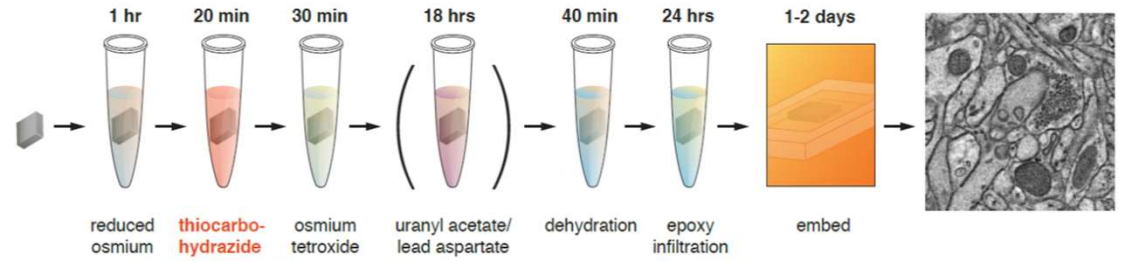
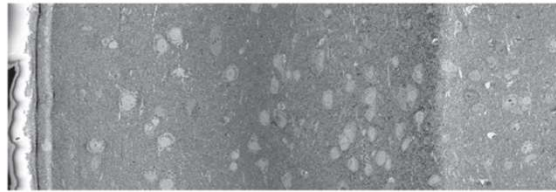
h



i



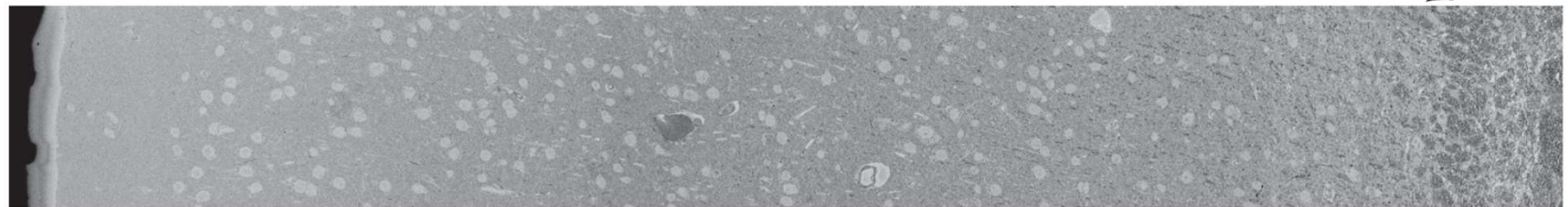
C ROTO



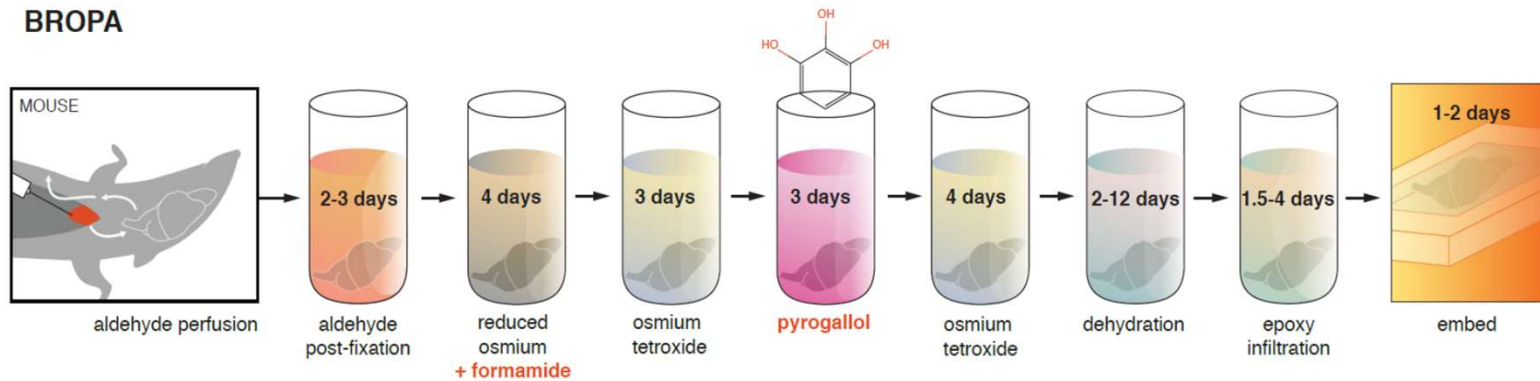
ROTO + ECS preservation



BROPA

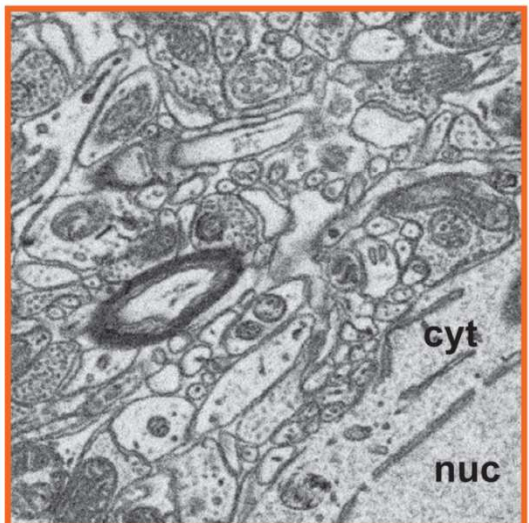
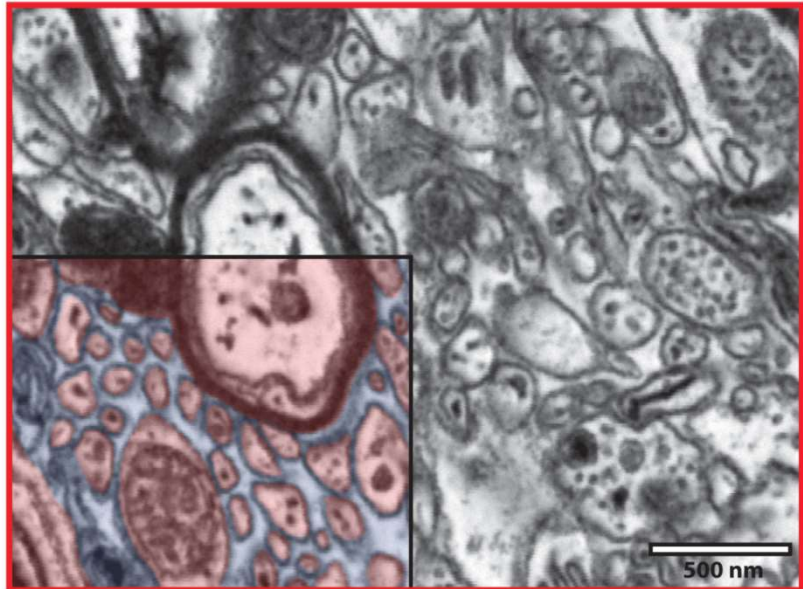
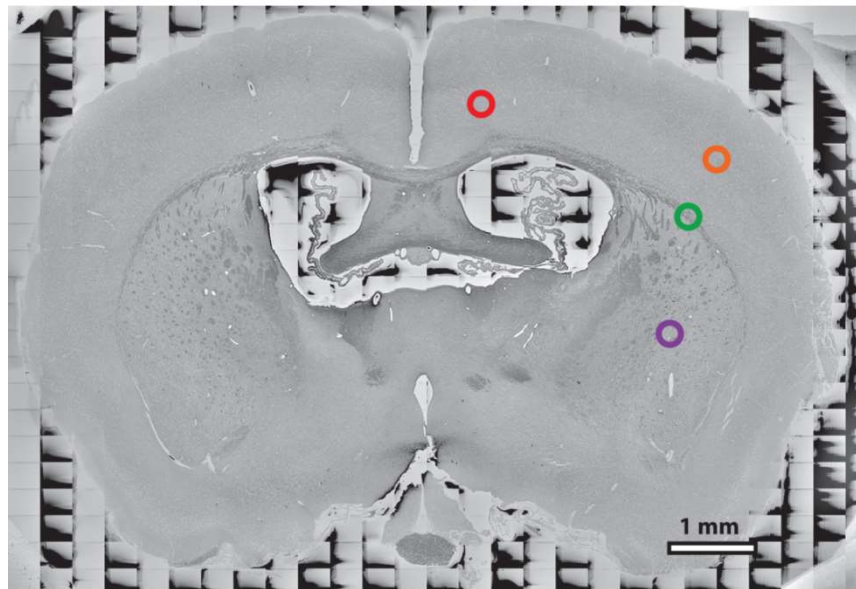


BROPA

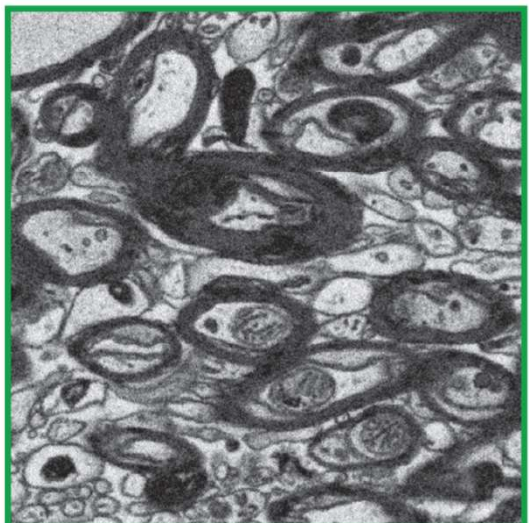


AP -0.96

cerebral cortex



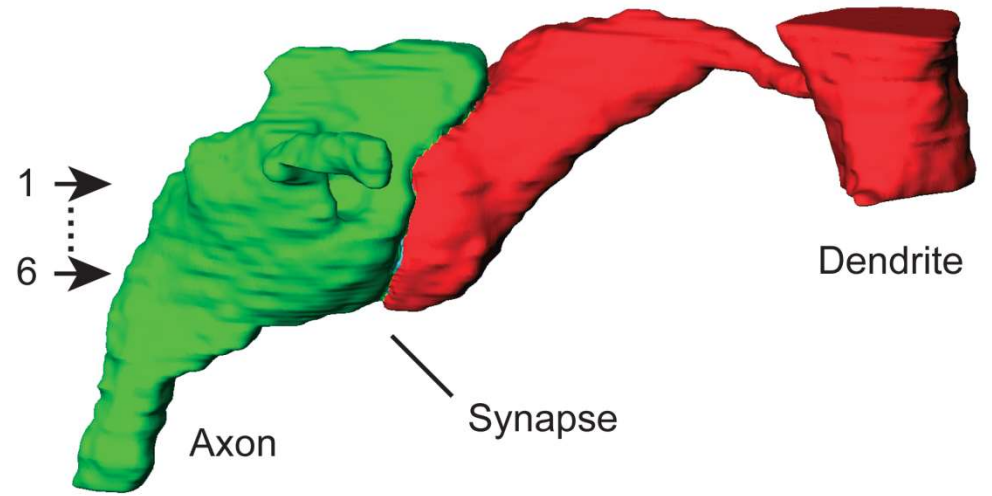
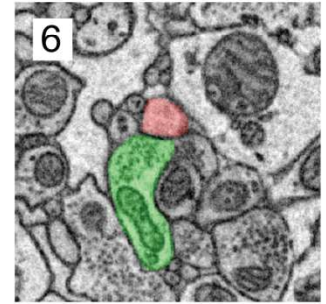
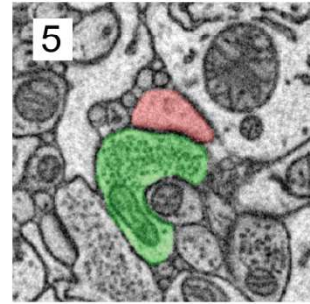
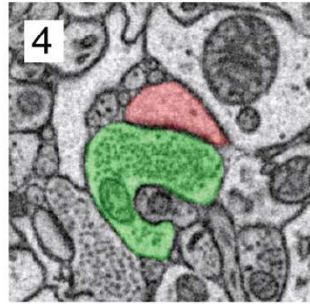
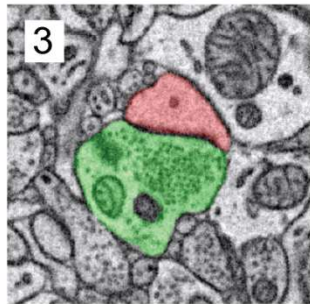
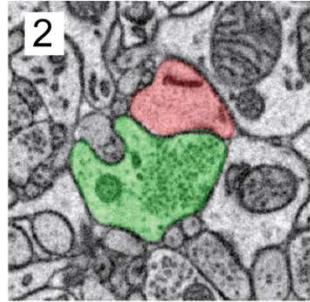
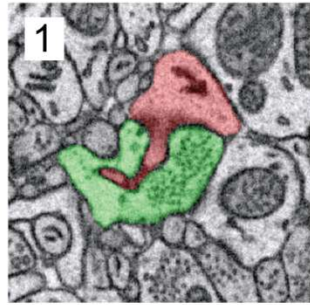
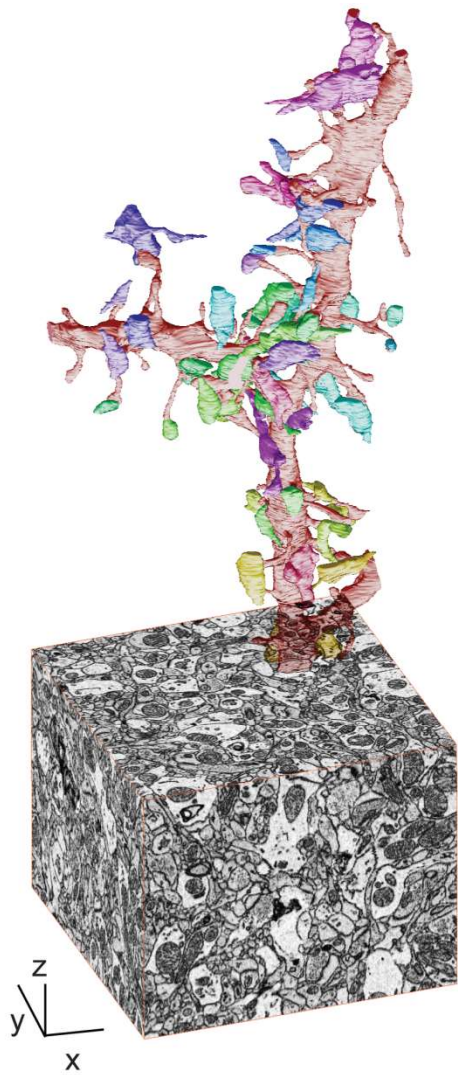
cerebral cortex

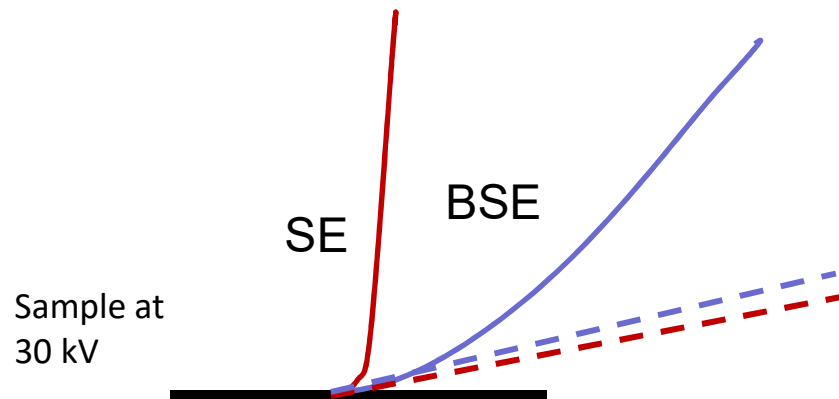
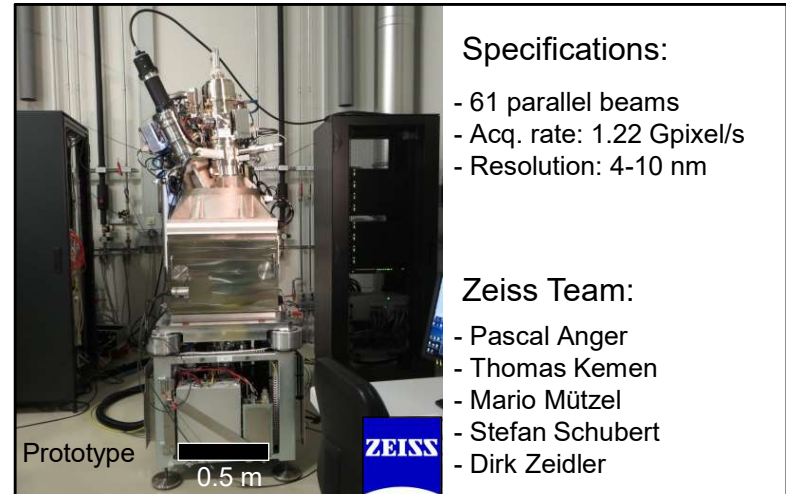
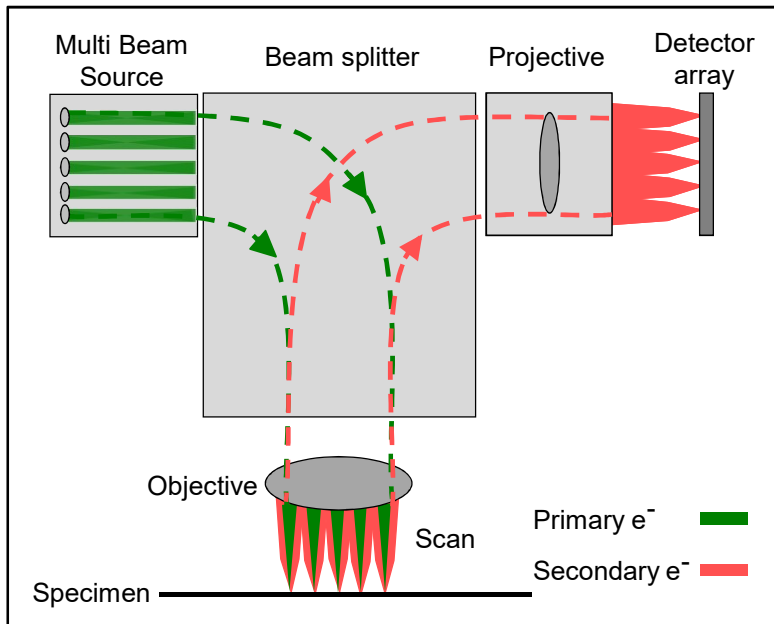


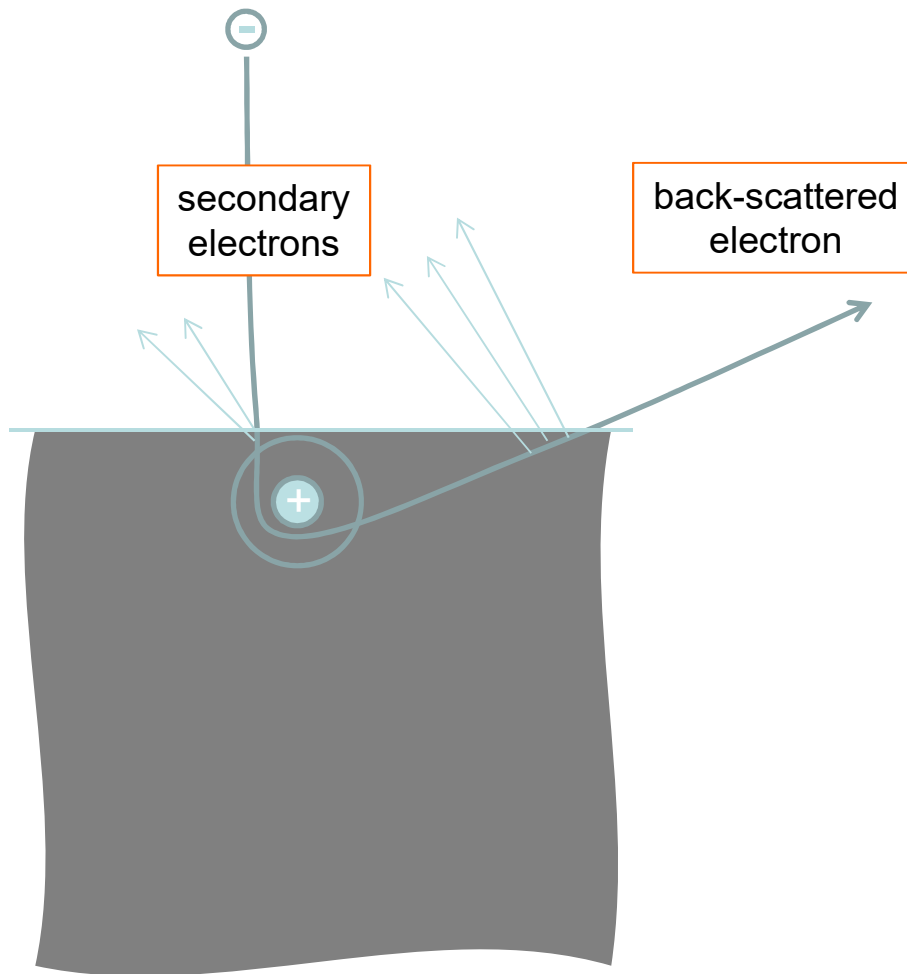
external capsule

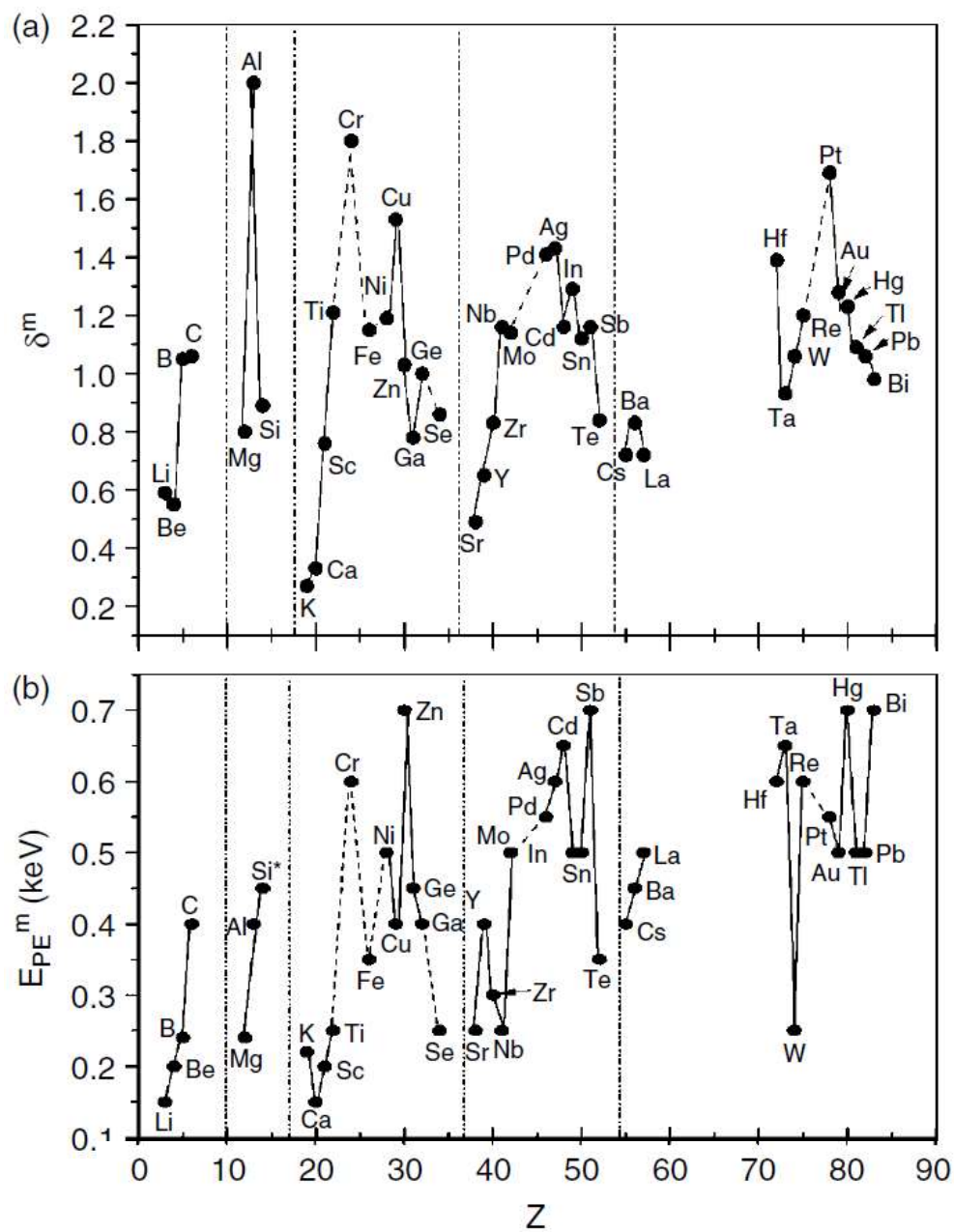


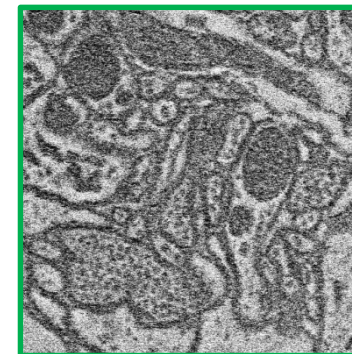
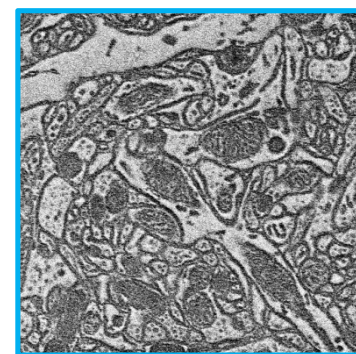
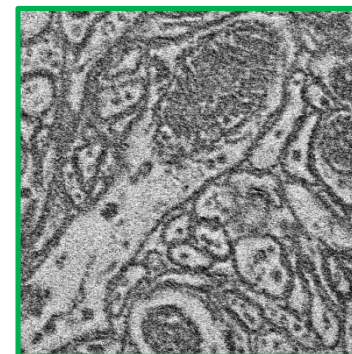
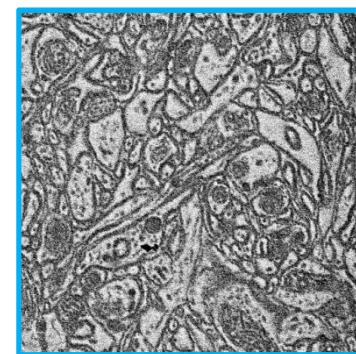
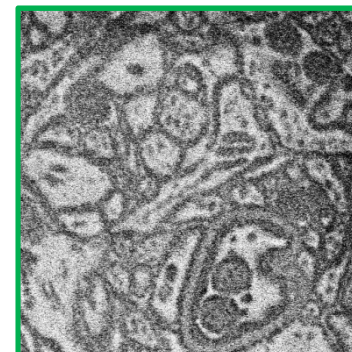
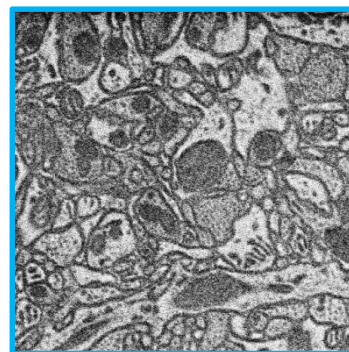
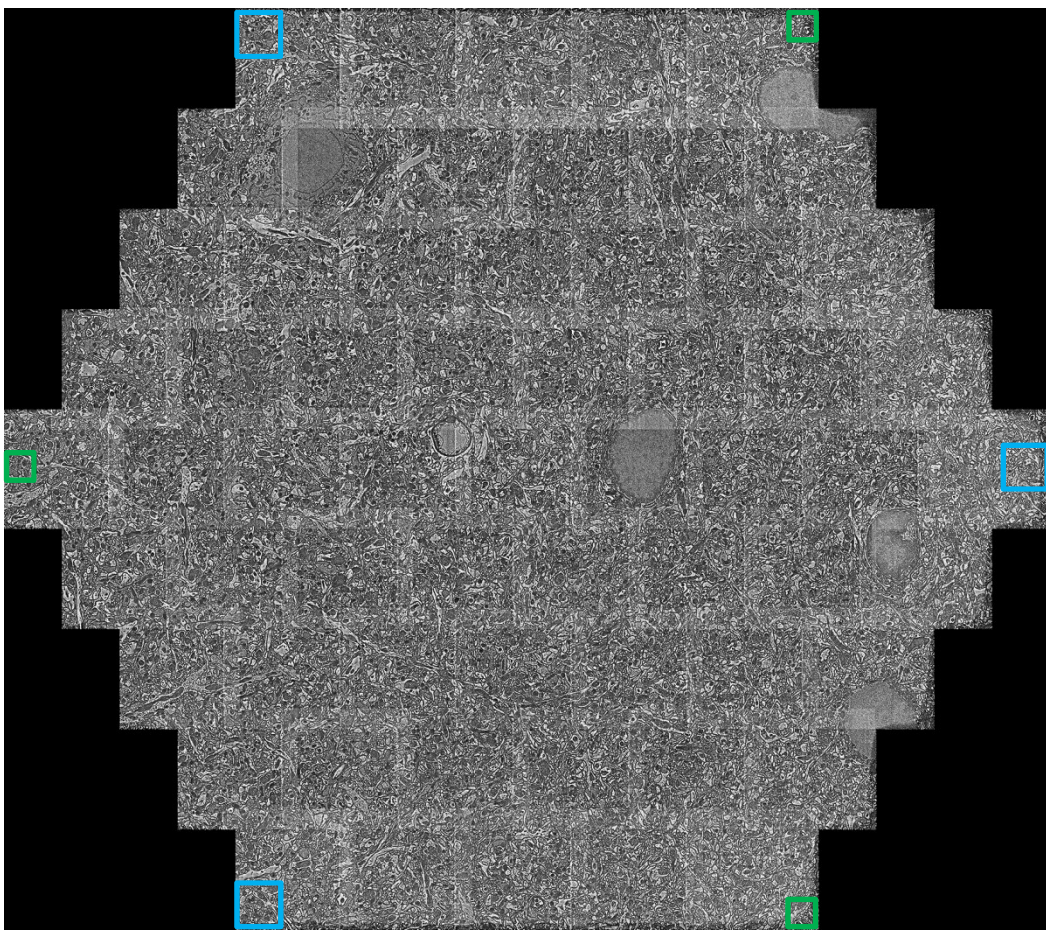
striatum











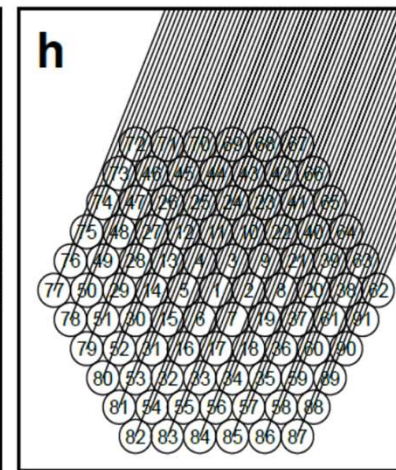
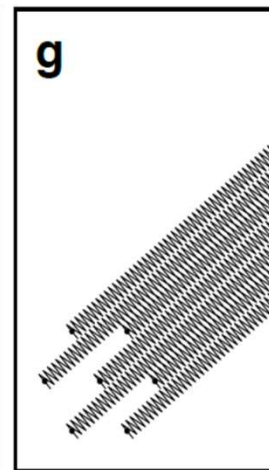
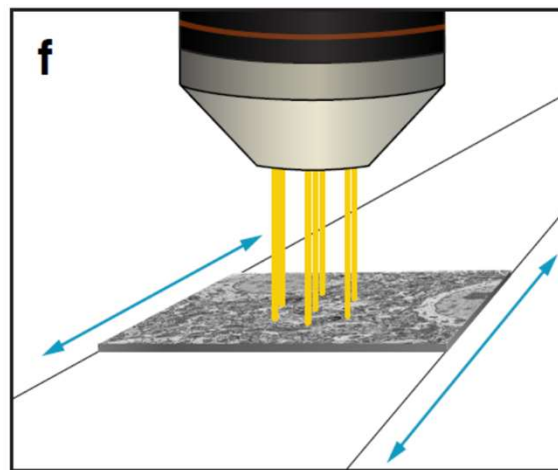
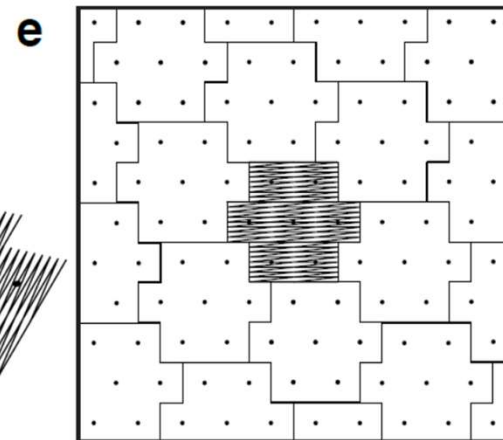
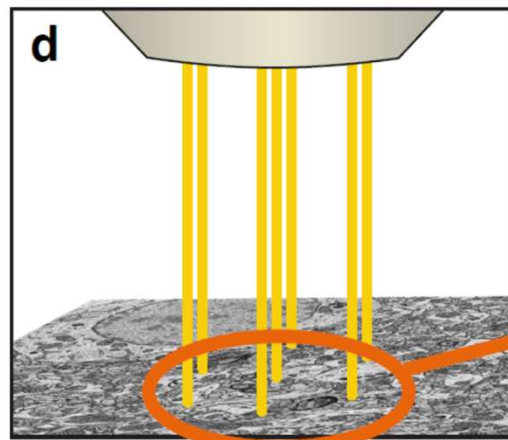
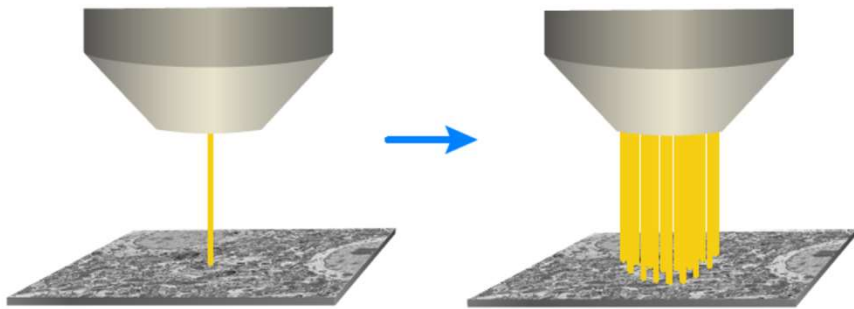
Landing energy: 1.5 kV
Beam deceleration: 30 kV
Pixel size: 6 nm
Dwell time: 50 nS
Acquisition rate: 1.22 GHz

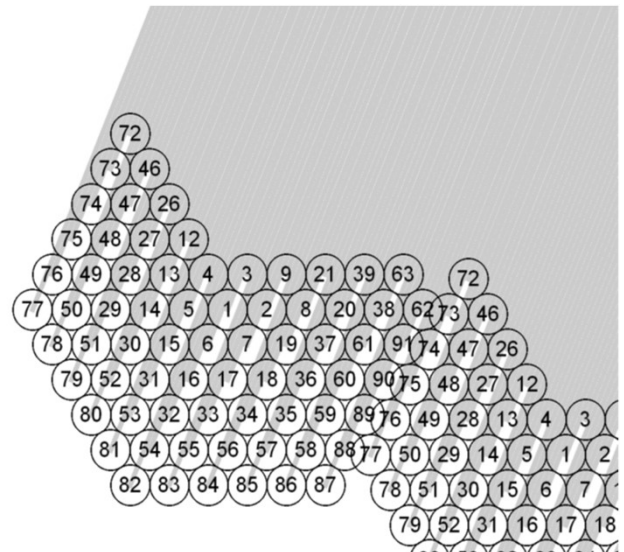
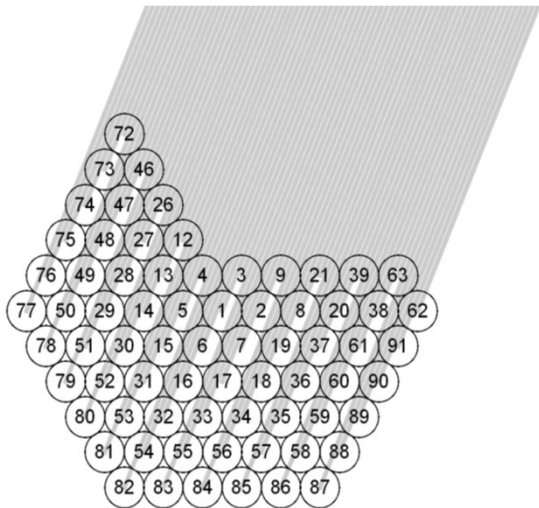
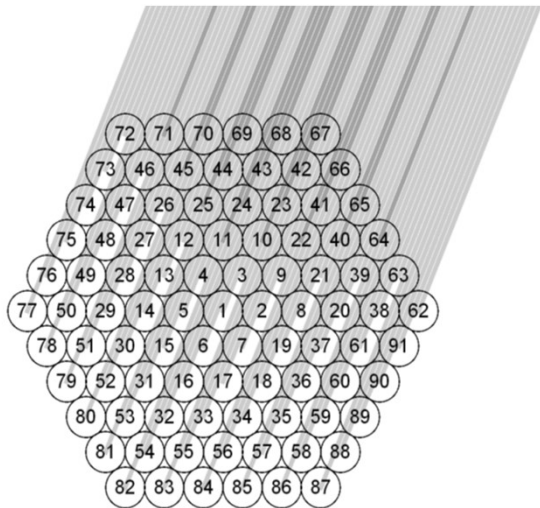
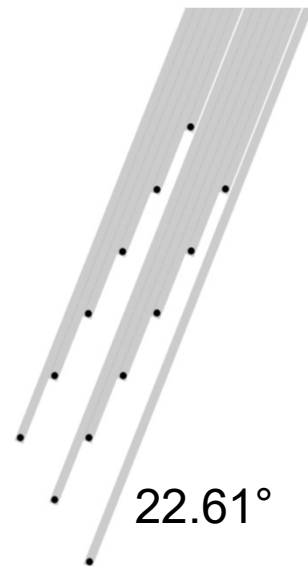
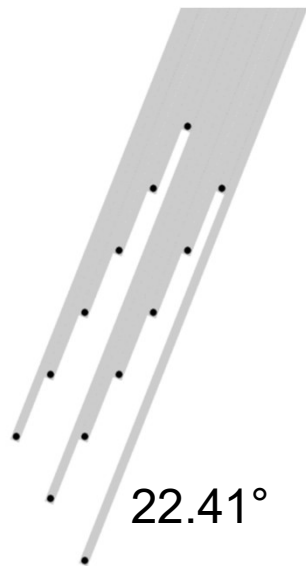
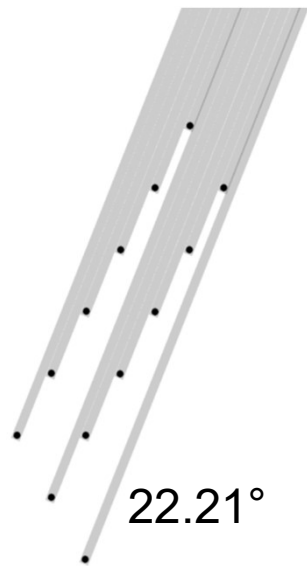
10 μ m

Sample: Shawn Mikula
Coating: Benjamin Titze
Imaging: Tomasz Garbowski & Dirk Zeidler
(Carl Zeiss Microscopy GmbH)
mSEM prototype system in development

1 μ m

500 nm





Serial Thick Section Gas Cluster Ion Beam Scanning Electron Microscopy

Kenneth J. Hayworth¹, David Peale¹, Zhiyuan Lu², C. Shan Xu¹ and Harald F. Hess¹

¹ Janelia Research Campus, Howard Hughes Medical Institute, Ashburn, United States.

² Department of Psychology and Neuroscience, Dalhousie University, Halifax, Canada.

Focused Ion Beam Scanning Electron Microscopy (FIB-SEM) is used to volume image heavy metal-stained, plastic-embedded biological samples with resolutions below 10 x 10 x 10nm, an ability that is especially important in connectomics [1]. FIB-SEM samples are typically restricted to be <50µm in the direction of the FIB beam because glancing angle milling results in artifacts over longer distances [1]. Removal rate is also restricted due to a current/spot size tradeoff. These limitations are especially problematic when one contemplates combining FIB with the increased speed offered by multibeam SEMs like the 91 beam Zeiss MultiSEM [2]. The MultiSEM's *minimum* field of view is ~180µm, and its imaging rate is approximately two orders of magnitude faster than FIB's milling rate. These considerations appear to preclude the integration of traditional FIB milling with MultiSEM imaging.

To overcome these limitations we chose to develop a broad ion beam milling approach using Gas Cluster Ion Beams (GCIB). GCIB delivers low-energy atoms to a surface and therefore does not require the use of a glancing angle. GCIB has been used for semiconductor polishing and for profiling in mass spectroscopy [3]. We attached a GCIB-10s gun from Ionoptika to a Zeiss Ultra SEM. Using a 10kV beam of Ar₂₀₀₀ (clusters of 2000 argon atoms), we verified that smooth, sub-10nm removal was possible from the surface of 100nm thick tissue sections. In order to obtain surfaces sufficiently smooth to produce quality secondary electron (SE) images (using 1.2kV landing energy and InLens detection

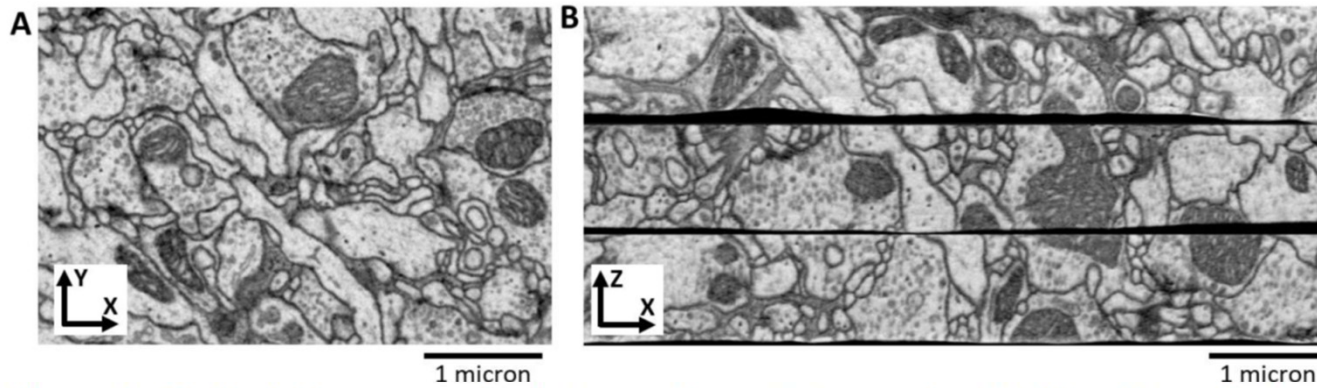


Figure 1. GCIB-SEM imaging. (A) SE image after multiple rounds of GCIB milling. (B) Cross section through dataset of three consecutive 1µm thick sections prior to computational flattening.

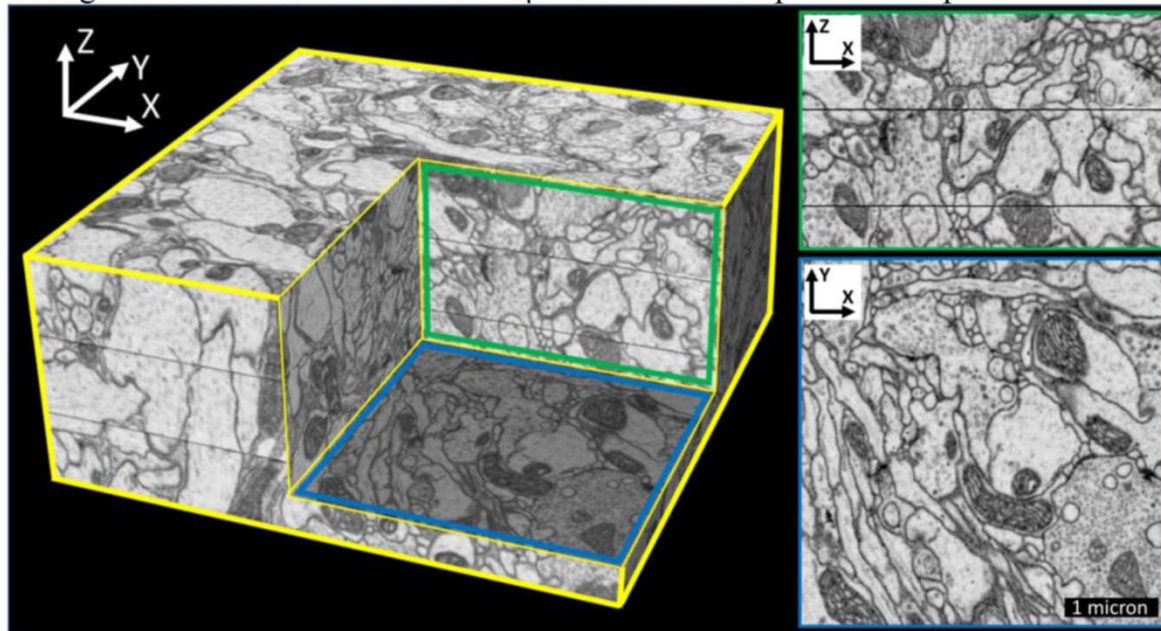
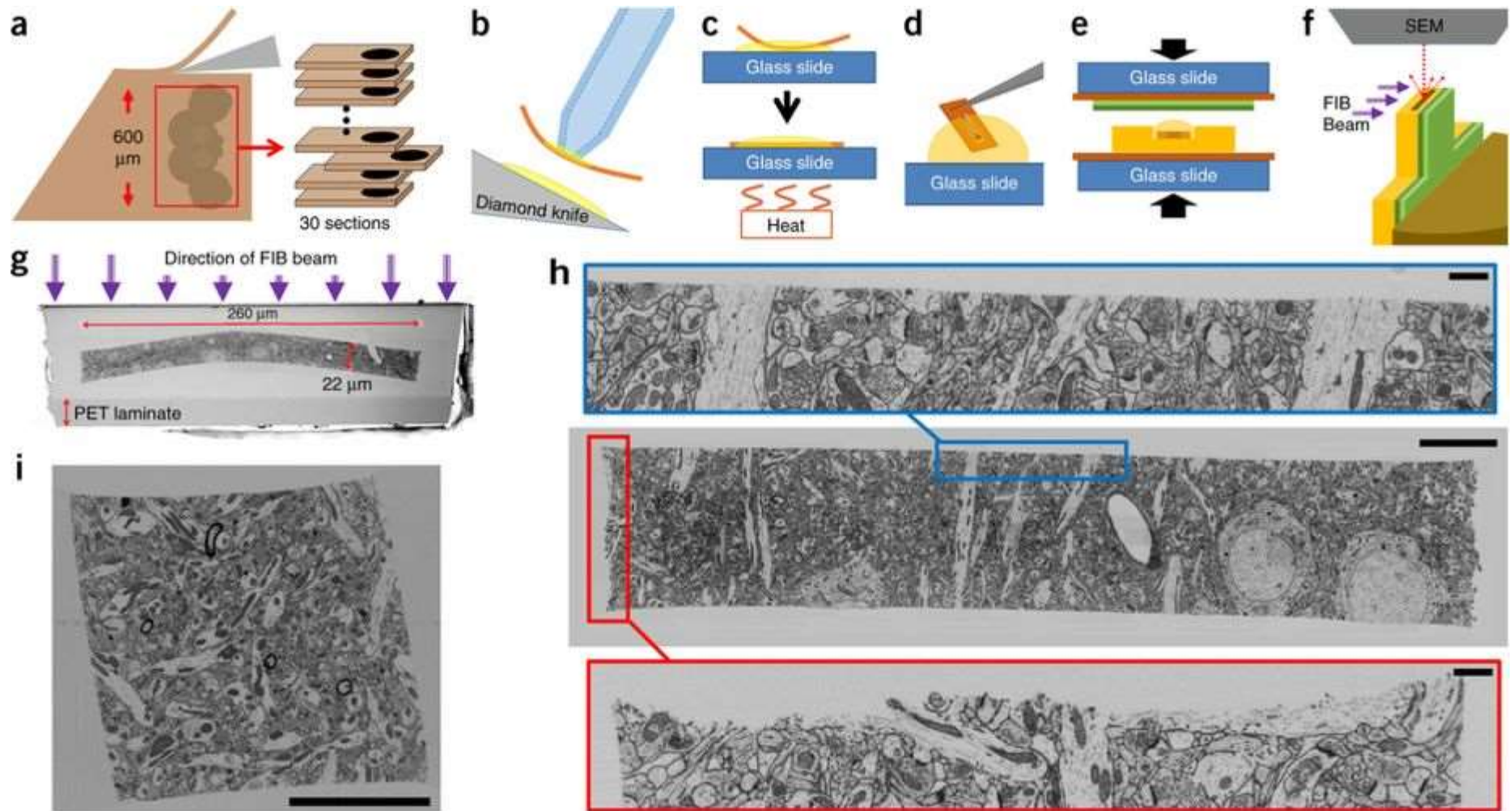
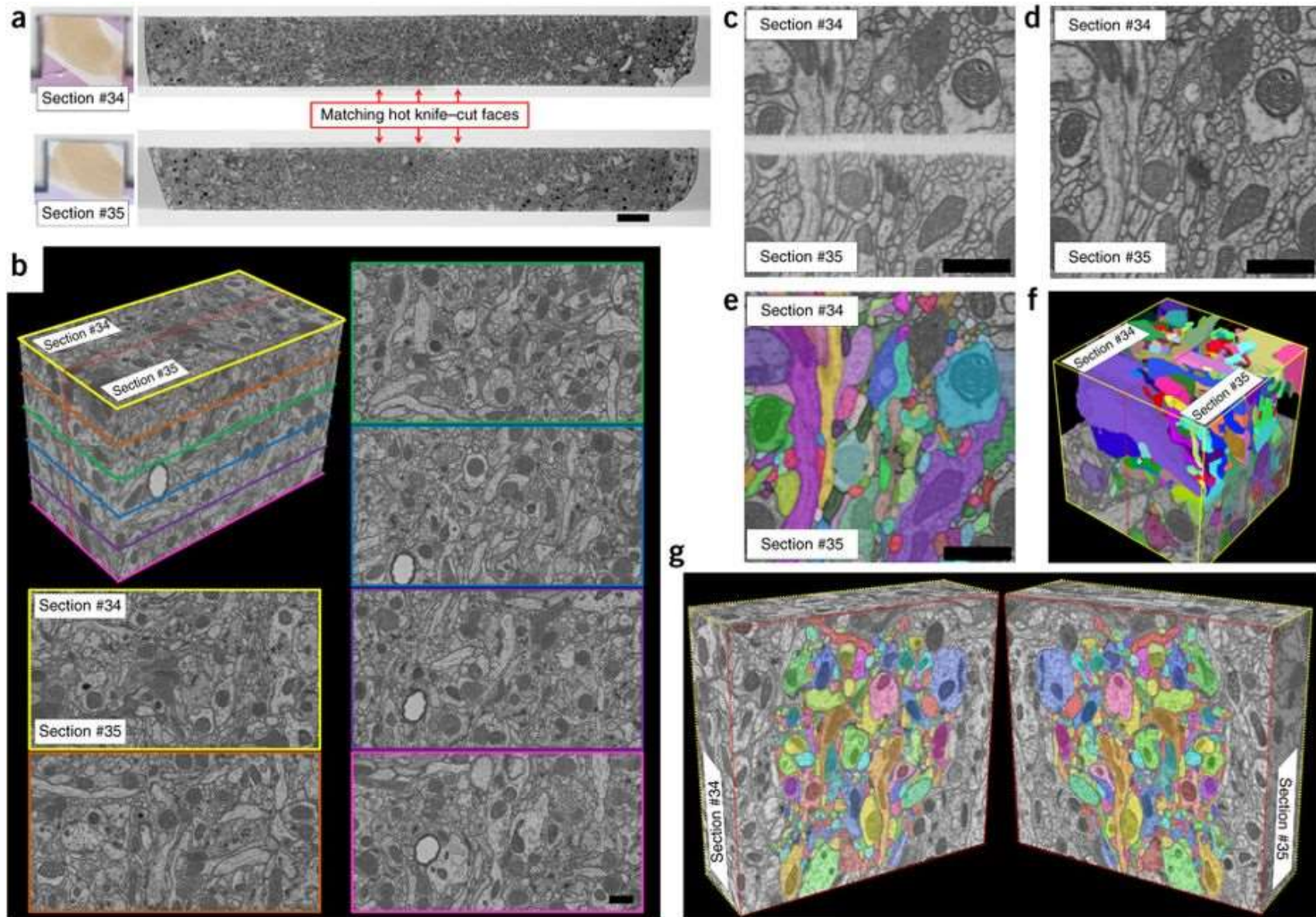


Figure 2. Final GCIB-SEM dataset after computationally flattening and volume-stitching the three consecutive 1µm thick sections together.



Hayworth, K. J., C. S. Xu, Z. Lu, G. W. Knott, R. D. Fetter, J. C. Tapia, J. W. Lichtman and H. F. Hess (2015). "Ultrastructurally smooth thick partitioning and volume stitching for large-scale connectomics." *Nature Methods* **12**: 319.



Hayworth, K. J., C. S. Xu, Z. Lu, G. W. Knott, R. D. Fetter, J. C. Tapia, J. W. Lichtman and H. F. Hess (2015). "Ultrastructurally smooth thick partitioning and volume stitching for large-scale connectomics." *Nature Methods* **12**: 319.



Maria Kormatcheva

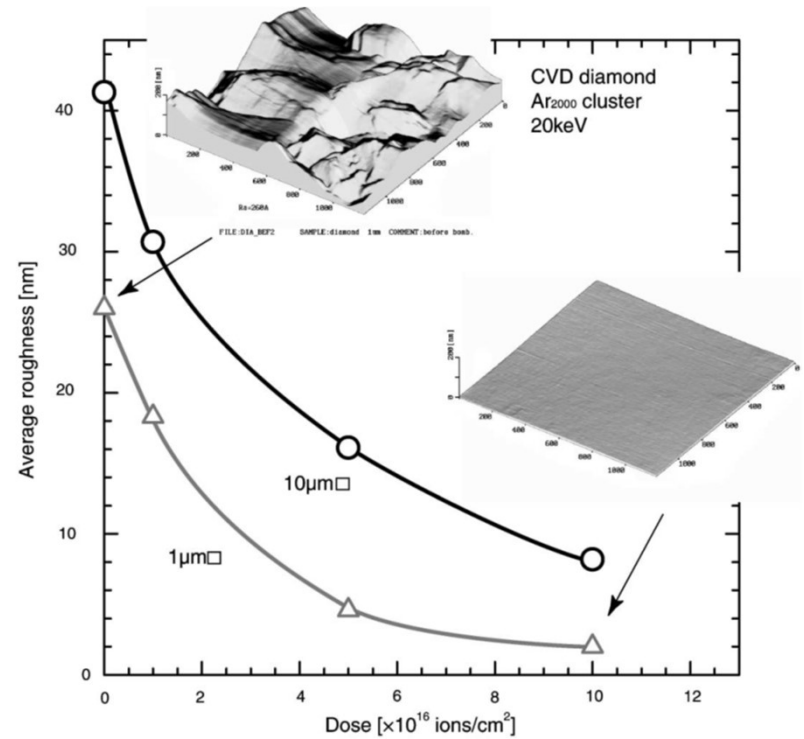
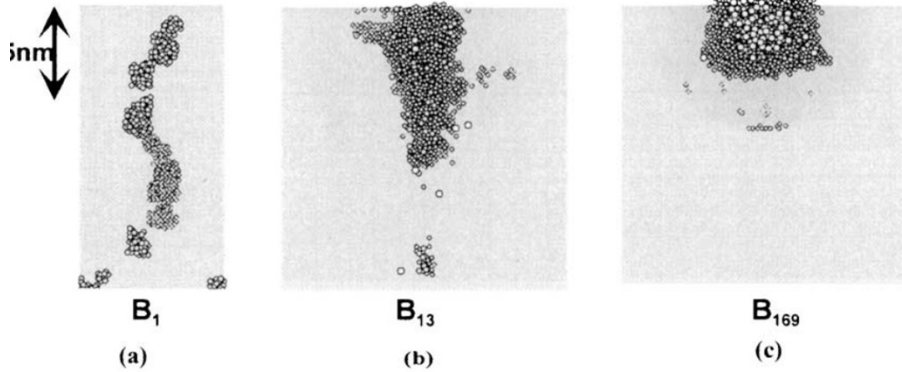
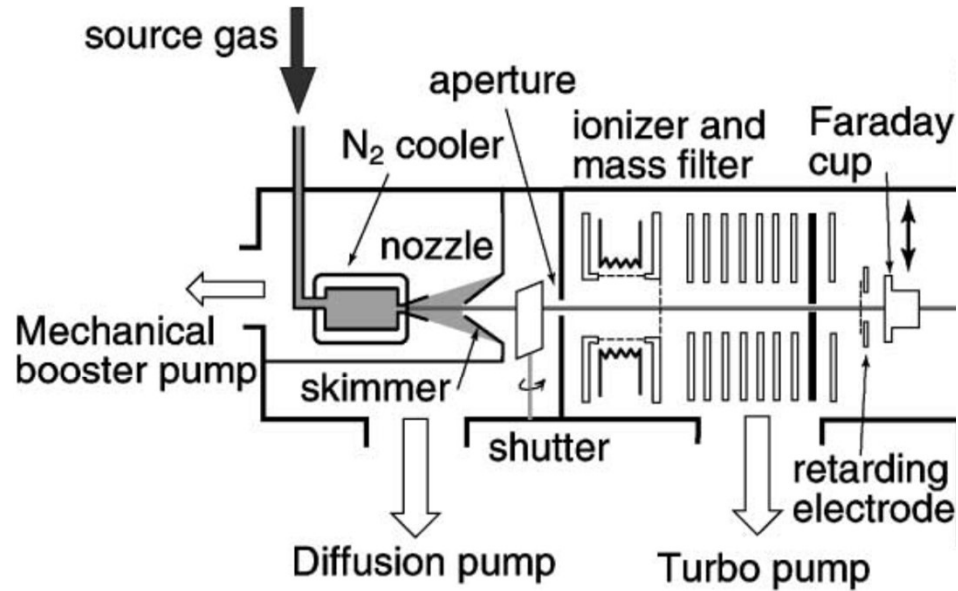


Illustration: Yamada et al., 2001



Stumbling Blocks, Pitfalls, Showstoppers, etc.:

Synapses (chemical), strength and other parameters

Synapses (electrical), existence etc.

Synapses (modulatory), etc.

Channel distributions

Variation between individuals

Isn't all that's interesting encoded in the genome?

stimuli >> organism >> behavior

stimuli >> circuits >> behavior

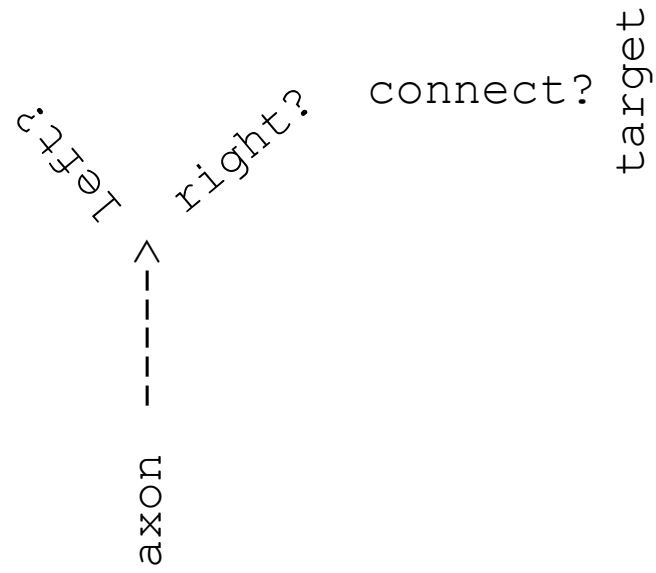
stimuli >> circuits >> behavior

genes -> Development ^

stimuli >> circuits >> behavior

genes -> proteins ->

Development ->



membrane

trans

membrane
signalling
molecule

membrane

cytoskeleton

membrane

trans lig
membrane and

signalling
molecule

<< activate

membrane

cytoskeletoncytoskeletoncytoskeletoncyto

ane membrane membrane membrane

membrane
trans
membrane
signalling
molecule

membrane

embranemembrane membrane membrane

cell-cell
adhesion
molecules
membrane

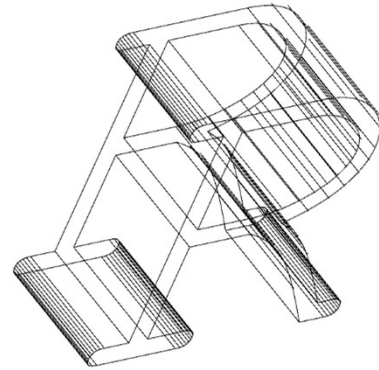
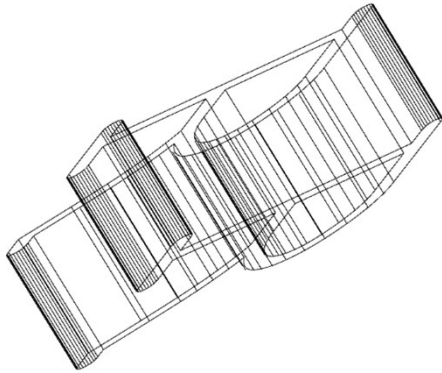
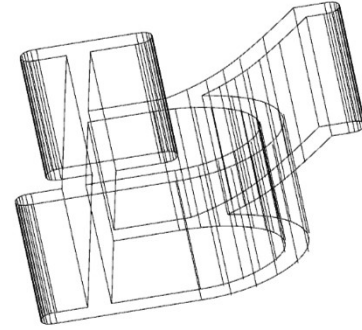
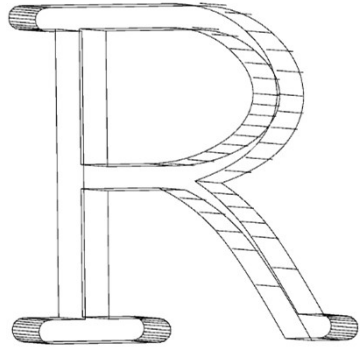
M^m
molecule
O=|
||
|
||
|
molecule
X₁nc₁ow
molecule
C=|
||
|
molecule
|
molecule

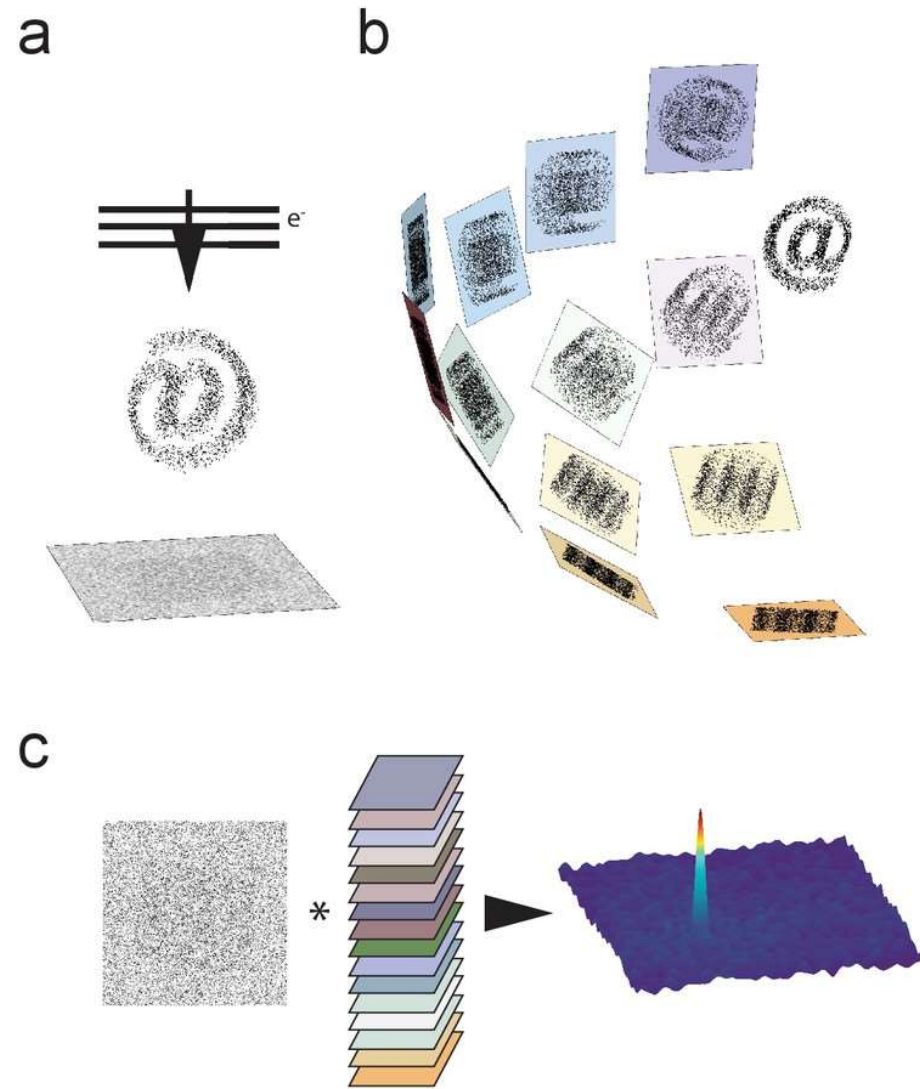


Peter
Rickgauer

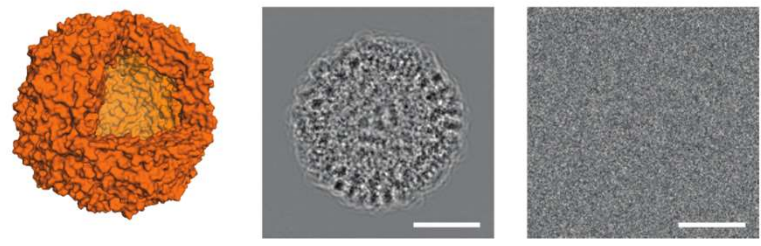
Niko Grigorieff (Janelia)
Tim Grant
Ruben Diaz-Avalos
Alexis Rohou

Janelia cryo-EM facility
Zhiheng Yu

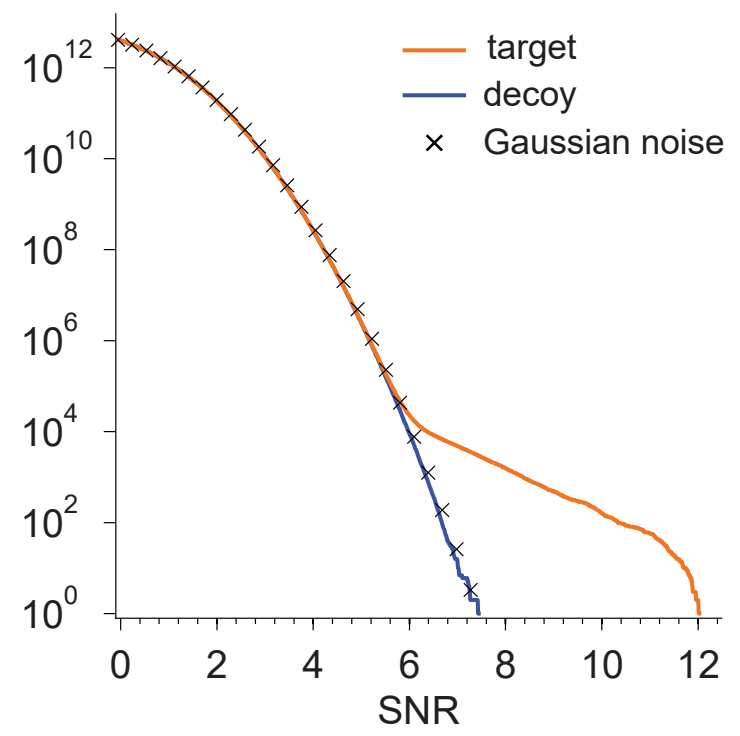
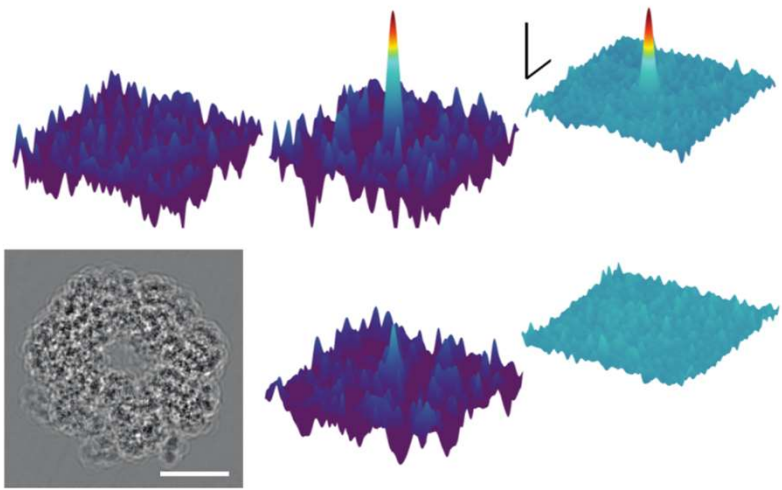




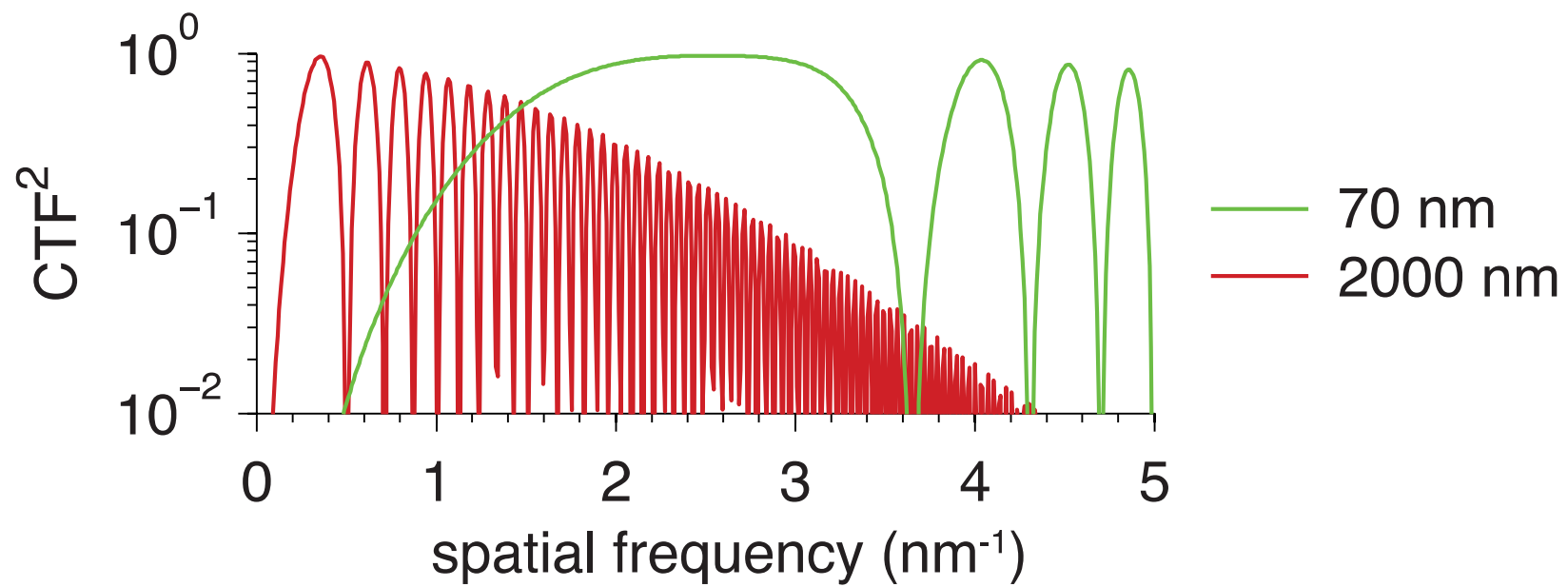
apoferritin

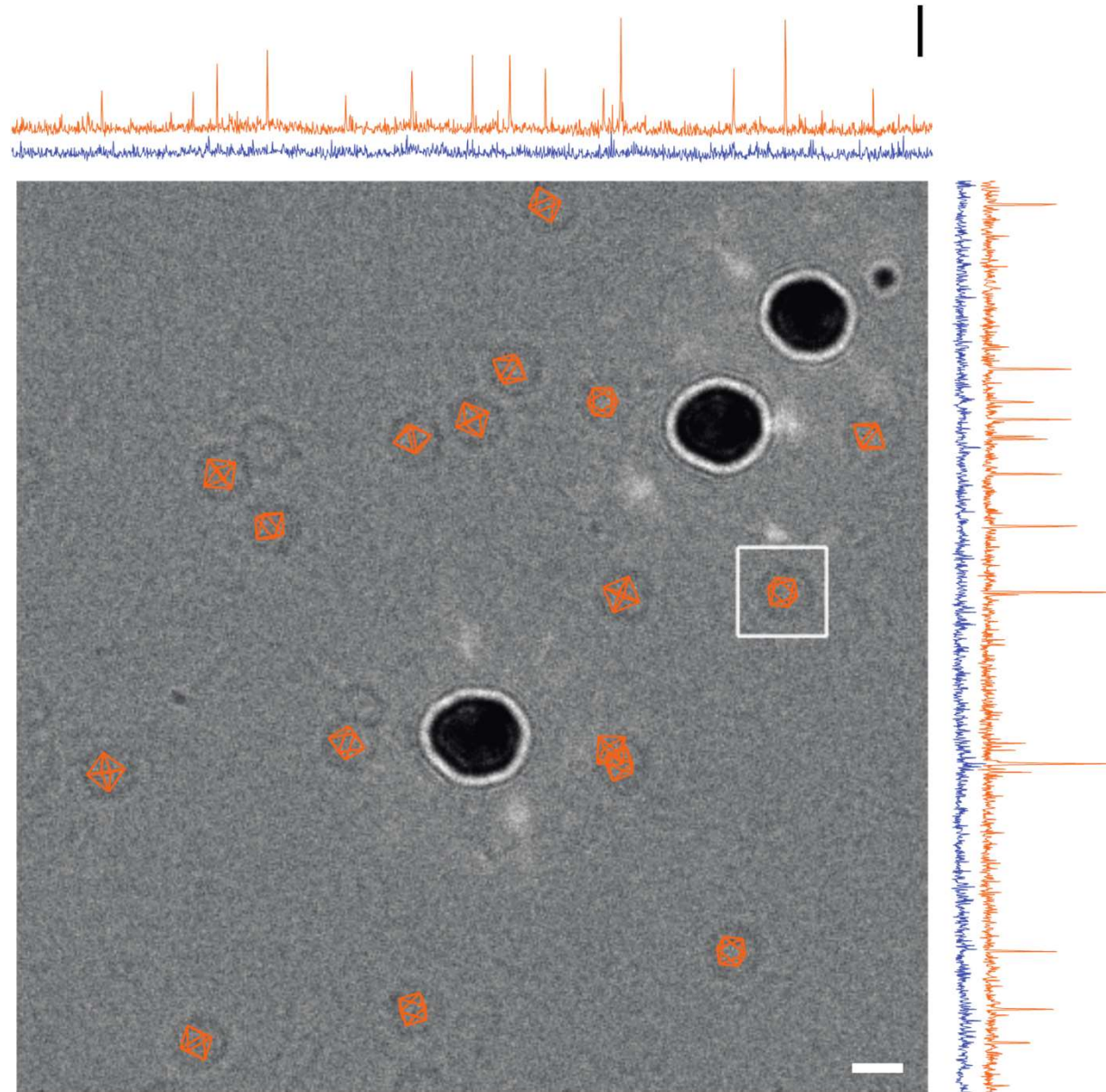


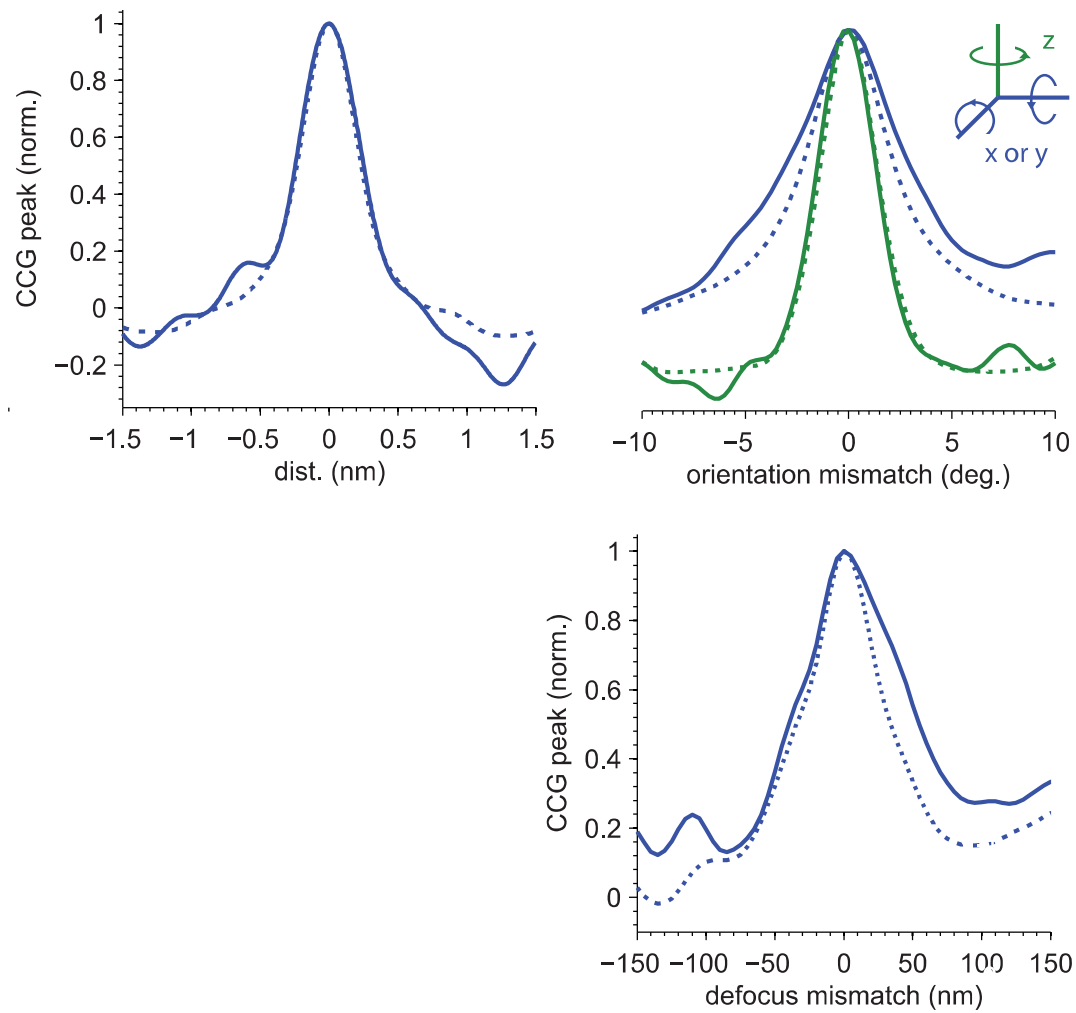
groEL

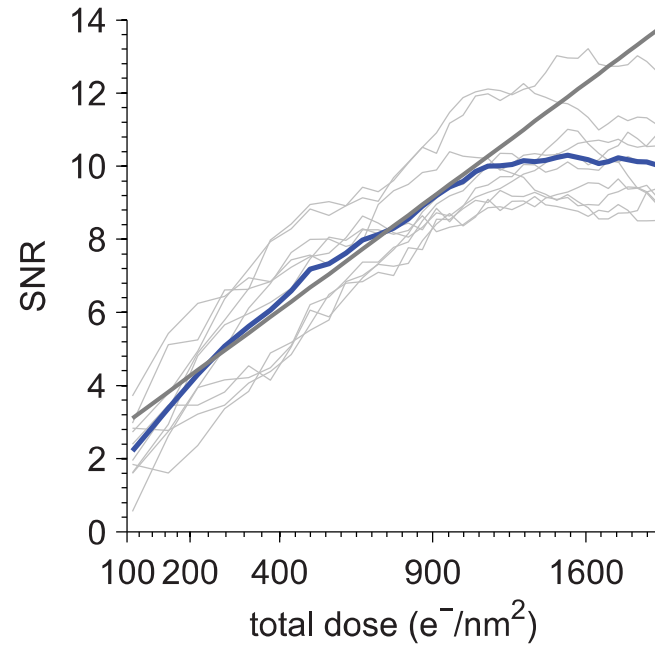
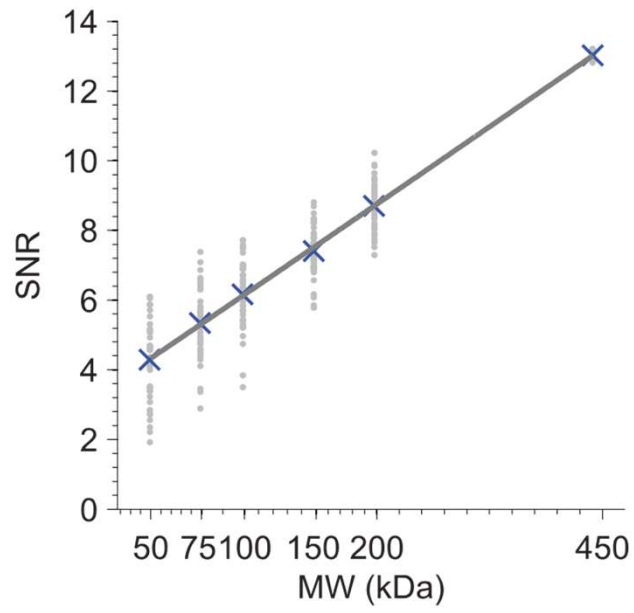


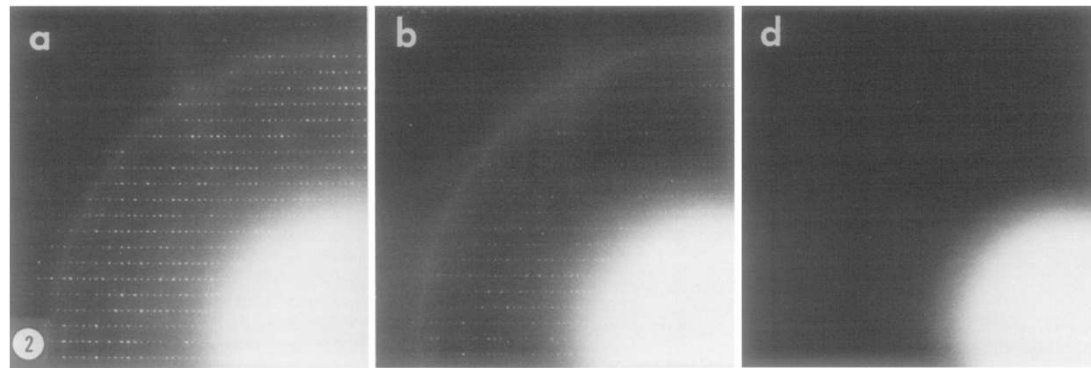




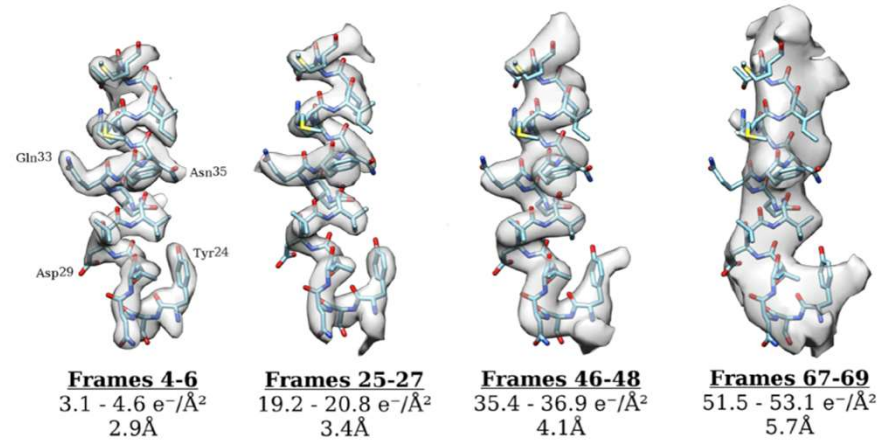








Taylor and Glaeser (1976)



Grant and Grigorieff (2015)

Simulations

